Strength of Cold-Formed Steel Jamb Stud-To-Track Connections

by

Albert Victor Lewis

A thesis
presented to the University of Waterloo
in fulfillment of the
thesis requirement for the degree of
Master of Applied Science
in
Civil Engineering

Waterloo, Ontario, Canada, 2008

Author's Declaration

I hereby declare that I am the sole author of this thesis. This is a true copy of the thesis, including any required final revisions, as accepted by my examiners.

I understand that my thesis may be made electronically available to the public.

Abstract

Cold-formed steel structural members are used extensively in building construction, with a common application being wind load bearing steel studs. The studs frame into horizontal steel track members at the top and bottom of the wall assembly, with the stud-to-track connection typically being made with self-drilling screws or welds. The wall studs are designed to carry lateral loads only and must be checked for web crippling at the end reactions. While a design expression currently exists for the single stud-to-track connection, there is no similar design expression for multiple jamb stud members.

An experimental investigation was carried out, consisting of 94 jamb stud assembly tests subjected to end-one-flange loading. The stud-to-track connections consisted of single C-section studs located at the end of a track simulating a door opening, and a built-up jamb made up of two studs simulating framing at either a window or door opening. The members were attached to the track with self-drilling screws. The research objective was to determine the failure modes and develop a design expression for these structural assemblies.

The scope of the experimental investigation covered the following range of parameters:

i) Stud and track depths of 92 mm and 152 mm;

ii) Stud and track thickness (0.84 mm, 1.12 mm, 1.52 mm and 1.91 mm);

iii) Configuration of jamb studs (back-to-back, toe-to-toe and single);

iv) Location of jamb studs in the track (interior and end);

v) Screw size (#8, #10 and #12);

vi) Screw location (both flanges and single flange).

Based on the findings of this investigation, design expressions are proposed to predict the capacity of this connection for two limit states: web crippling of the jamb stud; and, punch-through of the track. The web crippling design expression was taken from the North American Specification for the Design of Cold-Formed Steel Structural Members [AISI 2007a; CSA 2007] with new coefficients developed from the test data of the jamb stud-to-track assemblies. A new design expression is also proposed for the track punch-through failure mode, which differs from the approach currently used in the North American Standard for Cold-Formed Steel Framing – Wall Stud Design [AISI 2007b]. A proposal is also recommended to revise the wording in the North American Standard for Cold-Formed Steel Framing – Wall Stud Design [AISI 2007b] to include provisions for the design of jamb studs based on the results of this research.

Acknowledgements

I would like to offer my deep gratitude to my thesis supervisor, Prof. Reinhold Schuster, for introducing me to the field of cold formed steel research and engineering, for his guidance and patience as I slowly learn to find my way in this field, and for his generosity in offering me the benefit of his knowledge and experience both in this field and as an engineer. He has provided me with many rich opportunities over the years, and for all this, I am indeed grateful.

This project was funded by the American Iron and Steel Institute, the Steel Stud Manufacturers Association, and by the Canadian Sheet Steel Building Institute. The contributions of the other researchers in this field are also gratefully acknowledged. I also gratefully acknowledge the donation of materials from Bailey Metal Products Limited.

Dr. Steven Fox has been a mentor and friend to me from the beginning of my career in the of cold formed steel industry. His love of science and his appetite for investigation continue to be a source of great motivation for me. I am very grateful for all the help and encouragement he has provided me throughout the course of this project; without his energy and enthusiasm, I doubt I would have been able to finish.

Finally, I would like to thank my wife Angela, for her support, patience, and encouragement throughout this research. I could not have done this without her.

Table of Contents

List of Figures

List of Tables

Chapter 1
Introduction

1.1 Cold-Formed Steel Construction

Cold-formed steel structural members are used extensively in building construction throughout the world due to a combination of their high strength-to-weight ratio, stiffness, recyclability, and the relatively low cost associated with their supply and installation. Infill wall framing is a common application for a subset of cold-formed steel structural members referred to as "wind load bearing" studs. Shown in the photograph of Figure 1-1, are typical wind load bearing walls or 'curtain walls', which are used to support the exterior wall finishes and to transfer the lateral loads, such as those imposed by wind pressure. These studs 'infill' the space between the main structural elements framing the floor, such as hot-rolled steel beams or concrete slabs, which carry the gravity loads.

Figure 1-1: Curtain Wall Construction

Cold-formed steel stud walls are constructed with a combination of stud and track sections as illustrated in Figure 1-2. A stud is a 'C'-shaped section that typically ranges from 92 mm to 203 mm in depth with flanges from 32 mm to 41 mm in width and with stiffening lips on the outside edges of the flanges. Studs are commonly available in steel thicknesses ranging from 0.84 mm to 1.91 mm. The track sections are of the same nominal size and thickness as the studs, but without the stiffening lips on the outside edge of the flanges. A steel stud wall assembly is constructed with a top and bottom track into which the steel studs are fastened at regular intervals. The track is anchored to the structure and the studs are usually connected to the track with self-drilling screws through each flange at both the top and bottom stud-to-track connection. The stud is designed to carry a uniform lateral load, which is transferred at the ends of the stud to the track, and then through the anchors to the supporting structure.

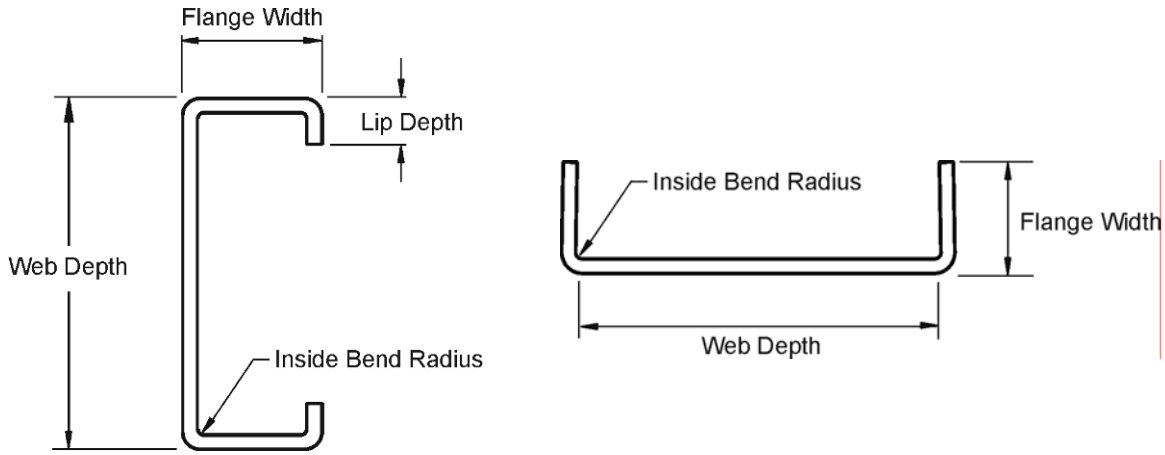

Figure 1-2: Stud and Track

In wind load bearing applications, there is some type of deflection assembly installed at the top track to accommodate the anticipated movement of the upper floor so that the wall studs do not become axially loaded. One type of deflection detail is illustrated in Figure 1-3, which uses a double top track arrangement, where the length of the flanges of the outer top track is determined by the amount of deflection anticipated. One leg of the outer top track is assumed to be loaded uniformly by the inner top track, which distributes the reactions from the studs. A description of a design procedure is provided by the Lightweight Steel Framing Design Manual [CSSBI 2006]. The behaviour of these deflection type connections was not included in the scope of the experimental work reported herein.

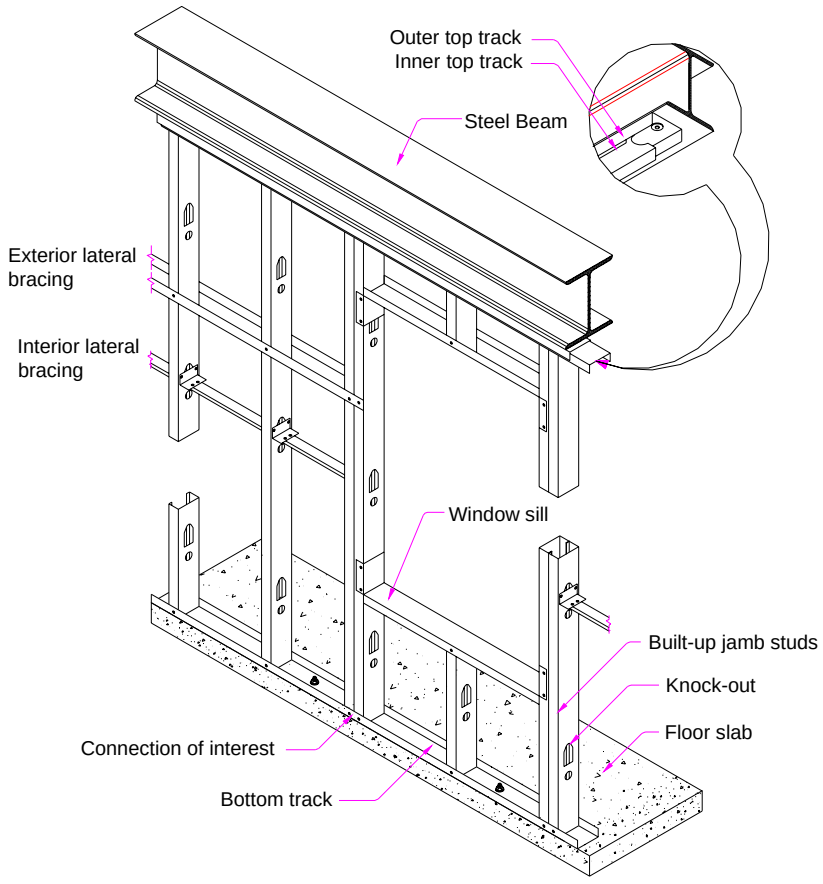

Figure 1-3: Typical Infill Wall Application

1.2 Description of the Problem

The design of cold-formed steel structural members in North America is governed by the North American Specification for the Design of Cold-Formed Steel Structural Members [AISI 2007a; CSA 2007], hereafter referred to as the NASPEC. In Canada, this document is published by the Canadian Standards Association as CAN/CSA-S136-07 [CSA 2007], and in the United States by the American Iron and Steel Institute as AISI-S100-07 [AISI 2007a]. These design documents include provisions that cover the design of many common cold-formed steel structural elements and members, but do not have design criteria for the design of the stud-to-track connections commonly used in cold-formed wind load bearing steel stud construction.

The design of a wind load bearing steel stud takes into account the following limit states: flexure, shear, deflection and web crippling. Designing for the first three of these limit states can be performed by using the NASPEC. The web crippling limit state, however, poses special problems with wind load bearing steel stud applications. The web crippling expressions in the NASPEC assume that the flexural member (i.e. the steel stud) is resting on a rigid bearing surface. The stud-to-track connection in a wind load bearing wall, while it is an end-one-flange loading, is a condition that is not covered by the NASPEC. This difference is illustrated in Figure 1-4. As a consequence, testing is required to determine the appropriate design resistances for this type of connection.

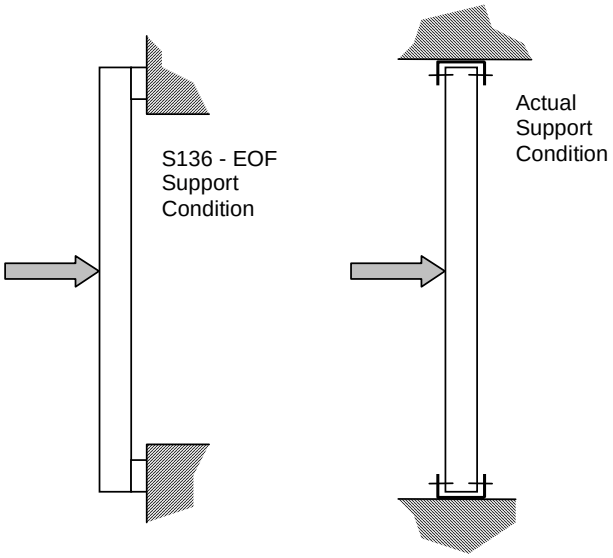

Figure 1-4: Idealized Web Crippling Compared to Stud-to-Track Connection

There are a number of parameters that affect the capacity of the stud-to-track connection, including:

i) The geometric and mechanical properties of the stud and track material;

ii) The thickness of the stud and track members relative to one another;

iii) The size of the gap between the end of the stud and the web of the track;

iv) Size and location of the fasteners making the stud-to-track connection;

v) Continuity of the track near the stud (i.e. jamb stud at a wall opening);

vi) Built-up stud members (i.e. jamb studs); and

vii) Axial load on the stud.

Tests on items i) through v) have been carried out by various researchers, leading to the design provisions that are currently contained in the North American Standard for Cold-Formed Steel Framing – Wall Stud Design, AISI S211-07 [AISI 2007b], hereafter referred to as the WSD. These design provisions are limited to single stud-to track connections where sufficient test data was available. Until now, no testing has been done on the strength of the built up jamb stud-to-track connections that are also common elements of a cold-formed steel wind load bearing wall assembly. The effect of axial load on the strength of the stud-to-track connection has not as yet been investigated.

1.3 Scope of Study

The research presented in this thesis is focused on the connection between built-up stud members and the bottom track, both at interior locations, as shown in Figure 1-3 above, and at end locations, such as would be found at a doorway or the corner of a building. The scope of the work was primarily experimental, with a total of 94 tests being conducted. The experimental work covered the following range of parameters:

i) Stud and track depths of 92 mm and 152 mm;

ii) Stud and track thickness (0.84 mm to 1.91 mm);

iii) Configuration of jamb studs (back-to-back, toe-to-toe and single);

iv) Location of jamb studs in the track (interior and end);

v) Screw size (#8, #10 and #12);

vi) Screw location (both flanges and single flange);

vii) Stud and track the same thickness;

viii) Yield strengths from 300 to 450 MPa.

After the experimental work was completed and the results were analyzed, design expressions were derived covering the two principal failure modes: web crippling of the stud, and punch-through of the track.

1.4 Organization of Thesis

An overview of previous research is presented in Chapter 2. The University of Waterloo has been the site of much of this earlier work that has led to the current design expressions.

The parameters of the experimental investigation and the test procedure are described in Chapter 3. The research scope comprised a total of 94 tests on various combinations of parameters relevant to these jamb stud connections.

Provided in Chapter 4 is a discussion of the various failure modes observed during the test program and a summary of the test results. Also included in this section is a discussion of the effects of screw size and placement on the strength and behaviour of the assembly.

The culmination of this research was the development of equations to predict the capacity of these connections as observed in the test program. These predictor equations are provided in Chapter 5 along with the calibrated resistance factors needed for design.

Another contribution of this work was to propose changes to the WSD to recognize these jamb stud members. Included in Chapter 6 is the current wording of the WSD related to

the stud-to-track connections with the proposed changes to incorporate the jamb stud members. This proposal will be forwarded to the AISI Committee on Framing Standards for their adoption consideration.

Listed in Chapter 7 is a summary of the conclusions, and presented in the Appendices are the detailed test data.

Chapter 2
Literature Review

2.1 Previous Research on Stud-To-Track Connections

The lateral strength and behaviour of stud-to-track connections has been studied by a number of earlier researchers, resulting in a valuable collection of data and observations. In this chapter, this previous research is reviewed as it pertains to this current investigation.

2.2 Drysdale and Breton (1991)

As part of a larger study on the performance of steel stud brick veneer wall assemblies, 109 stud-to-track connection tests were conducted at McMaster University by Drysdale and Breton [1991]. Of these tests, 70 were screwed stud-to-track connections, while the remaining tests were welded connections, deflection track connections which used double sections of track, and connections reinforced with various clips and box sections. Only the screwed stud-to-track connections will be discussed here, since the others are not germane to this investigation.

A number of parameters with the screwed stud-to-track connections were varied by Drysdale and Breton. These include the stud and track web depth and thickness, the distance (end gap) between the end of the stud and the web of the track, the location of the connection relative to its placement within a section of track, and whether the compression, tension, or both flanges of the stud and track were connected. Of the different number of test series, a number of tests were conducted in each series, and the parameters that were varied for each series are presented in Table 2-1.

Table 2-1: Stud-to-Track Screw-Fastened Connection Test Parameters [Drysdale and Breton, 1991]

Test Series	Connected Flange		End Gap	Connection Location	Stud		Track		Num. of Tests
	Comp.	Tension			Web	t_{stud}	Web	t_{track}	
20A-D1	Y	Y	min.	Interior	92mm	20 gauge	92mm	20 gauge	9
18A-D1	Y	Y	min.	Interior	92mm	18 gauge	92mm	18 gauge	5
20B-D1	Y	Y	min.	Interior	152mm	20 gauge	152mm	20 gauge	6
18B-D1	Y	Y	min.	Interior	152mm	18 gauge	152mm	18 gauge	6
20A-D2	Y	Y	12mm	Interior	92mm	20 gauge	92mm	20 gauge	4
20B-D2	Y	Y	12mm	Interior	152mm	20 gauge	152mm	20 gauge	4
18A-D2	Y	Y	12mm	Interior	92mm	18 gauge	92mm	18 gauge	4
18B-D2	Y	Y	12mm	Interior	152mm	18 gauge	152mm	18 gauge	3
20A-D3	N	Y	min.	Interior	92mm	20 gauge	92mm	20 gauge	3
18A-D3	N	Y	min.	Interior	92mm	18 gauge	92mm	18 gauge	4
20B-D3	N	Y	min.	Interior	152mm	20 gauge	152mm	20 gauge	3
18B-D3	N	Y	min.	Interior	152mm	18 gauge	152mm	18 gauge	3
18A-D4	Y	N	min.	Interior	92mm	18 gauge	92mm	18 gauge	4
20A-D5	N	Y	12mm	Interior	92mm	20 gauge	92mm	20 gauge	4
20B-D6	Y	Y	min.	End	152mm	20 gauge	152mm	20 gauge	2
20A-D10	Y	Y	min.	Interior	92mm	20 gauge	92mm	14 gauge	3
20B-D11	Y	Y	min.	Interior	152mm	20 gauge	152mm	18 gauge	3

The following observations are noteworthy:

1. #6 pan-head self-drilling screws were used for the stud-to-track connections, and in many cases, the screw pulled completely out of the stud compression flange at failure.

2. The data indicates that the connection between the stud and the track on the compression flange (bottom) influences the strength of the assembly more than a missing screw in the tension flange (top). The capacity of those assemblies without a screw in the compression flange had an average of only 88% of the capacity of an assembly with two screws.

3. Drysdale and Breton did not propose predictor equations for these types of connections.

2.3 Marinovic (1994)

Research was conducted at Cornell University by Marinovic [1994] on screw-connected stud-to-track connections that resulted in the development of the following predictor equation for the nominal resistance of a track punch-through failure:

$$P_n = 0.6twF_u \qquad (2.1)$$

Where:

P_n	=	Nominal stud capacity
t	=	Base steel thickness of track material
w	=	Stud flange width
F_u	=	Tensile strength of track material

The diameter of the screws used in these tests was 6 mm, and screw pull-out was not a failure mode with these tests.

Unfortunately, the test setup used for this study was unable to carry web crippling loads for many of these connections; consequently web crippling results and associated conclusions were not reported. While the test setup was sufficient to allow loads to develop that caused track punch-through failure in a number of tests, the higher loads required to cause a web crippling failure often resulted in the track tearing though the fasteners that held the track to the test frame, prematurely ending the test.

2.4 Schumacher (1998)

Schumacher at al. [1998] investigated combinations of built-up members typical of jamb studs. Two sizes of stud and track, 92 mm and 152 mm, with nominal thicknesses of 0.85 mm and 1.52 mm, respectively, were used to construct six different types of test specimen configurations. These configurations included pairs of single studs and built-up 'I' sections, with or without track sections nested and screw-fastened onto to the studs. Where track was nested over the stud(s), it was kept back 5 mm from the flange of the base track. In practice, it is impossible to fasten the track to the base track using screws; since they have the same cross-section, one cannot be nested inside the other.

Connections between built-up stud members were made using #10 hex-head screws, while track nested to the stud and the stud to base track connections used #8 wafer-head screws.

The effect of fastener location attaching the track to the substrate was investigated by varying the location to either directly between studs or adjacent to the studs. The fastener locations and the different configuration of test specimens are shown in Figure 2-1.

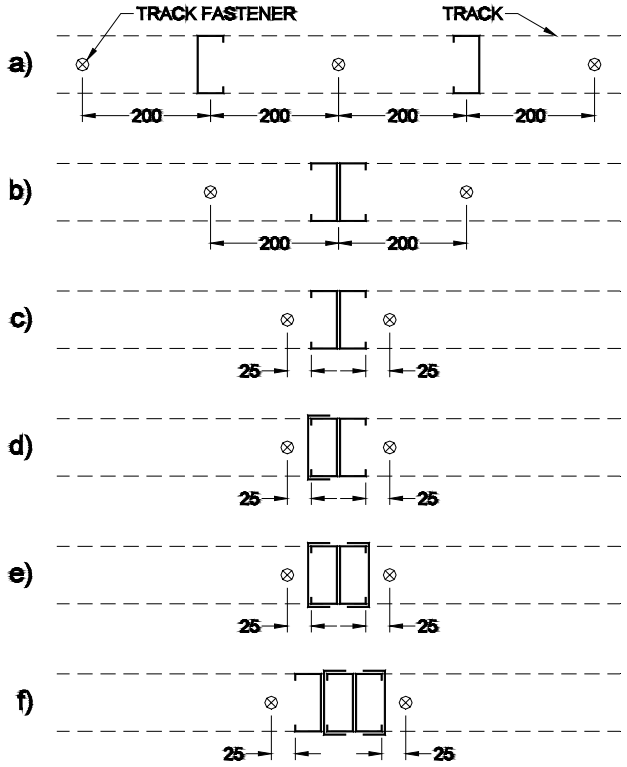

Figure 2-1: Built-up Stud Combinations with Track Fastener Locations [Schumacher et al., 1998]

The observed failure mode was typically web crippling followed by screw pullout of the compression flange (upper) screw. In most tests, the ultimate load directly preceded screw pullout.

The most noteworthy conclusions from this study were that that a single #10 screw between each stud connecting the track to the supporting frame was adequate for the lighter thickness single stud assemblies, but built-up members required a fastener at each side of the member to adequately transfer the load through the track to the supporting structure. As well, nesting track sections onto studs did not increase the strength of the connection, since the nested track could not be directly attached to the base track to transfer any shear.

2.5 Lewis (1999)

The web crippling equation used to design the stud-to-track connection was based on research into web crippling for a rigidly supported member. Lewis et al. [1999] concluded that since, in general practice, the wall track is attached to the substrate with a single fastener at intervals of up to 900 mm, it cannot be considered to be rigidly supported. The position of the fastener in the centre of the track web, as illustrated in Figure 2-2, cannot be considered to restrain the track flanges from deflecting and deforming under load.

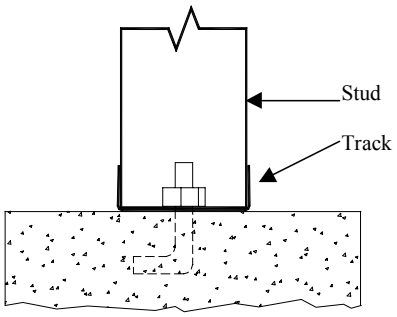

Figure 2-2: Stud-to-Track Connection

A series of end-one-flange tests on pairs of single stud-to-track connections was carried out using a single C-clamp directly between two adjacent studs to connect the track to the substrate, as shown on Figure 2-3.

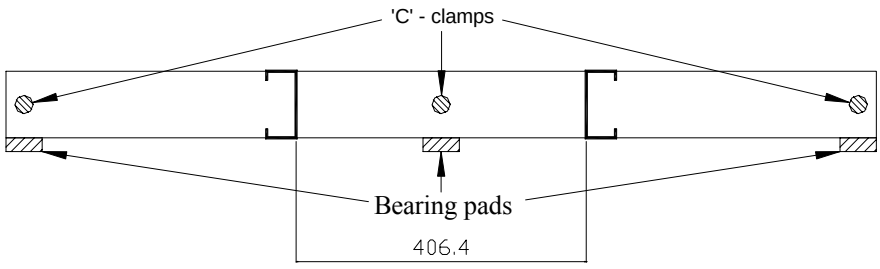

Figure 2-3: Test Apparatus--Clamping and Bearing Pad Detail

Stud and track sections with a nominal web depth of 92 mm, and standard thicknesses of 20, 18, 16, and 14 gauge (0.84 mm, 1.12 mm, 1.52 mm and 1.91 mm), were used to construct the test specimens. Each stud thickness was tested with track material of the same thickness, and with all thinner track thicknesses. The purpose of varying the stud-to-track thickness was to determine the effect on the connection behaviour of using thinner track than stud. One additional configuration was tested, incorporating a large end gap of 9.53 mm (3/8 in.), as shown on Figure 2-4. For all other specimens, the end gap was closed as tightly as possible, and the measured gap recorded.

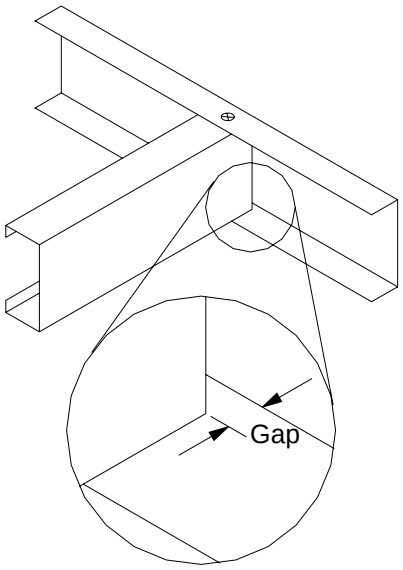

Figure 2-4: Test Procedure-Gap Measurement [Lewis 1999]

A total of 25 different assemblies were tested, and a designator system was established for ease of identification. For example, specimen **75S60T-1** is to be interpreted as follows:

‘75’ refers to the member thickness in one thousandth of an inch, i.e. 0.075 in. (1.91 mm)

‘S’ refers to the member type. In this case, it is a stud

‘60’ refers to the member thickness in one thousandth of an inch, i.e. 0.060 in. (1.52 mm)

‘T’ refers to the member type. In this case, it is a track

‘1’ refers to the test number for this series.

For specimen 36S33T-0.0375-1 & -2, the extra ‘0.375’ term refers to the large end gap built into the specimen. The test matrix and results are shown in Table 2-2.

Table 2-2: Test Results [Lewis, 1999]

Test Series	Gap (mm) Left	Gap (mm) Right	Observed Failure Mode	Load / Web (kN)
36S33T-0.375-1	9.53	9.53	Web Crippling	2.670
36S33T-0.375-2	9.53	9.53	Web Crippling	2.596
36S33T-1	1.22	1.73	Web Crippling	3.222
36S33T-2	1.52	0.94	Web Crippling	2.780
36S33T-3	1.14	1.14	Web Crippling	2.743
48S33T-1	0.76	0.86	Web Crippling	4.695
48S33T-2	0.51	0.76	Web Crippling	4.585
48S44T-1	0.76	0.64	Web Crippling	4.787
48S44T-2	1.27	1.09	Web Crippling	4.640
48S44T-3	0.86	1.02	Web Crippling	4.824
60S33T-1	0.64	1.52	Punch through	5.358
60S33T-2	1.52	1.40	Punch through	5.284
60S44T-1	1.73	0.20	Web Crippling & Punch Through	8.010
60S44T-2	1.65	1.02	Punch through	8.341
60S60T-1	0.00	1.93	Web Crippling, Excessive Deflection	8.267
60S60T-2	0.20	1.02	Web Crippling, Excessive Deflection	9.096
75S33T-1	0.10	0.20	Punch through	5.763
75S33T-2	1.78	0.51	Punch through	5.690
75S44T-1	2.03	1.35	Punch through	8.470
75S44T-2	0.64	1.65	Punch through	7.899
75S60T-1	0.51	0.10	Web Crippling	12.318
75S60T-2	0.00	0.00	Web Crippling	11.839
75S75T-2	0.00	0.00	Web Crippling, Excessive Deflection, Screw Pull-out	13.644
75S75T-3	0.91	0.51	Web Crippling	13.165

The results of this study indicated that there are two modes of failure; web crippling and track punch-through. Track punch-through occurred before the full web crippling

strength of the stud could be developed, and was a mode of failure only where the thickness of the track was less than the thickness of the stud. With the exception of the 60S44T series, for punch-through to occur, the track had to be 2 gauges thinner than the stud.

Hex-head self-drilling #10 screws for studs up to 1.52 mm thick, and #12 screws for the 1.91 mm thick studs, were used to connect the stud flanges to the track flanges. Only in the case with a 1.91 mm stud, was screw pull-out observed.

The main conclusion from this study was that to avoid a premature track punch-through failure, the track thickness must be greater than or equal to the thickness of the stud.

2.6 Fox and Schuster (2000)

In 2000 at the University of Waterloo, Fox and Schuster [2000] compiled test data for lateral load capacities of screw-attached stud-to-track connections from a variety of sources. From these tests, two different failure patterns were observed: web crippling of the stud and punch-through of the track flange.

Based on an analysis of the test data, the existing equations for nominal web crippling resistance and track punch-through failure were refined to better predict the failure capacity of screw-attached connections:

When the track thickness was greater than or equal to that of the stud thickness, end-one-flange web crippling of a C-section stud controlled, resulting in the nominal web crippling resistance as expressed in Eq. 2.2:

$$P_n = Ct_s^2 F_{ys}\left(1 - C_R\sqrt{R}\right)\left(1 + C_N\sqrt{N}\right)\left(1 - C_H\sqrt{H}\right) \qquad (2.2)$$

Where:

C = Web crippling coefficient = 5.6
C_R = Inside bend radius coefficient = 0.14
C_N = Bearing length coefficient = 0.30
C_H = Web slenderness coefficient = 0.01
F_{ys} = Yield strength of stud material
H = h/t_s
h = Flat dimension of stud web measured in plane of web
N = n/t_s
n = Stud bearing length
R = r/t_s
r = Stud inside bend radius
t_s = Stud thickness

When the track thickness was less than the stud thickness, punch-through shear failure of the track controlled, resulting in the nominal punch-through resistance as expressed in Eq. 2.3:

$$P_n = 0.7 t_t w_b F_{ut} \tag{2.3}$$

Where:

F_{ut} = Ultimate strength of track material
t_t = Track thickness
w_b = Track shear width
= $(20t_t + 14)$ in mm
= $(20t_t + 0.56)$ in inches

2.7 Daudet (2001)

Pilot tests were undertaken at Dietrich Industries where the stud-to-track connection was located at the end of the track, such as at an opening of a doorway. Daudet [2001] reported that for these connections, web crippling of the stud appeared to be the governing mode of failure, and that the connection strength was about one half the value predicted by using the method outlined by Fox and Schuster [2000].

2.8 Bolte (2003)

An experimental investigation was conducted at the University Of Missouri-Rolla by Bolte [2003] to determine the lateral load capacity of two stud-to-track connections found in wind load bearing cold-formed steel stud walls. The capacities of both deflection-track and screw-attached track connections typically found in curtain wall systems were examined.

Data from both this study and from Fox and Schuster [2000] were analyzed, and the following equation was developed to predict the nominal stud-to-track connection resistance, P_{nst}, where the connection is not adjacent to wall openings and where the track thickness is greater than or equal to the stud thickness:

$$P_{nst} = P_n + \Delta P_{not} \tag{2.4}$$

Where:

Δ = 0.756
P_n = Web crippling capacity in accordance with Section C3.4.1 of the AISI Specification (2001) for end-one-flange loading
P_{nst} = Nominal strength for the stud to track connection when subjected to transverse loads
P_{not} = Screw pull-out capacity in accordance with Section E4.4.1 of the AISI Specification (2001)

The original research report should be consulted for a listing and explanation of the parameters within which this equation is valid.

2.9 NASPEC (2007)

The North American Specification for the Design of Cold-Formed Steel Structural Members (NASPEC) [AISI 2007a, CSA 2007] does not give a design equation specifically for stud-to-track assemblies. Instead, the capacity of the screw-attached stud-to-track

connection is calculated based upon the nominal web crippling strength of the wall stud acting alone using the following equation.

$$P_n = Ct^2 F_y \sin\theta \left(1 - C_R\sqrt{\frac{R}{t}}\right)\left(1 + C_N\sqrt{\frac{N}{t}}\right)\left(1 - C_h\sqrt{\frac{h}{t}}\right) \quad (2.5)$$

Where:

P_n	=	Nominal web crippling strength
C	=	Web crippling coefficient (see Table 2-3)
C_h	=	Web slenderness coefficient (see Table 2-3)
C_N	=	Bearing length coefficient (see Table 2-3)
C_R	=	Inside bend radius coefficient (see Table 2-3)
F_y	=	Yield strength of stud material
h	=	Flat dimension of stud web measured in plane of web
N	=	Bearing length
R	=	Stud inside bend radius
t	=	Stud web thickness
θ	=	Angle between plane of web and plane of bearing surface, $45° < \theta \leq 90°$

Table 2-3: Web Crippling Coefficients, NASPEC (2007)

	C	**C_R**	**C_N**	**C_h**
Single Web Channel & C-Sections	4	0.14	0.35	0.02
Built-up Sections	10	0.14	0.28	0.001

P_n represents the nominal web crippling strength of a load or end reaction for one solid web element. The coefficients for screw-attached stud-to-track connections are based upon an end-one-flange loading case with stiffened or partially stiffened flanges fastened to the support, and are given in Table 2-3.

2.10 WSD (2007)

The North American Standard for Cold-Formed Steel Framing – Wall Stud Design (WSD) [AISI 2007b] does provide design equations specifically for curtain wall stud-to-track assemblies. In all cases, this document requires the designer to first check that the stud-to-track connection satisfies the web crippling strength of the stud, according to Section C3.4 of the NASPEC, and that the maximum gap between the end of the stud and the web of the track be less than 6.35 mm (1/4 in.).

For cases where the connection is not adjacent to a wall opening, both stud flanges are connected to both track flanges, and the track thickness is greater than or equal to the stud thickness, the following web crippling equation is used:

$$P_{nst} = Ct^2 F_y \left(1 - C_R\sqrt{\frac{R}{t}}\right)\left(1 + C_N\sqrt{\frac{N}{t}}\right)\left(1 - C_h\sqrt{\frac{h}{t}}\right) \qquad (2.6)$$

Where:

C	=	Web crippling coefficient = 3.7
C_R	=	Inside bend radius coefficient = 0.19
C_N	=	Bearing length coefficient = 0.74
C_h	=	Web slenderness coefficient = 0.019
R	=	Stud inside bend radius
N	=	Stud Bearing Length
h	=	depth of flat portion of stud measured along plane of web
t	=	Stud thickness
F_y	=	Yield strength of stud material
P_{nst}	=	Nominal strength of stud-to-track connection when subjected to transverse loads

For cases where the connection is not adjacent to a wall opening, both stud flanges are connected to both track flanges, but the track thickness is less than the stud thickness, the following track punch-through equation is used:

$$P_{nst} = 0.6 t_t w_{st} F_{ut} \quad (2.7)$$

Where:

t_t = Design track thickness
w_{st} = $20\ t_t + 0.56\alpha$
α = Coefficient for conversion of units
= 1.0 when t_t is in inches
= 25.4 when t_t is in mm
F_{ut} = Tensile (ultimate) strength of track
P_{nst} = Nominal strength of stud-to-track connection when subjected to transverse loads

For cases where the connection is adjacent to a wall opening, both stud flanges are connected to both track flanges, and the track terminates at the opening, the nominal resistance shall be taken as $0.5P_{nst}$, calculated using one of the equations above, depending on the ratio of track to stud thickness. The adoption of the $0.5P_{nst}$ factor at end-of-track locations is based on the results of the study by Daudet [2001].

For cases where both stud flanges are not attached to both track flanges, this standard offers two more methods for calculating stud-to-track connection resistance. Where the connection is not adjacent to a wall opening, and the track thickness is greater than or equal to the stud thickness, P_{nst} is set equal to P_n as calculated by using Section C3.4 of the NASPEC. In those cases where the connection is adjacent to a wall opening, and the track thickness is greater than or equal to the stud thickness, P_{nst} is set equal to $0.5P_n$ as calculated by using Section C3.4 of the NASPEC.

Chapter 3
Experimental Investigation

3.1 Experimental Parameters

The parameters that were varied in the test program consisted of the stud and track thickness, stud and track web depth, screw size, screw location, and the location and configuration of the studs in the test samples. These parameters are described in more detail in the following sections.

3.1.1 Mechanical Properties

For each type of section (i.e. stud and track) three tensile coupons were taken from the web elements for the determination of the mechanical properties. The coupon specimens were tested according to the American Standard of Testing and Materials A370 [ASTM 2005]. The galvanized coating was removed from the specimens using a solution of hydrochloric acid and water to allow for measurement of the base steel thickness. Listed in Table A-1 of Appendix A are the mechanical properties for each specimen tested.

3.1.2 Stud and Track Sizes

The test specimens used in this study were constructed of C-shaped stud and track sections as illustrated in Figure 3-1. Listed in Table B-1 of Appendix B are the web depth, flange length, lip length, inside bend radius at the flange-web junction and base steel thickness of the stud and track specimens used in each of the test assemblies.

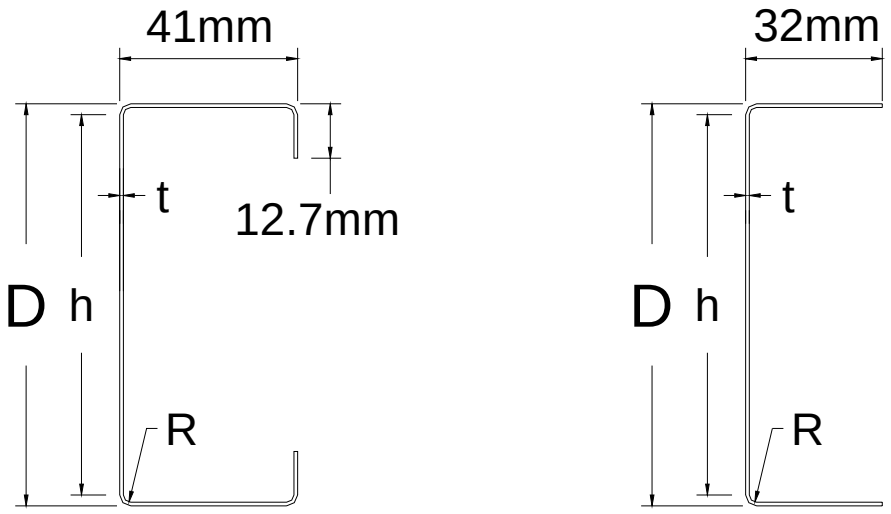

Figure 3-1: Geometric Section Parameters

To limit the number of test specimen configurations, various combinations of stud and track thicknesses were considered and reviewed. In earlier tests with single studs, it was discovered that when the track thickness was as thick, or thicker, than the stud, the failure mode was web crippling of the stud [Fox and Schuster 2000]. Since the web crippling failure mode is not dependent on the thickness of the track, it was decided that test combinations with the track thicker than the studs was unnecessary. Fox and Schuster also found that track punch-through by a single stud did not occur when the thickness of the track was at least as thick as the stud. It is common practice for load bearing stud applications to specify the thickness of the stud and track to be the same. Therefore, based on these considerations it was decided to test only combinations of stud and track with equal nominal thickness.

The standard thicknesses for steel stud framing in Canada at the time of testing were as follows:

- 0.84 mm (33 mil, 20 gauge);

- 1.12 mm (44 mil, 18 gauge);
- 1.52 mm (60 mil, 16 gauge); and,
- 1.91 mm (75 mil, 14 gauge).

Test assemblies were constructed with stud and track sections in all four sizes.

The web crippling capacity of a member is partly a function of the slenderness of the member's web (web depth divided by the thickness). Consequently, the strength of the stud-to-track connection is also partly a function of the depth of the stud. The most common sizes of studs are 92 mm and 152 mm deep, although the 203 mm deep sections may sometimes be necessary in higher walls. A decision was made to limit the web depths of the test specimens to 92 mm and 152 mm, which represent the majority of the sizes used in practice, and also reduced the number of assembly combinations. Of the 152 mm sections tested, only the toe-to-toe configuration was tested.

Stud sections can also be manufactured with varying flange widths to meet certain structural requirements, with flange widths from 32 mm to 76 mm. Since the primary failure modes that occur in these stud-to-track connections are web crippling and track punch-through, neither of which are a function of the flange width, it was decided to limit the test assemblies to only the 41 mm stud flange width, and to the standard 32 mm track flange width.

3.1.3 Built-Up Jamb Studs at an Interior Track Location

Framing an opening in a wall for a window usually requires leaving a solid surface at the jambs for the attachment of the window itself. To save time and material, framers prefer

using jamb studs in a toe-to-toe configuration to eliminate the need for an additional track section to close the opening. However, in some cases due to the strength requirements or the framing methods, jamb studs will be connected back-to-back. This configuration makes it easier to connect the members together to act as a built-up section, but does require an additional piece of track to close off the opening. Illustrated in Figure 3-2 are two jamb configurations at a window opening showing the studs framing into a bottom wall track that is continuous past the jamb.

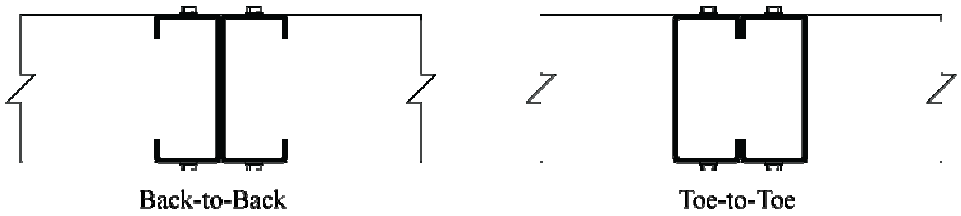

Figure 3-2: Jamb Studs at Interior Location

When the jamb is made from back-to-back members, a piece of track is added to the inside stud to provide a solid surface in the opening required for the installation of the door or window. This track may be continuous along the length of the jamb stud, but is cut short at the top and bottom since a track section cannot frame into another track section as a stud can do. Consequently, while the track adds to the flexural strength of the jamb, since it is not connected to the top and bottom wall track, the jamb track does not transfer any shear at the ends. The entire reaction at each end of the jamb is taken through the members that frame into the top and bottom wall track, specifically the studs. Even though it is common for a built-up jamb to include track sections, these members do not contribute to the strength of the jamb stud-to-track connection and so were not included in this test program.

3.1.4 Built-Up Jamb Studs at a Track End Location

In a similar manner to window framing, the built-up jambs at a doorway can also be configured in toe-to-toe or back-to-back shapes, but in a door opening the bottom wall track terminates at the jamb stud. Given that the bottom track is no longer continuous, the strength of the stud-to-track connection will be affected. Illustrated in Figure 3-3 are the configurations of jamb studs at a door opening that were tested. In addition to the built-up configuration, two configurations of single member were also tested.

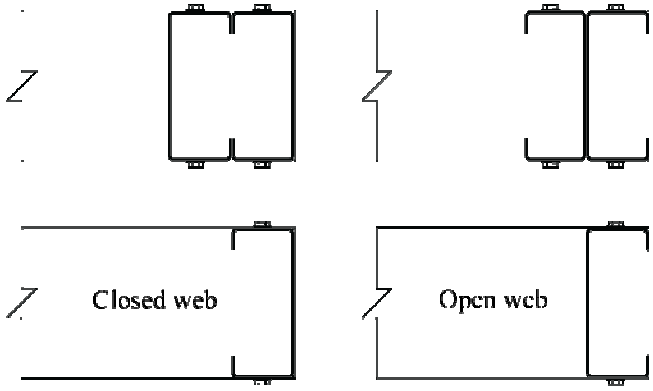

Figure 3-3: Jamb Studs at End Location

3.1.5 Screw Size and Location

Standard practice for steel stud framing is to use self drilling screws to connect both flanges of the stud to the track into which it frames, and the minimum size (diameter) for these screws is a #8. For some of the thicker steel sections, a #8 screw is not recommended since the diameter is too small and it can shear off as it is being installed. To avoid this limitation, most of the tests in this program used #10 screws to make the connections. A

series of tests were carried out with #8 and #12 screws to investigate whether the screw size does affect the strength of the connection.

In practice, it may be possible to find installations where the screws had been inadvertently omitted from one side of the stud or the other. Without the screws connecting both flanges of the stud to the track, the load transfer within the connection will be different and the ultimate strength may change. A series of tests were carried out where screws were only installed in one flange of the stud. Illustrated in Figure 4 are the test configurations that were used to investigate the various screw sizes and placements.

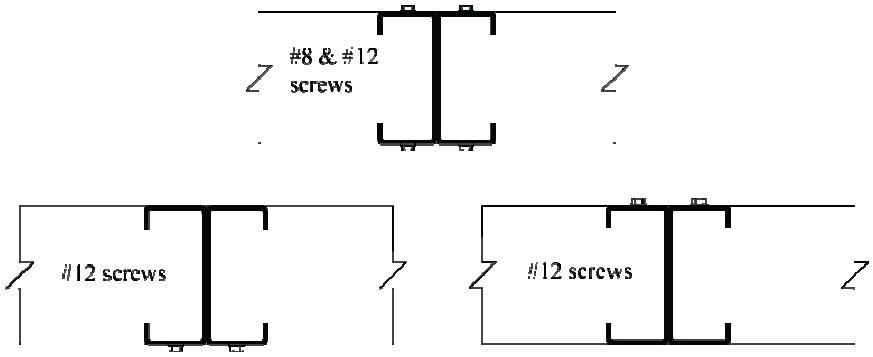

Figure 3-4: Test Configurations with Different Screw Size and Placements

3.2 Test Specimen Designation

Listed in Table B-2 of Appendix B are all the test specimen configurations, with the screw size and location, stud designation and track designation. The designation system used to define the test specimen can be illustrated by the following example:

Test specimen **TS4-33-1**

where,

TS4 = refers to “Test Series 4” which is a specific configuration of stud size, orientation and location in the track (TS1 through TS12)

33 = Nominal steel thickness in mils (33, 44, 60 or 75 mil)

1 = Test number in that series (usually 1 or 2)

The stud and track designations provided in Table B-2 follow the designation system illustrated by the following example:

Stud size **362S162-44**

where,

362 = Web depth (in 1/100 of an inch)

S = “S” for stud and “T” for track

162 = Flange width (in 1/00 of an inch)

44 = Minimum base steel thickness (in mils or 1/000 of an inch)

Even though the designation system is based on Imperial units, the same designator was used to describe the metric sections, which was done to standardize the designation system throughout North America.

3.3 Test Setup

The test setup involved conducting a series of single point loading tests on simply supported built-up jamb assemblies. The jamb studs were cut to 1220 mm lengths and connected in the toe-to-toe or back-to-back configuration. For the single stud tests, the single stud was reinforced with a second stud, but the end of the reinforcing stud was kept back 152 mm from the track, and the single jamb stud made the stud-to-track connection.

To prevent a flexural failure or a web crippling failure of the jamb stud at the point of applied load, the assemblies were reinforced with additional pieces of track. The track into

which the jamb studs framed was bolted to an 8 mm thick steel angle with two 12.7 mm steel bolts and 25 mm washers, spaced no more than 152 mm apart, with a bolt on either side of the stud-to-track connection. Connecting the track to the supporting structure in this manner avoided potential flexural failure of the track or failure of the track-to-structure connectors.

The unconnected end of the test specimen was supported on a load cell, making the specimen statically determinate. The readings from this load cell subtracted from the load cell measuring the total applied load gave an accurate reading of the load at the stud-to-track connection. The photograph in Figure 4-5 and the sketch in Figure 4-6 illustrate the test setup.

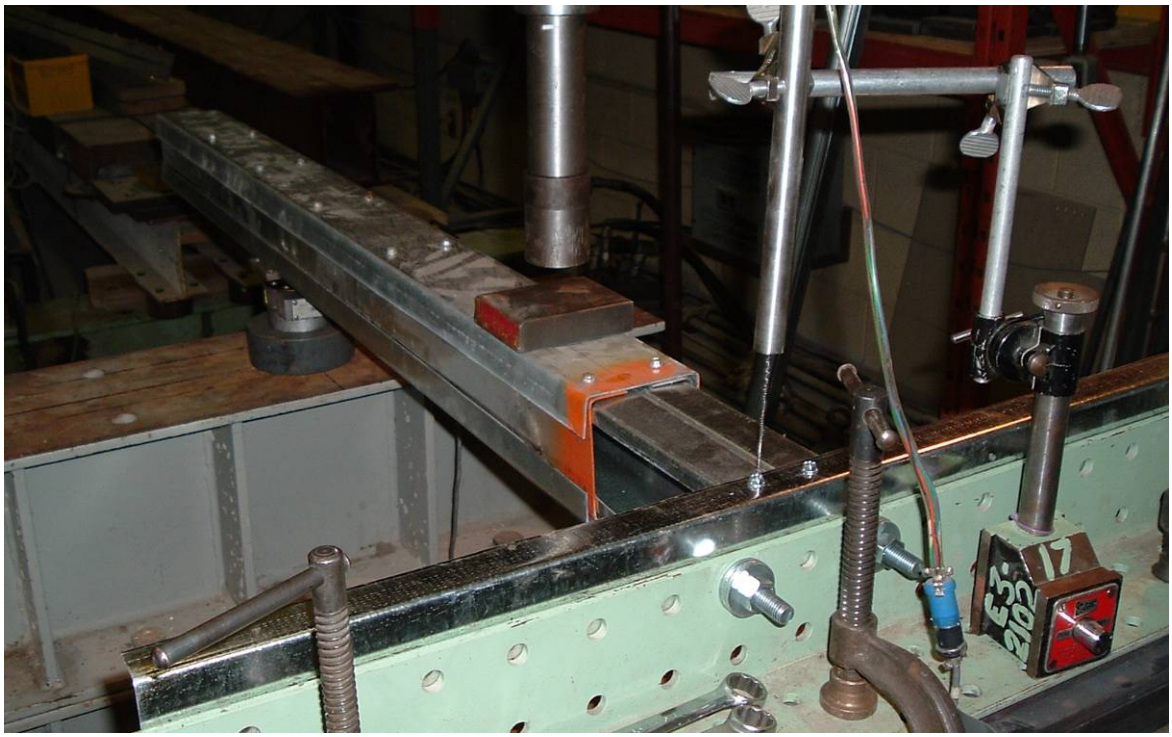

Figure 3-5: Photograph of a Typical Test Setup

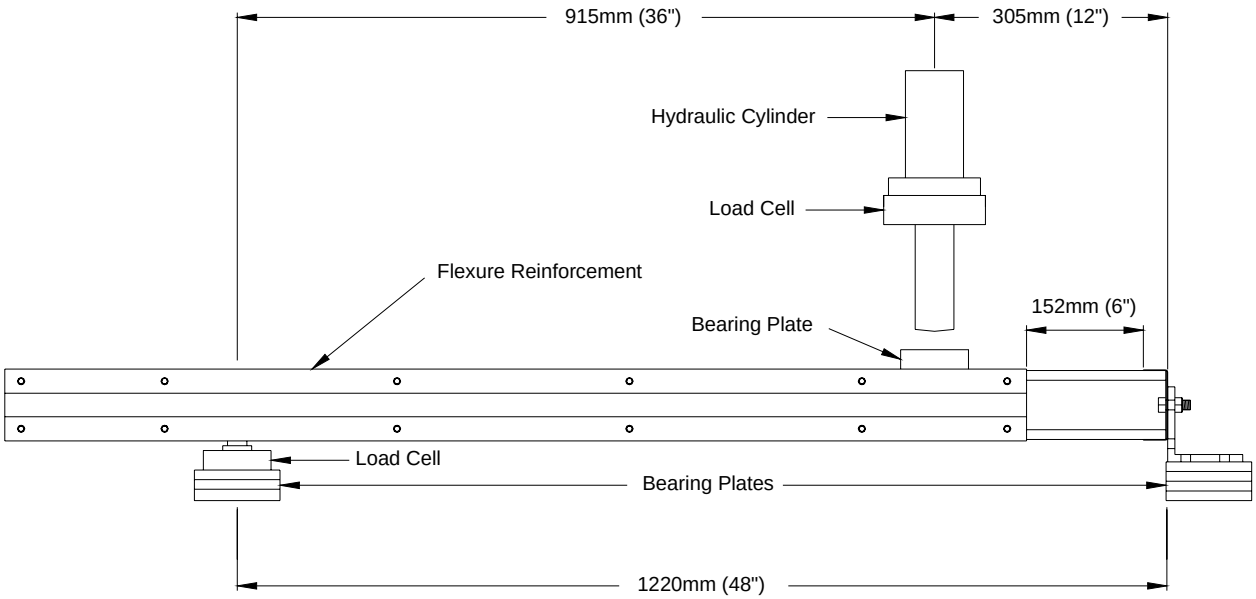

Figure 3-6: Schematic of a Typical Test Setup

3.4 Test Procedure

To maximize the load acting on the connection, the concentrated load was applied one foot from the stud-to-track connection. The ultimate failure load was recorded when the test specimen was no longer capable of carrying an increase in load. In addition to recording the ultimate failure load, an effort was made to record the onset of web crippling, and to record other failure modes as they occurred. For example, as some specimens started to fail in web crippling, track punch-through began, and then screw failure occurred, effectively ending the test. The various failure modes were noted, and the applied load was also recorded, whenever possible, at the onset of each mode.

The test setup was not appropriate to assess the track displacement, nor was that the intent of these tests; however, to qualify the failure modes, it was decided to record the displacement of the connection itself. Excessive displacement or deformation of the

connection was considered a failure mode. The displacement data was obtained by placing a low-voltage displacement transducer (LVDT) directly above the junction of the stud and track connection (shown in Figure 3-5).

Due to faulty equipment with some tests, some of the load-displacement curves are discontinuous (caused by the LVDT sticking) or are erratic (caused by signal noise). The data acquisition system was unable to incorporate a real-time load-displacement monitor, and so these problems were not detected until the test data was analyzed at a later date.

Chapter 4
Test Results

4.1 Failure Modes

The predominant failure mode observed was web crippling (WC), often with excessive deformation (Def) at the stud-track connection. Other observed failure modes were track punch-through (PT), failure of the screw or screws themselves, and screw pull-out (SPU). Where the connection failed due to failure of the screw(s), failure appeared to be a shear failure (SS), a tension failure (ST), or a combined failure between the two modes.

4.1.1 Web Crippling

Web crippling is the local crushing of the web of a flexural member at a location of a concentrated load. Web crippling of the stud was the most common failure mode observed in this test program and occurred in all cases where studs were paired toe-to-toe, or when single stud configurations were tested. Web crippling also occurred in almost half of the cases where the studs were paired back-to-back and had one fastener in each of the top and bottom flanges. In fact, web crippling occurred in 62 of the 94 assemblies tested.

At interior locations, the toe-to-toe configuration was found to have roughly the same web crippling resistance as the back-to-back configuration, stud webs being equal. Specimens with 152 mm deep webs resulted in a lower web crippling resistance than the equivalent assemblies made with 92 mm deep webs, as would be expected based on the current NASPEC web crippling equations.

At end locations, the back-to-back configuration was significantly stronger than the toe-to-toe arrangement. This behaviour was reflected in the improved performance of single-stud specimens in the (open web) configuration, i.e. where the stud web is not adjacent to the end of the track as illustrated in Figure 3-3. End single stud (closed web) specimens had a lower web crippling resistance than (open web) specimens because the load transfer through the stud web acted right at the end of the unsupported track flange.

Web crippling was often accompanied by excessive deformations of the connection due to the collapse of the stud web under load. The initial load transfer from the stud to the track within the connection was by bearing of the stud on the track flange with minimal deformation. After web crippling occurred, the deformation of the connection started to be restrained by the screw connecting the top flange of the stud to the top flange of the track. This load re-distribution can lead to an increased load resistance beyond the stud web crippling limit until some other failure mode (e.g. screw pull-out) occurs.

Illustrated in Figure 4-1 is a typical web crippling failure of specimen TS3-44-1 with a 152 mm stud depth. Shown in Figure 4-2 are the load vs. displacement curves for both TS3-44-1 and TS3-44-2 tests, showing the characteristic peaks in the load associated with web crippling. Load vs. displacement curves for all of the tests are provided in Appendix D.

The photograph shown in Figure 4-1 and the load vs. displacement plot in Figure 4-2 illustrate the amount of deformation that can be associated with a web crippling failure. In these cases, the web crippling failure load can clearly be determined. After this point, any increased load that the connection may carry, due to load redistribution within the

connection, comes at the cost of high degrees of deformation, was not considered to be useable. In general practice, there is a serviceability limit of 3 mm (1/8 in.) of deflection at the stud-to-track connection. In addition to the more common issues related to excessive deflection, such as cracking of finishes, too much deflection at a jamb-stud location could prevent the proper operation of windows and doors. In this case, excessive deflection would be a limit state on safety rather than serviceability. To illustrate the relationship of this limit state to the other failure modes discussed, a vertical asymptote has been added to each of the load vs. displacement plots where displacement equals 3 mm, as shown on Figure 4-2.

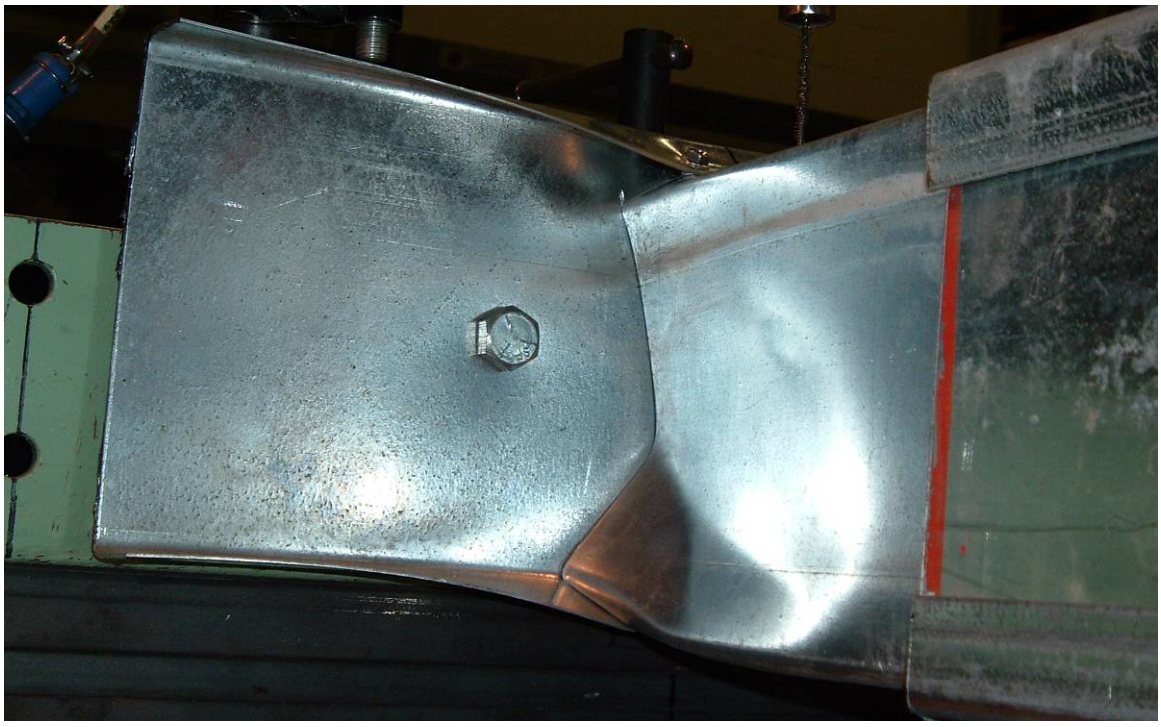

Figure 4-1: Typical Web Crippling Failure (Specimen TS3-44-1)

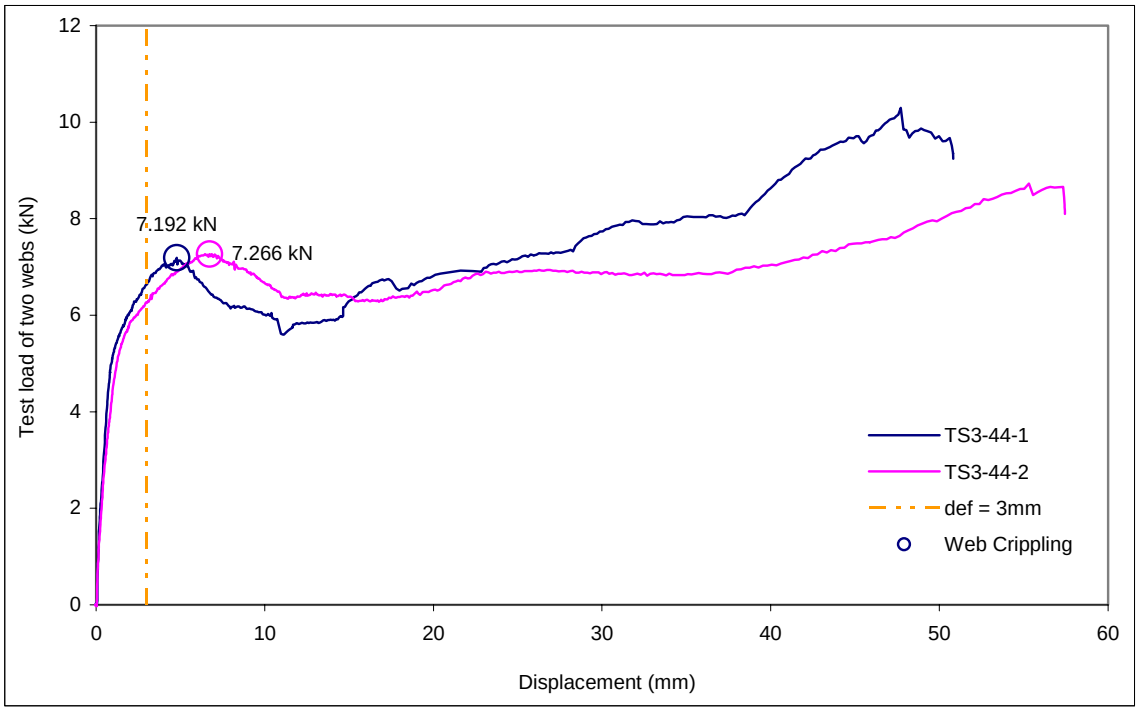

Figure 4-2: Test Load vs. Displacement (TS3-44 Test Series)

4.1.2 Track Punch-through

Track punch-through happens when the corner of the jamb stud shears through the track flange at the end of the member. This causes a rupture of the track in a line parallel to the member length at the stud to flange corner radius. This mode occurs most often when the studs are thicker than the track (or when the studs are back-to-back) and/or when the web crippling of the stud does not happen.

Punch-through occurred in all back-to-back configurations, interior and end, where there were fasteners in both the top and bottom flanges. With one exception for test TS5-44-2, the punch-through failures only occurred in material 1.52 mm and 1.91 mm (60 and 75 mil) thick: in the thinner sections stud web crippling was the failure mode.

For test series TS11 where only one #12 screw was used in the lower flange to connect the stud and track, only one specimen, using 1.12 mm thick material, did not fail in track punch-through. Without the screw in the top flange, all of the load transfer in the connection was through bearing under the end of the stud, increasing the likelihood of a punch-through failure. It is of interest to note that the punch-through loads for specimen TS10, which had one fastener in each of the top and bottom flanges, was noticeably higher than the punch-through load for specimen TS11, which only had one screw in the bottom flange. This confirms the importance of the load transfer that occurs between the stud and the track through the top screw.

Test series TS5 was a back-to-back configuration at an end location, and even though the track was unrestrained at the end, the stud web punched through the track with little or no web crippling. The load vs. displacement curves in Figure 4-4 show a small peak when the studs punched through the web, followed by an increase in displacement with no increase in load resistance.

The photograph in Figure 4-3 shows a punch-through failure of a 92 mm stud from test TS5-44-2. Shown in Figure 4-4 are the load vs. displacement curves for both specimens TS5-44-1 and TS5-44-2. With this particular test configuration, one of the two tests failed in track punch-through, whereas the second test failed in web crippling.

Figure 4-3: Photograph of Track Punch-Through (Specimen TS5-44-2)

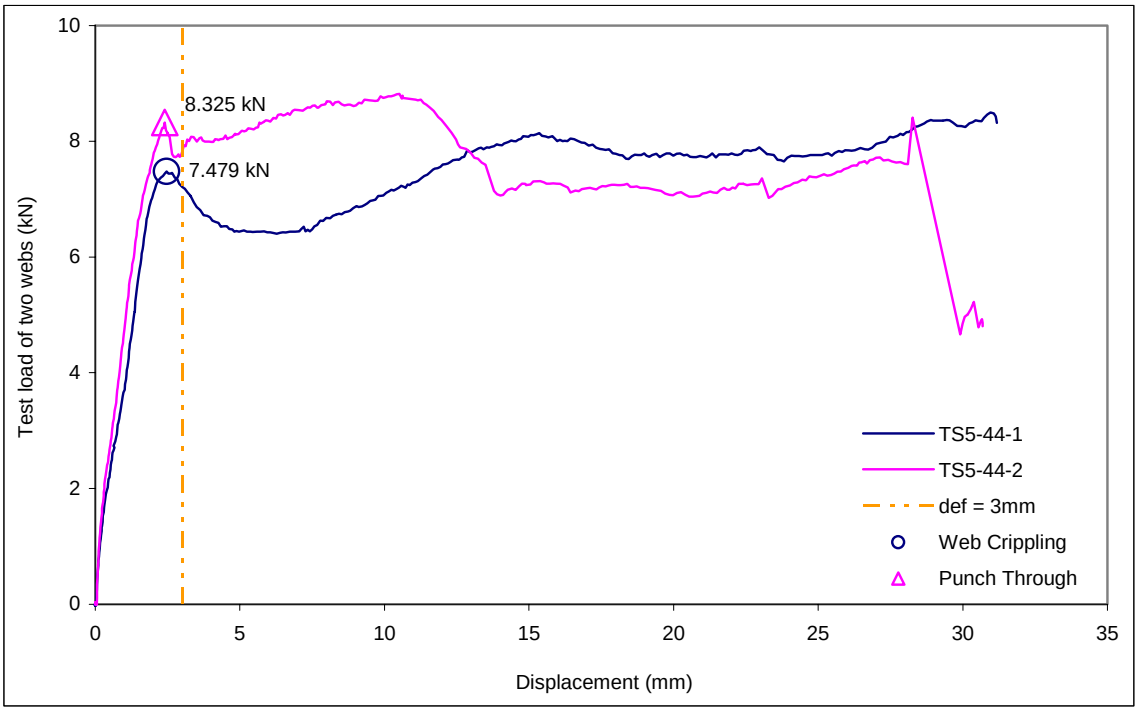

Figure 4-4: Test Load vs. Displacement (TS5-44 Test Series)

4.1.3 Displacement

Two types of excessive displacements were observed: due to web crippling of the stud, and due to track deformation. The photograph in Figure 4-1 shows a web crippling failure where the deformation is associated with a combination of the collapse of the stud web and the bending of the track flanges. The other type of deformation failure is illustrated in the photograph in Figure 4-5 where the stud web is intact but the track web is actually being rolled over.

Displacement of the stud-to-track connection was not considered to be a failure limit state: the load at the point of equivalent web crippling or track punch-through failure was taken to be the failure load for all tests (how this load is determined is discussed in Chapter 5). Although these connections could be capable of carrying an increased load, it was decided that displacements in excess of 12.7 mm would be unacceptable from a serviceability limit state perspective. Consequently, for tests that exhibited these large deformations, the failure load was taken from the load-displacement plot at some defined discontinuity in the curve at a displacement in the order of 3 mm to 5 mm.

The load vs. displacement curves of both TS4-33-1 and TS4-33-2 tests are shown in Figure 4-6. With test TS4-33-1 the displacement reached a value close to 25 mm, at which time the stud web had not yet crippled, and the load was still increasing. At this degree of deformation the members came in contact with the testing equipment, (i.e. the stud flange was bearing on a mounting bolt), at which point the test was stopped. The equivalent web crippling failure loads for these two tests are indicated on Figure 4-6.

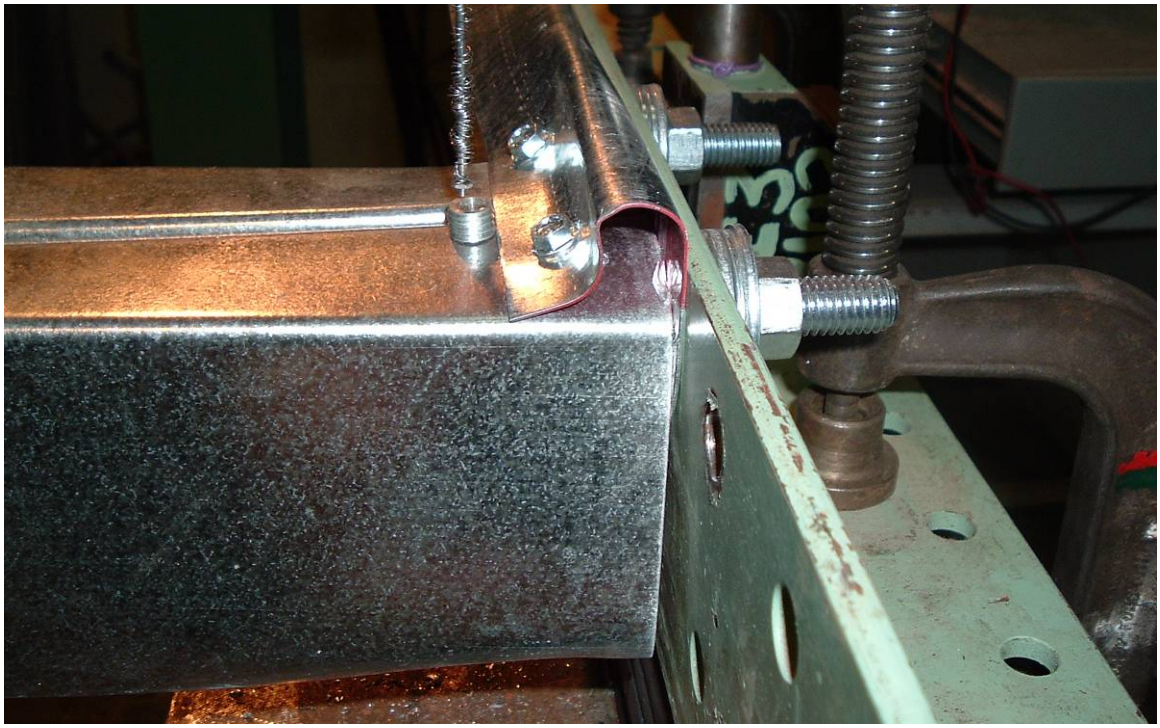

Figure 4-5: Photograph of Excessive Track Displacement (Specimen TS4-33-1)

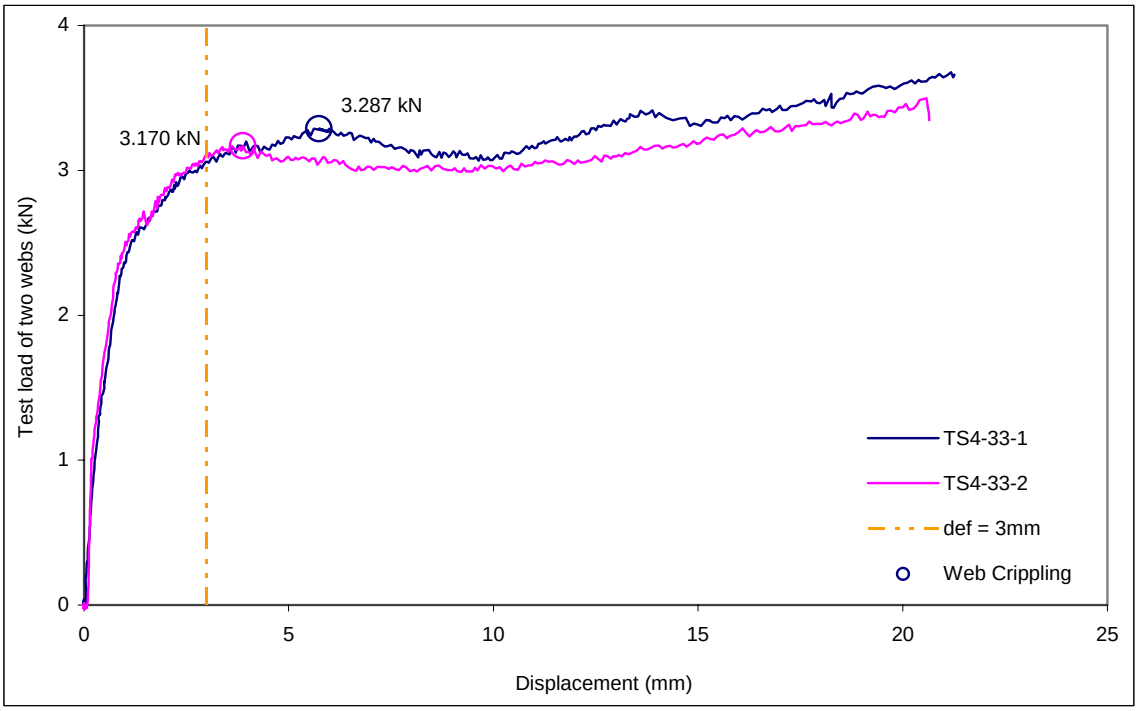

Figure 4-6: Test Load vs. Displacement (TS4-33 Test Series)

4.1.4 Screw Pull-out

Of the three screw failure modes reported herein, screw pullout was the easiest to characterize, and always occurred in conjunction with web crippling and/or excessive displacement. The assembly does not lose its ability to carry an increased load until the screw has pulled out, as is shown in Figure 4-7. The load-displacement curves in Figure 4-8 do not have the characteristic web crippling peak as shown in Figure 3.2, but there is a definite decrease in slope/stiffness after the onset of web crippling.

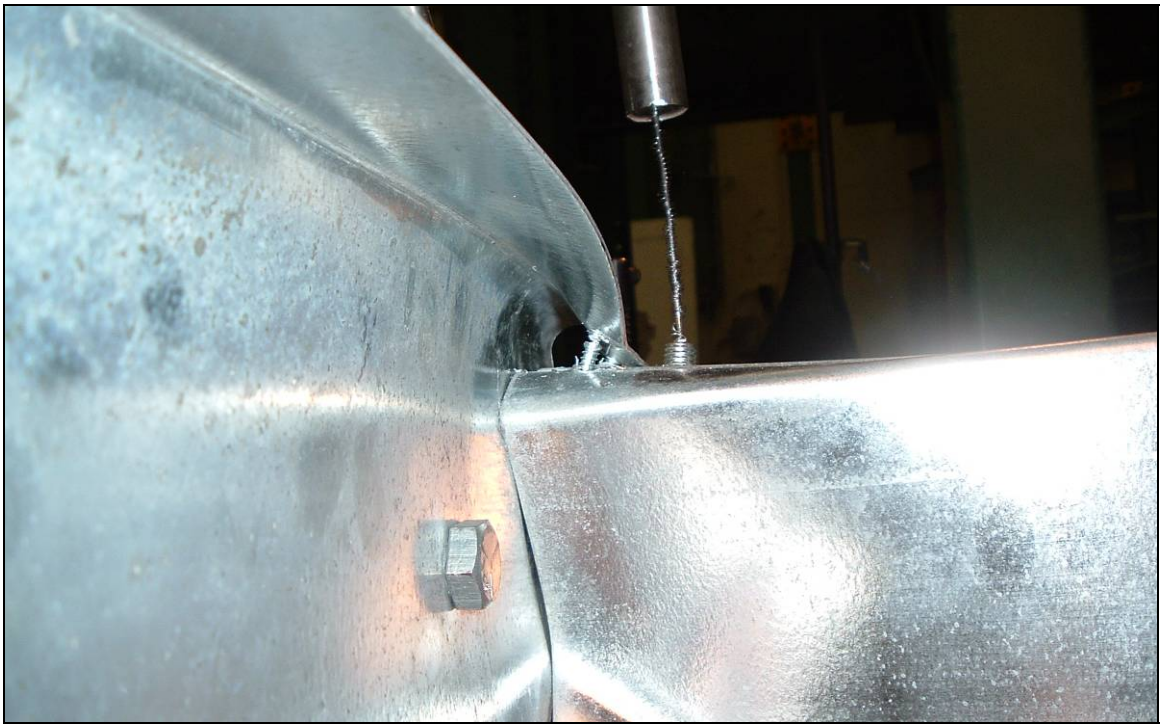

Figure 4-7: Photograph of Screw Pull-out after Web Crippling (Specimen TS6-60-2)

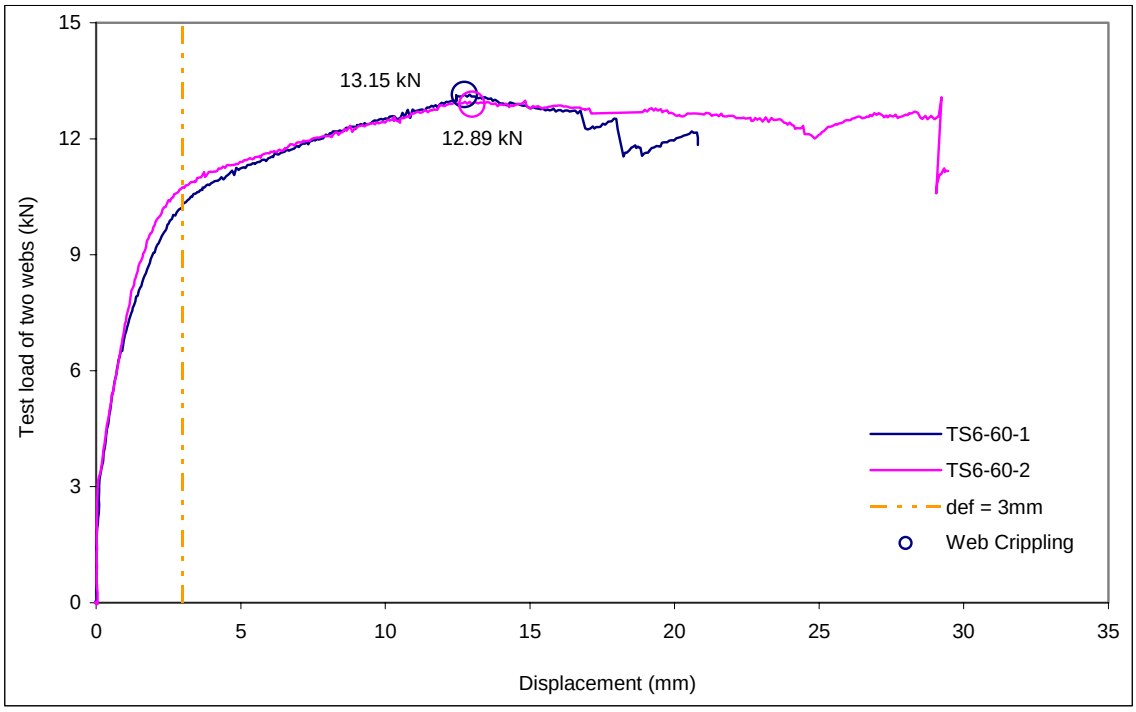

Figure 4-8: Test Load vs. Displacement (TS6-60 Test Series)

4.1.5 Screw Shear and Tension

Failure of the screws in tension and failure of the screws in shear are two different failure modes, but in the absence of any data analysis, it is difficult to make an accurate assessment as to which failure was observed. Generally, if there was no lateral movement of the screw holes relative to one another directly after the screw failed, the failure was assumed to be a tension failure. The rationale was that if shear were the failure mode, there would be an immediate lateral displacement of one hole relative to the other as soon as the screw failed. With all 94 tests, only three tests failed in this manner. Next to track punch-through, screw shear was the most frequent failure mode. Shown in Figure 4-9 is a photograph of test TS2-75-2, where the deflecting stud sheared through the screws. The load-displacement curve for test TS2-75-1 shown in Figure 4-10 drops suddenly at 9 mm displacement when

one screw failed, but continued to pick up load until the abrupt failure near 13 mm of defection when the remaining screw failed. Marks on the track shown in Figure 4-9 indicate where the stud gouged through the galvanizing as it moved relative to the track in a shearing action.

By way of comparison, the two halves of the screw shown in Figure 4-11 are in relatively close proximity, indicating that this screw may have failed in tension. The load-displacement curves in Figure 4-12 are similar to those in Figure 4-10, but the slope decreases more before the sudden failure.

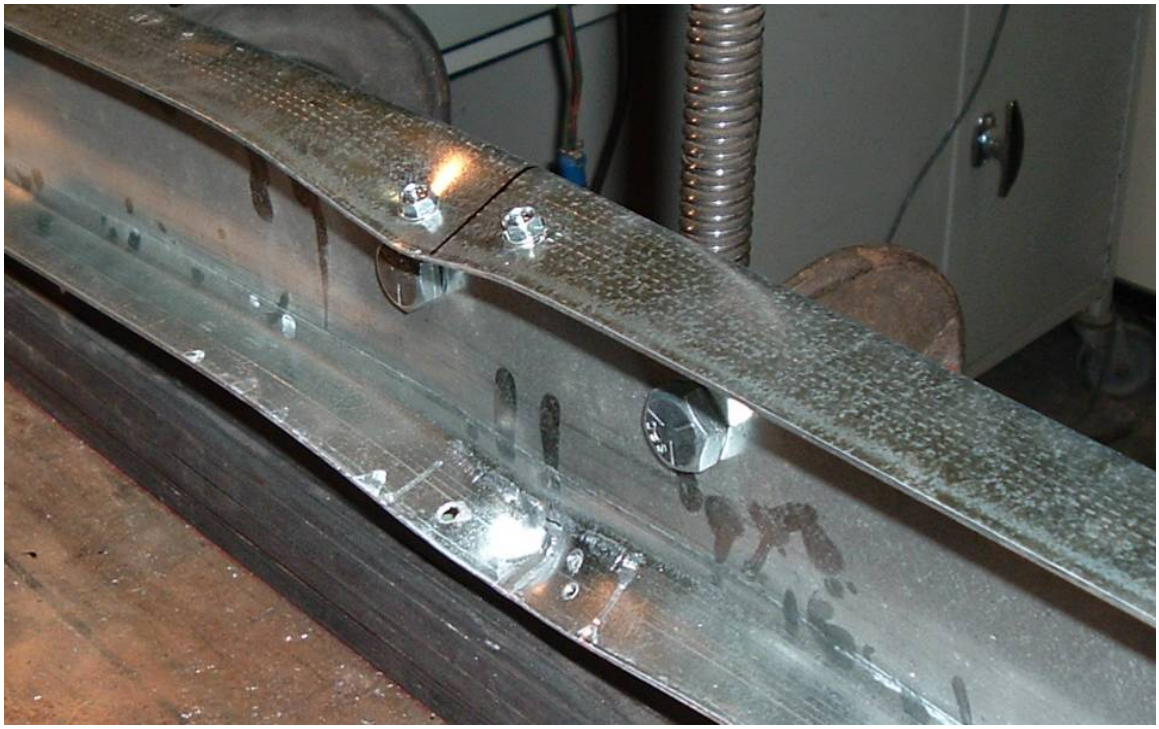

Figure 4-9: Photograph of Screw Shear Failure (Specimen TS2-75-2)

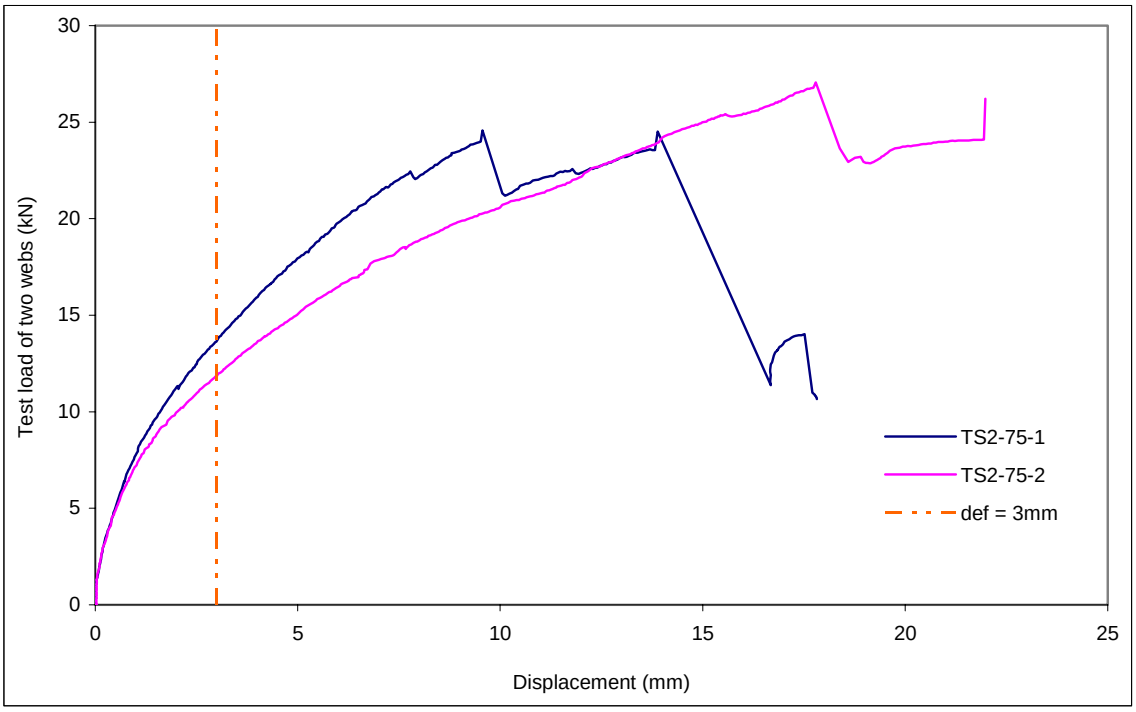

Figure 4-10: Test Load vs. Displacement (TS2-75 Test Series)

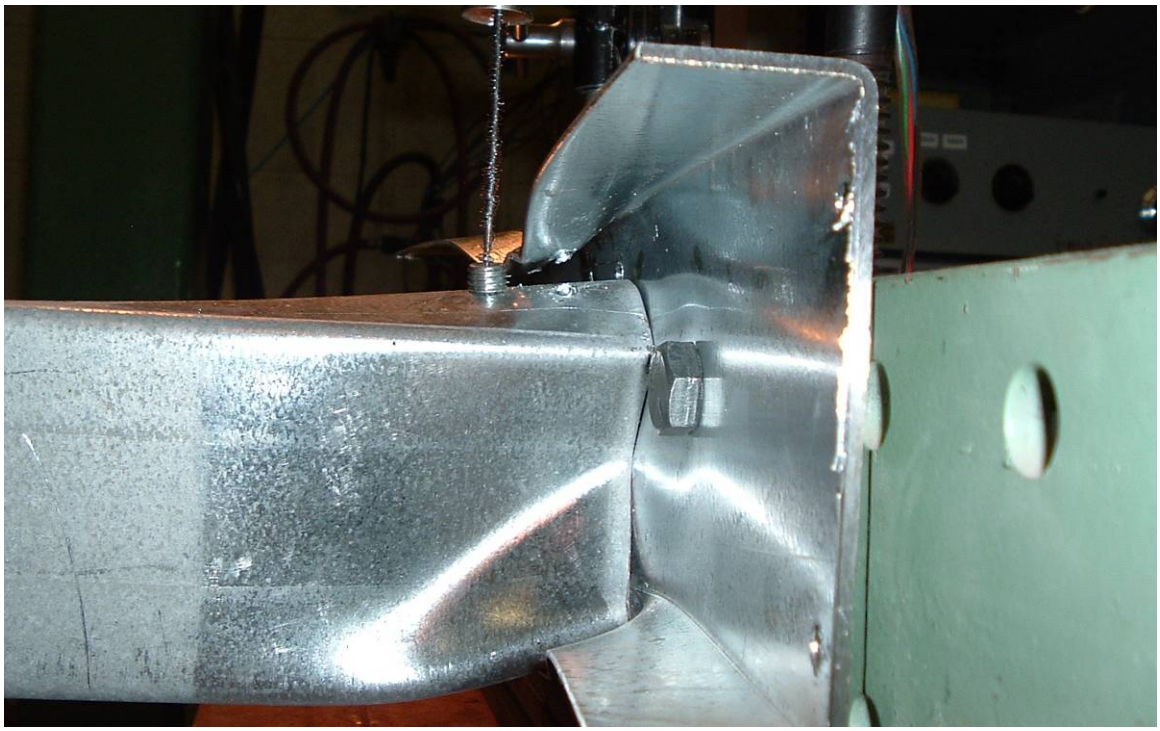

Figure 4-11: Web Crippling with Screw Tension Failure (Specimen TS1-75-2)

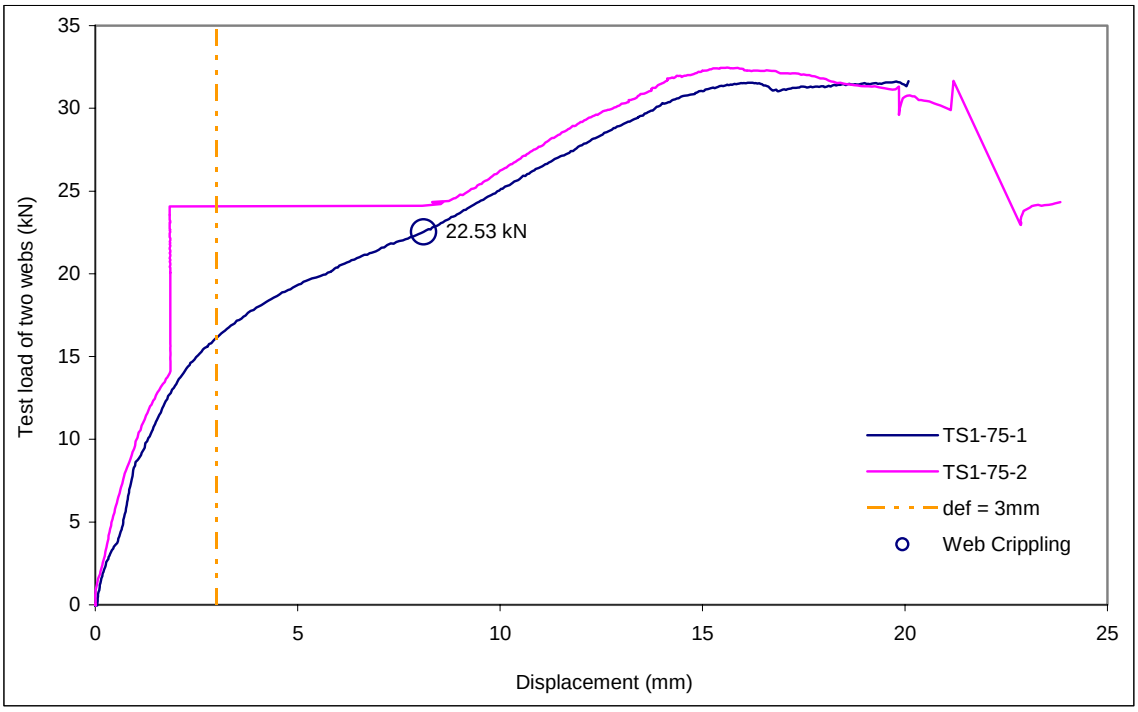

Figure 4-12: Test Load vs. Displacement (TS1-75 Test Series)

4.2 Selecting Failure Load

The selection of the appropriate failure load for each test was done by visual observations during the test and by using the load-displacement curve data. For many tests the failure mode and failure load were clearly defined. For example, with test TS9-75-1 (refer to Figure D9.4 in Appendix D) the failure mode was screw shear and the load-displacement curve shows a steadily increasing load until sudden failure. Similarly for web crippling failure, the load-displacement curve shows a local peak load when the web crippling occurs that can be followed by an increased load as the connection deforms. This was illustrated in Figure 4-2 for test TS3-44.

Not all failure loads were clearly defined, hence, some judgment was used to select an appropriate value. The load-displacement curves shown in Figure 4-13 are examples of assemblies (in this case TS4-75) that failed in web crippling, but there was no local maximum load that could be identified with web crippling. The maximum test load could not be established because it occurred in combination with excessive displacements. In cases such as this, the web crippling load was taken at the point of inflection of the load-displacement curve. The rational for selecting this point was based on the assumption that the load is initially carried through bearing of the stud, which starts to drop off as web crippling occurs and then will increase again as the load in the connection is redistributed to the track and starts to increase again. The inflection point was taken as the transition between these two modes.

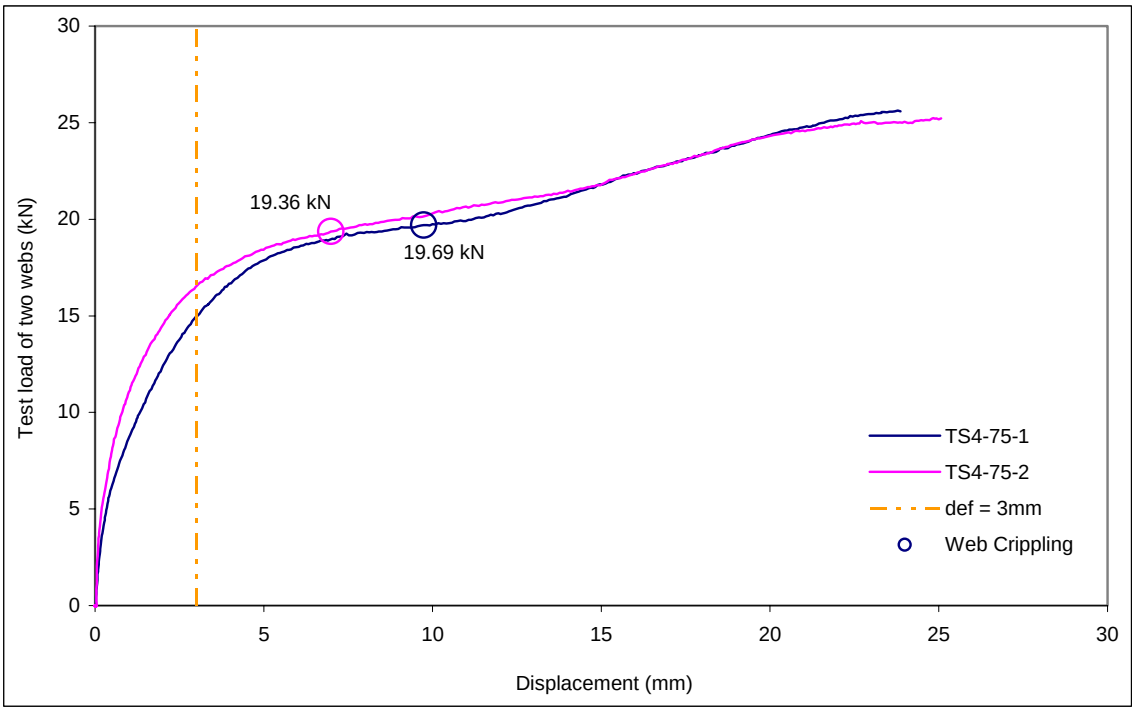

Figure 4-13: Web Crippling Failure Load Based on Load-Displacement Curve

The load-displacement curves for all of tests are provided in Appendix D. Indicated on the curves are the loads associated with web crippling (using a circle) and track punch-through (using a triangle), but not screw failure or excessive displacement. The web crippling (WC) and punch-through (PT) failure loads are identified because these values were used to develop the predictor equations for these failure modes. Unfortunately, due to faulty equipment with some tests, some of the load-displacement curves are discontinuous (caused by the LVDT sticking) or are erratic (caused by signal noise). The data acquisition system was unable to incorporate a real-time load-displacement monitor, and so these problems were not detected until the test data was analyzed at a later date.

4.3 Summary of Test Results

Presented in Table C-1 of Appendix C are all of the test results. Included in that table are the test sample configurations, failure loads, observed failure modes, and the relevant physical properties. The initial onset of web crippling is recorded, as is the punch through load per web, and the ultimate failure load. A discussion of the behaviour of the various specimen configurations along with the development predictor equations is provided in the following chapter.

4.4 Effect of Screw Size and Location

One of the parameters investigated in this research was the effect of the size and location of the screws connecting the stud to the track. In the WSD [AISI 2007b] the minimum size of screw is specified to be a #8, which is the smallest diameter screw used for structural connections. These screws are “self-drilling, self-tapping” and have a drill point on

the tip that drills the pilot hole through the connected sheets, allowing the threaded shank to tap the threads in the hole. These screws come in a variety of sizes from #6 to ¼", with different lengths of drill point depending on the thickness of material to be connected, and varying heads style depending on the end use and type of driver. The most common self-drilling screws for cold-formed steel structural applications are #10 or #12 diameter with a hex head.

The screws connecting the stud and track in a jamb stud are subjected to varying forces during a general loading cycle and will contribute to the resistance of the assembly. However, as long as the screw does not fail, the screw size does not add to the resistance of the stud-to-track connection. With the majority of the tests, #10 screws were used to make the connection, with an additional two series using #8 screws (TS9) and another series with #12 screws (TS10). These two test series provide a direct comparison with the #10 screw (TS2) tests.

Listed in Table 4-1 are the failure modes for the various combinations of screw size and stud/track thicknesses. It can be observed from this comparison that, to avoid a screw failure, it is necessary to specify the screw size according to the thickness of the material being connected. Like any structural connection, it is preferable to have failure occur in the member being connected in a ductile manner, and not in the connector, which tends to fail in a more brittle fashion.

Table 4-1: Effect of Screw Size on Failure Mode

#8 Screw Tests	Failure Mode	#10 Screw Tests	Failure Mode	#12 Screw Tests	Failure Mode
TS9-33-1	WC	TS2-33-1	WC		
TS9-33-2	WC	TS2-33-2	WC		
TS9-44-1	WC	TS2-44-1	WC	TS10-44-1	WC
TS9-44-2	WC	TS2-44-2	WC	TS10-44-2	WC
TS9-60-1	SS	TS2-60-1	PT	TS10-60-1	PT
TS9-60-2	SS	TS2-60-2	PT	TS10-60-2	PT
TS9-75-1	SS	TS2-75-1	SS	TS10-75-1	PT
TS9-75-2	SS	TS2-75-2	SS	TS10-75-2	PT

The location and number of screws making the connection will also have an impact on the resistance and behaviour of the assembly under load. A series of tests were carried out to determine the effect of only having one screw in one of the flanges, as illustrated in Figure 3-4. Test series TS10 was the standard configuration with screws in both stud flanges, while test TS11 had only one screw in the bottom flange, and test TS12 had only one screw in the top flange. The failure modes for each of these tests are listed in Table 4-2.

Table 4-2: Effect of Screw Location on Failure Mode

2 Screws	Failure Mode	Screw in Bottom	Failure Mode	Screw in Top	Failure Mode
		TS11-33-1	WC	TS12-33-1	Track Def
		TS11-33-2	PT	TS12-33-2	Track Def
TS10-44-1	WC	TS11-44-1	PT	TS12-44-1	Track Def
TS10-44-2	WC	TS11-44-2	PT	TS12-44-2	Track Def
TS10-60-1	PT	TS11-60-1	PT	TS12-60-1	Track Def
TS10-60-2	PT	TS11-60-2	PT	TS12-60-2	Track Def
TS10-75-1	PT	TS11-75-1	PT	TS12-75-1	Track Def
TS10-75-2	PT	TS11-75-2	PT	TS12-75-2	Track Def

The most significant difference is when the single screw is placed in the top flange only. When the assembly is loaded, the stud will load the bottom flange of the track that is unrestrained and will deflect without transferring much load. The top flange of the stud and track are connected and will pick up the majority of the load, thereby causing the screw to be in tension. Since the load transfer is through the top flange of the stud, there is no possibility of web crippling or track punch-through. As long as the screw has enough strength to carry the forces, the failure mode is excessive track deformation.

When the single screw is in the bottom flange, all of the forces are transferred through bearing of the stud onto the track with no load being transferred to the top flange of the track, as would be the case in a two-screw connection. If the bottom screw has sufficient strength, the failure mode will become web crippling or track punch-through. In all of these tests #12 screws were used to prevent screw failure, and the results cannot be extended to connections with smaller screws.

Chapter 5
Predictor Equations

5.1 Toe-to-Toe, Interior

Most of the interior toe-to-toe configurations failed in web crippling and behaved much like a single stud-to-track connection because the stud webs were separated from each other. The current predictor equation for web crippling of a single member stud-to-track connection given in the WSD [AISI 2007b] was used to predict the capacity of these toe-to-toe configurations. The results, listed in Table 5-1, show that the current WSD equation (multiplied by 2 to reflect there are two studs in the jamb) is an adequate predictor for these toe-to-toe jamb studs.

To develop a more accurate predictor equation, new web crippling coefficients were developed. How these coefficients were determined is discussed later in section 5.7. Listed in Table 5-1 are the predicted resistances, P_n, and the test-to-predicted ratios using the proposed web crippling coefficients, which are given in Table 5-9, section 5.8, for all of the various configurations.

Table 5-1: Comparison of Web Crippling Tested to Predicted Values - Interior Toe-to-Toe

Test Designation	Stud Properties						Test	WSD		New	
	d (mm)	t (mm)	F_y (MPa)	R (mm)	N (mm)	h (mm)	P_t (kN)	$2.0P_n$ (kN)	P_t/P_n	P_n (kN)	P_t/P_n
TS1-33-1	92	0.791	335.6	3.378	32.0	83.66	3.908	4.333	0.902	4.282	0.913
TS1-33-2	92	0.791	335.6	3.378	32.0	83.66	3.770	4.333	0.870	4.282	0.880
TS1-44-1	92	1.078	307.7	3.175	32.0	83.49	7.356	7.473	0.984	6.985	1.053
TS1-44-2	92	1.078	307.7	3.175	32.0	83.49	7.180	7.473	0.961	6.985	1.028
TS1-60-1	92	1.547	391.0	3.175	32.0	82.56	17.236	18.947	0.910	17.408	0.990
TS1-60-2	92	1.547	391.0	3.175	32.0	82.56	17.486	18.947	0.923	17.408	1.005
TS3-33-1	152	0.807	327.1	3.073	32.0	144.2	3.822	4.188	0.913	4.091	0.934
TS3-33-2	152	0.807	327.1	3.073	32.0	144.2	3.678	4.188	0.878	4.091	0.899
TS3-44-1	152	1.081	339.2	3.200	32.0	143.4	7.192	7.752	0.928	7.374	0.975
TS3-44-2	152	1.081	339.2	3.200	32.0	143.4	7.266	7.752	0.937	7.374	0.985
TS3-60-1	152	1.544	372.8	3.581	32.0	141.8	16.654	16.701	0.997	15.890	1.048
TS3-60-2	152	1.544	372.8	3.581	32.0	141.8	16.768	16.701	1.004	15.890	1.055
TS3-75-1	152	1.828	368.1	3.480	32.0	141.4	21.24	22.913	0.927	21.595	0.984
TS3-75-2	152	1.828	368.1	3.480	32.0	141.4	20.88	22.913	0.911	21.595	0.967
								Avg	0.932		0.980
								COV	0.044		0.058

5.2 Toe-to-Toe, End

With the toe-to-toe configuration at the end of the track, one of the studs is essentially at an interior location and the other stud is at the end. The current WSD design provisions for web crippling stipulate that a stud located at the track end has 50% of the capacity of a stud at an interior location. If the WSD design expressions are to be applied to a toe-to-toe configuration at the track end, one approach would be to take 150% of the calculated capacity based on a single stud to account for the reduction due to the end effect. A comparison of the test results with the WSD predictor design expressions (multiplied by 1.50 to account for the end effect) is given in Table 5-2. New web crippling coefficients were also developed based on the test data: the resulting test-to-predicted ratios are also given in Table 5-2. Refer to Table 5-9 in section 5.8 for the web crippling coefficients.

Table 5-2: Comparison of Web Crippling Tested to Predicted Values - End Toe-to-Toe

Test Designation	Stud Properties						Test	WSD		New	
	d (mm)	t (mm)	F_y (MPa)	R (mm)	N (mm)	h (mm)	P_t (kN)	$1.50P_n$ (kN)	P_t/P_n	P_n (kN)	P_t/P_n
TS4-33-1	92	0.791	335.6	3.368	32.0	83.68	3.288	3.253	1.011	3.622	0.908
TS4-33-2	92	0.791	335.6	3.368	32.0	83.68	3.17	3.253	0.974	3.622	0.875
TS4-44-1	92	1.078	307.7	3.175	32.0	83.49	5.58	5.604	0.996	5.490	1.016
TS4-44-2	92	1.078	307.7	3.175	32.0	83.49	6.458	5.604	1.152	5.490	1.176
TS4-60-1	92	1.547	391.0	3.186	32.0	82.53	12.122	14.202	0.854	12.590	0.963
TS4-60-2	92	1.547	391.0	3.186	32.0	82.53	12.212	14.202	0.860	12.590	0.970
TS4-75-1	92	1.874	454.0	3.195	32.0	81.86	19.694	23.609	0.834	20.045	0.982
TS4-75-2	92	1.874	454.0	3.195	32.0	81.86	19.358	23.609	0.820	20.045	0.966
TS6-33-1	152	0.807	327.1	3.062	32.0	144.26	3.444	3.144	1.095	3.638	0.947
TS6-33-2	152	0.807	327.1	3.062	32.0	144.26	3.150	3.144	1.002	3.638	0.866
TS6-44-1	152	1.081	339.2	3.203	32.0	143.43	5.842	5.812	1.005	6.062	0.964
TS6-44-2	152	1.081	339.2	3.203	32.0	143.43	5.700	5.812	0.981	6.062	0.940
TS6-60-1	152	1.544	372.8	3.572	32.0	141.77	13.146	12.532	1.049	11.929	1.102
TS6-60-2	152	1.544	372.8	3.572	32.0	141.77	12.894	12.532	1.029	11.929	1.081
TS6-75-1	152	1.828	368.1	3.473	32	141.40	15.638	17.191	0.910	15.558	1.005
TS6-75-3	152	1.828	368.1	3.473	32	141.40	16.252	17.191	0.945	15.558	1.045
								Avg	0.970		0.988
								COV	0.098		0.083

5.3 Single Stud, End Closed

The single stud at the end of the track, with the stud web closing the opening, is covered by the current WSD design provisions, which takes 50% of the web crippling capacity of a stud at an interior location. A comparison of the test results with the WSD predictor design expression (multiplied by 0.50 to account for the end effect) is given in Table 5-3. New web crippling coefficients were also developed based on the test data: the resulting test-to-predicted ratios are also given in Table 5-3. Refer to Table 5-9 in section 5.9 for the web crippling coefficients.

Table 5-3: Comparison of Web Crippling Tested to Predicted Values - Single Stud, End Closed

Test Designation	Stud Properties						Test	WSD		New	
	d (mm)	t (mm)	F_y (MPa)	R (mm)	N (mm)	h (mm)	P_t (kN)	$0.50P_n$ (kN)	P_t/P_n	P_n (kN)	P_t/P_n
TS7-33-1	92	0.791	335.6	3.368	32.0	83.68	1.258	1.084	1.160	1.498	0.840
TS7-33-3	92	0.791	335.6	3.368	32.0	83.68	1.396	1.084	1.287	1.498	0.932
TS7-44-2a	92	1.078	307.7	3.175	32.0	83.49	2.687	1.868	1.438	2.246	1.196
TS7-44-3	92	1.078	307.7	3.175	32.0	83.49	2.668	1.868	1.428	2.246	1.188
TS7-60-1	92	1.547	391.0	3.186	32.0	82.53	5.039	4.734	1.064	5.080	0.992
TS7-60-2	92	1.547	391.0	3.186	32.0	82.53	5.682	4.734	1.200	5.080	1.119
TS7-75-1	92	1.874	454.0	3.195	32.0	81.86	7.310	7.870	0.929	8.023	0.911
TS7-75-2	92	1.874	454.0	3.195	32.0	81.86	8.225	7.870	1.045	8.023	1.025
								Avg	1.194		1.025
								COV	0.153		0.129

5.4 Single Stud, End Open

The single stud at the end of the track, with the stud edge stiffeners at the opening, is not covered by the current WSD design provisions. The jamb stud web is not at the end of the track, but there is still some effect of the track termination. One way of recognizing this configuration is to consider that it is half way between an interior and an end condition, as defined in the WSD. To reflect this transitional condition, it might be appropriate to consider this stud as only having 75% of the web crippling capacity of a stud at an interior location. A comparison of the test results to the WSD predictor design expression (multiplied by 0.75 to account for the end effect) is given in Table 5-4. New web crippling coefficients were also developed based on the test data: the resulting test-to-predicted ratios are also given in Table 5-4. Refer to Table 5-9 in section 5.8 for the web crippling coefficients.

Table 5-4: Comparison of Web Crippling Tested to Predicted Values - Single Stud, End Open

Test Designation	Stud Properties						Test	WSD		New	
	d (mm)	t (mm)	F_y (MPa)	R (mm)	N (mm)	h (mm)	P_t (kN)	$0.75P_n$ (kN)	P_t/P_n	P_n (kN)	P_t/P_n
TS8-33-1	92	0.791	335.6	3.368	32.0	83.68	1.491	1.626	0.917	1.932	0.772
TS8-33-3	92	0.791	335.6	3.368	32.0	83.68	1.754	1.626	1.078	1.932	0.908
TS8-44-2a	92	1.078	307.7	3.175	32.0	83.49	3.350	2.802	1.195	3.056	1.096
TS8-44-3	92	1.078	307.7	3.175	32.0	83.49	3.680	2.802	1.313	3.056	1.204
TS8-60-1	92	1.547	391.0	3.186	32.0	82.53	7.092	7.101	0.999	7.204	0.984
TS8-60-2	92	1.547	391.0	3.186	32.0	82.53	N/R				
TS8-75-1	92	1.874	454.0	3.195	32.0	81.86	11.940	11.804	1.011	11.591	1.030
TS8-75-2	92	1.874	454.0	3.195	32.0	81.86	11.230	11.804	0.951	11.591	0.969
								Avg	1.066		0.995
								COV	0.133		0.138

5.5 Back-to-Back, Interior and End

The interior back-to-back configurations in the thinner gauges (33 and 44 mil) failed in web crippling before track punch-though and at loads much like the toe-to-toe configuration. The WSD equation for calculating the web crippling of a single member stud-to-track connection was used to predict the capacity of these back-to-back configurations, but was multiplied by 2 to reflect there are two studs in the jamb. The results, listed in Table 5-5, show that the WSD equation can be considered an adequate predictor for the back-to-back configurations, much the same as the toe-to-toe jamb studs.

The capacity of the back-to-back configuration at the track end was also compared to the results using the WSD predictor equation: this comparison is given in Table 5-6. Since the test results for the end and interior locations were adequately predicted using the WSD equation, all of the back-to-back tests were combined and compared to the WSD predictor equation: this comparison is presented in Table 5-7. Based on these results, it does not seem

necessary to differentiate the location of the back-to-back jambs studs with their respective location in the track.

New web crippling coefficients have also developed, resulting in a more accurate predictor equation for both the end and interior locations. How these coefficients were determined is discussed later in section 5.7. Listed in Tables 5-5 and 5-6 are the predicted resistances, P_n, and the test-to-predicted ratios using the proposed web crippling coefficients. The coefficients are given in Table 5-9, section 5.8, for all of the various configurations.

Table 5-5: Comparison of Web Crippling Tested to Predicted Values - Interior Back-to-Back

Test Designation	Stud Properties						Test	WSD		New	
	d (mm)	**t** (mm)	**F_y** (MPa)	**R** (mm)	**N** (mm)	**h** (mm)	**P_t** (kN)	**$2.0P_n$** (kN)	**P_t/P_n**	**P_n** (kN)	**P_t/P_n**
TS2-33-1	92	0.791	335.6	3.378	32.0	83.66	3.714	4.333	0.857	4.182	0.888
TS2-33-2	92	0.791	335.6	3.378	32.0	83.66	4.248	4.333	0.980	4.182	1.016
TS2-44-1	92	1.078	307.7	3.175	32.0	83.49	8.070	7.473	1.080	8.216	0.982
TS2-44-2	92	1.078	307.7	3.175	32.0	83.49	7.140	7.473	0.956	8.216	0.869
TS9-33-1	92	0.791	335.6	3.378	32.0	83.66	4.216	4.333	0.973	4.182	1.008
TS9-33-2	92	0.791	335.6	3.378	32.0	83.66	4.324	4.333	0.998	4.182	1.034
TS9-44-1	92	1.078	307.7	3.175	32.0	83.49	8.758	7.473	1.172	8.216	1.066
TS9-44-2	92	1.078	307.7	3.175	32.0	83.49	7.914	7.473	1.059	8.216	0.963
TS10-44-1	92	1.078	307.7	3.175	32.0	83.49	8.920	7.473	1.194	8.216	1.086
TS10-44-2	92	1.078	307.7	3.175	32.0	83.49	8.492	7.473	1.136	8.216	1.034
TS11-33-1	92	0.791	335.6	3.378	32.0	83.66	4.408	4.333	1.017	4.182	1.054
								Avg	1.038		1.000
								COV	0.098		0.070

Table 5-6: Comparison of Web Crippling Tested to Predicted Values - End Back-to-Back

Test Designation	Stud Properties						Test	WSD		New	
	d (mm)	t (mm)	F_y (MPa)	R (mm)	N (mm)	h (mm)	P_t (kN)	$2.0P_n$ (kN)	P_t/P_n	P_n (kN)	P_t/P_n
TS5-33-1	92	0.791	335.6	3.378	32.0	83.66	4.392	4.333	1.014	4.383	1.002
TS5-33-2	92	0.791	335.6	3.378	32.0	83.66	4.374	4.333	1.009	4.383	0.998
TS5-44-1	92	1.078	307.7	3.175	32.0	83.49	7.478	7.473	1.001	7.478	1.000
								Avg	1.008		1.000
								COV	0.006		0.002

Table 5-7: Comparison of Web Crippling Tested to Predicted Values - Back-to-Back

Test Designation	Stud Properties						Test	WSD	
	d (mm)	t (mm)	F_y (MPa)	R (mm)	N (mm)	h (mm)	P_t (kN)	$2.0P_n$ (kN)	P_t/P_n
TS2-33-1	92	0.791	335.6	3.378	32.0	83.66	3.714	4.333	0.857
TS2-33-2	92	0.791	335.6	3.378	32.0	83.66	4.248	4.333	0.980
TS2-44-1	92	1.078	307.7	3.175	32.0	83.49	8.070	7.473	1.080
TS2-44-2	92	1.078	307.7	3.175	32.0	83.49	7.140	7.473	0.956
TS9-33-1	92	0.791	335.6	3.378	32.0	83.66	4.216	4.333	0.973
TS9-33-2	92	0.791	335.6	3.378	32.0	83.66	4.324	4.333	0.998
TS9-44-1	92	1.078	307.7	3.175	32.0	83.49	8.758	7.473	1.172
TS9-44-2	92	1.078	307.7	3.175	32.0	83.49	7.914	7.473	1.059
TS10-44-1	92	1.078	307.7	3.175	32.0	83.49	8.920	7.473	1.194
TS10-44-2	92	1.078	307.7	3.175	32.0	83.49	8.492	7.473	1.136
TS11-33-1	92	0.791	335.6	3.378	32.0	83.66	4.408	4.333	1.017
TS5-33-1	92	0.791	335.6	3.378	32.0	83.66	4.392	4.333	1.014
TS5-33-2	92	0.791	335.6	3.378	32.0	83.66	4.374	4.333	1.009
TS5-44-1	92	1.078	307.7	3.175	32.0	83.49	7.478	7.473	1.001
								Avg	1.032
								COV	0.087

5.6 Track Punch-Through of Back-to-Back Jamb Studs

The punch-through failure mode is a function of the material properties of the track.

The WSD includes a design expression for predicting this failure load as discussed in Section

2.10. A different equation is proposed for the track punch-through with back-to-back members as given in Eq. 5.1. This equation was derived by analyzing the test data and trying various types of predictor equations. It may be possible to develop an equation that results in a more accurate prediction of the test data, but the form recommended in Eq. 5.1 was selected because of its simplicity.

$$P_n = 15.2 C_{pt} t^2 F_u \quad (5.1)$$

where,

P_n = Nominal track punch-through resistance (N)

C_{pt} = Punch-through coefficient

= $0.4687 + (t\,F_u)\,(2.821\text{x}10^{-3}) - (t\,F_u)^2\,(2.604\text{x}10^{-6})$

or conservatively can be taken as 1.0

F_u = Tensile strength of the track material (MPa)

t = Base steel thickness of track (mm)

Listed in Table 5-8 are the tested punch-through failure loads, P_t, the predicted resistances, P_n, the ratios P_t/P_n, the average of all ratios and the coefficient of variation, COV, of these ratios. Two punch-through coefficients are being proposed. For a simpler, but less accurate predictor, a value of 1.0 can be used for C_{pt}. This coefficient has the advantage of making the predictor equation easier to calculate, but the COV increases. A second, more complicated value of C_{pt} is proposed (shown above) that was determined from a regression analysis of the data to give a better prediction. In both cases the predictor equation must be used with SI units and is limited to back-to-back configurations, end or interior location, and 92 mm deep studs with thicknesses of 1.1 mm to 1.9 mm. It is also important to note that the capacity being predicted is the resistance of the connection, made up of two stud members.

The predictor equation for track punch-through given in the WSD [AISI 2007b] is similar to Eq. 5.1, but was developed based only on tests of single members. The WSD predictor equation was applied to the test data for the built-up sections and the resulting P_t/P_n ratios are also given in Table 5-8. It appears from the average test to predicted ratio of 0.845 that track punch-through occurs at a lower load for the built-up members than for the single web members. A definitive conclusion cannot be made from the available test data to explain this difference. Some possible explanations could include:

- The inside bend radii for the built-up sections were smaller, thereby causing higher localized stresses.
- The two studs back-to-back reduced the deformation of the stud webs under load, creating a stiffer section that would more easily shear through the track.
- The material properties of the track used in the two test programs could have been significantly different.
- The number of tests was limited, and so the difference may be within experimental error.

Table 5-8: Track Punch -Through Prediction Results

Test Designation	Test Sample Configuration	Track			P_t	C_{pt} = 1				WSD	
		Web	Thickness	F_u	Test Load	P_n	P_t/P_n	C_{pt}	P_t/P_n	P_n	P_t/P_n
		(mm)	(mm)	(MPa)	(kN)	(kN)				(kN)	
TS2-60-1	Interior back-to-back	92	1.516	615	19.11	21.34	0.90	0.84	1.07	24.80	0.77
TS2-60-2	Interior back-to-back	92	1.516	615	19.44	21.34	0.91	0.84	1.09	24.80	0.78
TS5-44-2	End back-to-back	92	1.078	403	8.325	7.07	1.18	1.20	0.98	9.27	0.90
TS5-60-1	End back-to-back	92	1.516	615	17.42	21.34	0.82	0.84	0.98	24.80	0.70
TS5-60-2	End back-to-back	92	1.516	615	17.42	21.34	0.82	0.84	0.98	24.80	0.70
TS5-75-1	End back-to-back	92	1.830	436	23.49	22.05	1.07	1.06	1.00	24.23	0.97
TS5-75-2	End back-to-back	92	1.830	436	23.76	22.05	1.08	1.06	1.02	24.23	0.98
TS10-44-2	Interior back-to-back	92	1.078	403	9.752	7.07	1.38	1.20	1.15	9.27	1.05
TS10-60-1	Interior back-to-back	92	1.516	615	18.18	21.34	0.85	0.84	1.02	24.80	0.73
TS10-60-2	Interior back-to-back	92	1.516	615	22.55	21.34	1.06	0.84	1.26	24.80	0.91
TS10-75-1	Interior back-to-back	92	1.830	436	25.20	22.05	1.14	1.06	1.08	24.23	1.04
TS10-75-2	Interior back-to-back	92	1.830	436	27.83	22.05	1.26	1.06	1.19	24.23	1.15
TS11-33-2	Interior back-to-back	92	0.806	373	4.260	3.66	1.16	1.08	1.08	5.43	0.78
TS11-44-1	Interior back-to-back	92	1.078	403	7.704	7.07	1.09	1.20	0.91	9.27	0.83
TS11-44-2	Interior back-to-back	92	1.078	403	7.532	7.07	1.07	1.20	0.89	9.27	0.81
TS11-60-1	Interior back-to-back	92	1.516	615	13.84	21.34	0.65	0.84	0.78	24.80	0.56
TS11-60-2	Interior back-to-back	92	1.516	615	14.04	21.34	0.66	0.84	0.79	24.80	0.57
TS11-75-1	Interior back-to-back	92	1.830	436	22.51	22.05	1.02	1.06	0.96	24.23	0.93
TS11-75-2	Interior back-to-back	92	1.830	436	21.49	22.05	0.97	1.06	0.92	24.23	0.89
						AVG	**1.00**	AVG	**1.01**		**0.845**
						COV	**0.192**	COV	**0.124**		**0.187**

5.7 Determination of Web Crippling Coefficients

The observed web crippling behaviour at the end of the stud adjacent to the track is similar to the buckling of a thin flat rectangular plate, but is not easy to analyze from a solely theoretical perspective. Yu (1985) stated that the theoretical analysis of web crippling for cold rolled steel beams is complicated by:

1. "Non-uniform stress distribution under the applied load and adjacent portions of the web.
2. Elastic and inelastic stability of the web element.
3. Local yielding in the immediate region of the load application.
4. Bending produced by eccentric load or reaction when it is applied on the bearing flange.
5. Initial out-of-plane imperfections in the plate elements.
6. Various edge restraints provided by beam flanges and interaction between flanges and web elements."

The web crippling equation presented in Eq. 5-1 is semi-empirical in nature and was developed by Prabarakan and Schuster [1998]. Additional testing was carried out by Gerges and Schuster [1998], Beshara and Schuster [2002] and Wallace and Schuster [2004], just to mention the latest published references. The web crippling coefficients contained in the NAS

[2007] are the result of all the published data found in the literature. Beshara and Schuster [2002] developed the first consistent set of web crippling coefficients.

$$P_n = Ct^2 F_y \left(1 - C_R\sqrt{\frac{R}{t}}\right)\left(1 + C_N\sqrt{\frac{N}{t}}\right)\left(1 - C_h\sqrt{\frac{h}{t}}\right) \quad (5.1)$$

Where:

C	=	Web crippling coefficient
C_R	=	Inside bend radius coefficient
C_N	=	Bearing length coefficient
C_h	=	Web slenderness coefficient
R	=	Stud inside bend radius
N	=	Stud Bearing Length
h	=	Depth of flat portion of stud measured along plane of web
t	=	Stud thickness
F_y	=	Yield strength of the stud material
P_n	=	Nominal resistance of stud-to-track connection when subjected to transverse loads

It was determined in the course of this research that since the range of each of these coefficients had been decreasing with the work done by successive researchers, it might be possible to use an indexing algorithm to compute and compare every solution of the web crippling equation within a certain range and increment size for all values of the four web crippling coefficients. By summing the square of the difference between the calculated web crippling result, P_n, and the test result, P_t, and saving the coefficients that generated the lowest residual sum, the 'best fit' coefficients could be obtained.

A FORTRAN computer program was written to read and process a text file containing one dataset with test data arranged into records so that the measured parameters and results for each test made up one record. The six data sets were defined according to

whether the connection was single stud or built-up, back-to-back or toe-to-toe, and at an end or interior location. Each dataset was processed independently of the others. To calculate the residual sum for every combination of coefficients within the determined range, a series of nested loops were used such that one coefficient at a time would be incremented by the determined step size. The computer program would increment one coefficient, one step at a time through its full range, and then increment the next coefficient, before repeating the process. For each coefficient increment, the web crippling result, P_n, would be calculated for each record in the dataset, and the difference between it and the test result, P_t, would be squared, and summed. The step of squaring the difference was necessary to avoid summing both positive and negative numbers; such a sum would not be meaningful. When all records were read, and the residual sum for that set of coefficients had been calculated, it was compared to the previously stored residual sum. If the new residual sum was less than the previously stored sum, then the new sum and set of coefficients that was generated was saved for the next comparison, and the previous results were discarded.

Since the method to determine the coefficients described herein is numeric and 'brute force' in nature, the issue of how to avoid arriving at a solution that could be a local minima needed to be addressed. This was accomplished by using the current NASPEC and WSD coefficients, as shown in Table 5.1, as the guidelines for both the range and step size of the coefficients in the program, and running multiple iterations using different ranges and step sizes.

Regardless of the range and step size, the coefficients always tended towards the range of the current published results, and did not appear to tend towards some unrelated local minima.

Table 5-9: Current Web Crippling Coefficients

Coefficient	WSD	NASPEC	
	Single	Single	Built-up
C	3.7	4	10
C_R	0.19	0.14	0.14
C_N	0.74	0.35	0.28
C_h	0.019	0.02	0.001

The largest web crippling coefficient shown in Table 5-9 is '10', and the smallest is '0.001'. Using these values as a guide, it was decided to use a starting range of 0 to 20 for all coefficients, followed by a range of 0.001 to 20 for all coefficients, to see the effect of starting from zero. Successive iterative runs using smaller steps and narrower ranges were based on output of previous iterations, bracketing the previous coefficients with a sufficiently large range to attempt to avoid local minima.

It was decided that for the final computation of the coefficients, the step size for a coefficient should not be smaller than the smallest precision currently used for that coefficient. For example, the smallest precision for the web slenderness coefficient, C_h, is three decimal places, or 0.001, whereas for the web crippling coefficient, C, it is one decimal place, or 0.1. The configurations for the six datasets, and the resulting coefficients, are presented in Table 5-10.

5.8 Web Crippling Equation and Coefficients

The web crippling equation from the NASPEC was used with new regression coefficients determined from the test data. Web crippling coefficients are proposed for each test configuration that exhibited web crippling failure. The applicability of these design expressions should not be extended beyond the limits of the material properties and sizes of the tested specimens. The NASPEC web crippling predictor equation is given in Eq. 5.1 and the coefficients are provided in Table 5-9. This web crippling equation is non-dimensional and can be used with any consistent system of units. It is important to note that the coefficients in Table 5-10 are for the jamb stud assembly, which will be for two studs or a single stud depending on the configuration.

Table 5-10: Web Crippling Coefficients for Jamb Stud-to-Track Assemblies

Test Configuration	C	C_R	C_N	C_h
Toe-to-Toe, Interior, 2 webs	12.6	0.01	0.15	0.015
Toe-to-Toe, End, 2 webs	3.6	0.01	0.62	0.001
Single web, End Closed (web on opening)	1.0	0.01	1.00	0.001
Single web, End Open (reinforcing lips on opening)	1.7	0.12	1.01	0.003
Back-to-back, Interior, 2 webs	10.2	0.29	0.86	0.024
Back-to-back, End, 2 webs	11.2	0.18	0.34	0.006

5.9 Calibration of Resistance Factors

If the intention is to propose separate design expressions for the different jamb configurations, it is necessary to establish the appropriate resistance factors to be used for design. This is done using the provisions of Chapter F1 of the NASPEC [CSA 2007, AISI

2007a] with the statistical data from the tests. The statistical values used to calculate the resistance factor are summarized in Table 5-11. The calculated resistance factors and safety factors for the proposed predictor expressions are listed in Table 5-12, and for the WSD in Table 5-13.

Table 5-11: Statistical Data for Resistance Factor Calibrations

Value	US LRFD	Canada LSD
C_φ	1.52	1.42
M_m	1.1	1.1
F_m	1	1
P_m	Avg. P_t/P_n by test	Avg. P_t/P_n by test
β_o	2.5	3
V_M	0.1	0.1
V_F	0.05	0.05
n	By test	By test
C_P	1.266	1.266
V_P	Test COV 0.065 min	Test COV 0.065 min
V_Q	0.21	0.21

Table 5-12: Resistance Factors and Safety Factors for Web Crippling, NASPEC

Jamb Configuration	No. of Tests	V_p	P_m	Canada	US and Mexico	
				ϕ	ϕ	Ω
Toe-to-Toe, Interior	14	0.065(1)	0.980	0.73	0.88	1.82
Toe-to-Toe, End	16	0.083	0.988	0.72	0.87	1.83
Single, End Open	7	0.138	0.995	0.63	0.79	2.03
Single, End Closed	8	0.129	1.025	0.68	0.83	1.92
Back-to-Back, Interior	11	0.070	1.000	0.73	0.89	1.79
Back-to-Back, End	3	0.065(1)	1.008	0.67	0.83	1.93

(1) Minimum variance allowed by NASPEC

Table 5-13: Resistance Factors and Safety Factors for Web Crippling, WSD

Jamb Configuration	No. of Tests	V_p	P_m	Canada	US and Mexico	
				ϕ	ϕ	Ω
Toe-to-Toe, Interior	14	0.065(1)	0.932	0.69	0.84	1.91
Toe-to-Toe, End	16	0.098	0.970	0.69	0.84	1.91
Single, End Open	7	0.133	1.066	0.69	0.84	1.91
Single, End Closed	8	0.153	1.194	0.75	0.93	1.72
Back-to-Back	14	0.087	1.032	0.75	0.91	1.76

(1) Minimum variance allowed by NASPEC

Chapter 6

Recommended Changes to the AISI North American Wall Stud Design Standard 2007

One of the objectives of this study was to make recommendations for changes to the WSD [AISI 2007b] to incorporate the results of these tests into the design standard. The following is an excerpt from the WSD with the proposed changes to incorporate provisions for the jamb stud members.

B2.2 Stud-to-Track Connection for C-Section Studs

The *stud*-to-*track* connection shall satisfy the requirements for web crippling resistance [resistance] of the *stud*, in accordance with sections B1.6 and C1 of this standard, or as defined in this section.

(a) For *curtain wall studs* that are not adjacent to wall openings and where both *stud flanges* are connected to the *track flanges* and the *track* thickness is greater than or equal to the *stud* thickness, the nominal resistance [resistance], P_{nst}, shall be determined in accordance with Eq. B2.2-1, as follows:

$$P_{nst} = Ct^2F_y\left(1-C_R\sqrt{\frac{R}{t}}\right)\left(1+C_N\sqrt{\frac{N}{t}}\right)\left(1-C_h\sqrt{\frac{h}{t}}\right) \qquad (Eq.\ B2.2\text{-}1)$$

Where:

C	=	web crippling coefficient; See Table B2.2-1
C_R	=	inside bend radius coefficient = 0.19
C_N	=	bearing length coefficient = 0.74
C_h	=	web slenderness coefficient = 0.019
R	=	stud inside bend radius
N	=	stud bearing length = 1.25 in. (32 mm)
h	=	depth of flat portion of stud web measured along plane of web
t	=	stud design thickness
Ω	=	1.70 for ASD for single stud interior configuration
	=	1.90 for ASD for all other configurations listed in Table B2.2-1
ϕ	=	0.90 for LRFD for single stud interior configuration

= 0.85 for LRFD for all other configurations listed in Table B2.2-1
= 0.75 for LSD for single stud interior configuration
= 0.70 for LSD for all other configurations listed in Table B2.2-1

Table B2.2-1 Web Crippling Coefficients

	Configuration	Web crippling coefficient, C
Single stud	Interior	3.70
Single stud	Adjacent to wall opening with reinforcing lips facing opening	2.78
Single stud	Adjacent to wall opening with stud web facing opening	1.85
Double stud	Toe-to-Toe Interior	7.40
Double stud	Toe-to-Toe Adjacent to opening	5.55
Double stud	Back-to-back Interior	7.40
Double stud	Back-to-back Adjacent to opening	7.40

The above equation is valid within the following range of parameters:

Screw Size: No. 8 minimum for 44 mil (1.12 mm) minimum stud thickness
No. 10 minimum for 54 mil (1.37 mm) minimum stud thickness
No. 12 minimum for 68 mil (1.73 mm) minimum and thicker stud thickness

Stud Section
Design Thickness: 0.0346 inch to 0.0770 inch (0.88 mm to 1.96 mm)
Design Yield Strength: 33 ksi to 50 ksi (228 MPa to 345 MPa)
Nominal Depth: 3.50 inch to 6.0 inch (88.9 mm to 152.4 mm)

Track Section
Design Thickness: 0.0346 inch to 0.0770 inch (0.88 mm to 1.96 mm)
Design Yield Strength: 33 ksi to 50 ksi (228 MPa to 345 MPa)
Nominal Depth: 3.50 inch to 6.0 inch (88.9 mm to 152.4 mm)
Nominal Flange Width: 1.25 inch to 2.375 inch (31.8 mm to 60.3 mm)

(b) For single *curtain wall studs* that are not adjacent to wall openings and where both *stud flanges* are connected to the *track flanges* and the *track* thickness is less than the *stud* thickness, the nominal strength [resistance], P_{nst}, is the lesser of Equations B2.2-1 or B2.2-2, which is defined as follows:

$$P_{nst} = 0.6\ t_t\ w_{st}\ F_{ut} \qquad (Eq.\ B2.2\text{-}2)$$

Where:

t_t	=	design *track* thickness
w_{st}	=	$20\ t_t + 0.56\alpha$
α	=	coefficient for conversion of units
	=	1.0 when t_t is in inches
	=	25.4 when t_t is in mm
F_{ut}	=	tensile strength of the *track*
Ω	=	1.70 for ASD
ϕ	=	0.90 for LRFD
	=	0.80 for LSD

The above equation is valid within the following range of parameters:

Screw Size:	No. 8 minimum
<u>Stud Section</u>	
Design Thickness:	0.0346 inch to 0.0770 inch (0.88 mm to 1.96 mm)
Design Yield Strength:	33 ksi to 50 ksi (228 MPa to 345 MPa)
Nominal Depth:	3.50 inch to 6.0 inch (88.9 mm to 152.4 mm)
<u>Track Section</u>	
Design Thickness:	0.0346 inch to 0.0770 inch (0.88 mm to 1.96 mm)
Design Yield Strength:	33 ksi to 50 ksi (228 MPa to 345 MPa)
Nominal Depth:	3.50 inch to 6.0 inch (88.9 mm to 152.4 mm)
Nominal Flange Width:	1.25 inch to 2.375 inch (31.8 mm to 60.3 mm)

(c) For *curtain wall* jamb *studs* made up of two studs connected back-to-back where both *stud flanges* are connected to the *track flanges* and the *track* thickness is the same as the *stud* thickness, the nominal strength [resistance], P_{nst}, is the lesser of Equations B2.2-1 or B2.2-3, which is defined as follows:

$$P_{nst} = 15.2\ t_t^2\ F_{ut} \qquad (Eq.\ B2.2\text{-}3)$$

Where:

t_t	=	design *track* thickness
F_{ut}	=	tensile strength of the *track*

Ω	=	2.10 for ASD
ϕ	=	0.75 for LRFD
	=	0.65 for LSD

The above equation is valid within the following range of parameters:

Screw Size:	No. 10 minimum
Stud Section	
Design Thickness:	0.0346 inch to 0.0770 inch (0.88 mm to 1.96 mm)
Design Yield Strength:	33 ksi to 50 ksi (228 MPa to 345 MPa)
Nominal Depth:	3.50 inch to 6.0 inch (88.9 mm to 152.4 mm)
Track Section	
Design Thickness:	0.0346 inch to 0.0770 inch (0.88 mm to 1.96 mm)
Design Yield Strength:	33 ksi to 50 ksi (228 MPa to 345 MPa)
Nominal Depth:	3.50 inch to 6.0 inch (88.9 mm to 152.4 mm)
Nominal Flange Width:	1.25 inch (31.8 mm)

(d) For *curtain wall studs* that are not adjacent to wall openings and do not have both *stud flanges* connected to the *track flanges* and the *track* thickness is greater than or equal to the *stud* thickness, the nominal strength [resistance], P_{nst} shall equal P_n, along with Ω and ϕ, as determined by Section C3.4.1 of AISI S100 [CSA S136].

(e) For *curtain wall studs* that are adjacent to wall openings and do not have both *stud* flanges connected to the *track* flanges and the *track* thickness is greater than or equal to the *stud* thickness, nominal strength [resistance], P_{nst} shall equal $0.5P_n$, along with Ω and ϕ, as determined by Section C3.4.1 of AISI S100 [CSA S136].

Chapter 7
Conclusions

The following is a summary of the conclusions resulting from this work:

- The web crippling resistance of all jamb stud configurations can be predicted using the current design expression in the North American Standard for Cold-Formed Steel Framing – Wall Stud Design, AISI S211-07 [AISI, 2007b], taking into account the number of studs in the assembly and location relative to the track end.
- Specific web crippling coefficients have been developed based on a regression analysis of the test data.
- It is necessary to specify the screw size according to the thickness of the material being connected. Similar to any structural connection, it is preferable to have the failure occur in the member being connected in a ductile manner, and not in the connector which tends to be of a more brittle nature.
- A single screw in the top flange will preclude a web crippling or track punch-through failure and result in excessive deformation of the track flange. A single screw in the bottom flange will behave in a similar manner as a connection with two screws, as long as the screw is large enough not to fail first.
- Recommended changes have been proposed to the North American Standard for Cold-Formed Steel Framing – Wall Stud Design, AISI S211-07 [AISI, 2007b] to incorporate provisions for the design of jamb studs.

Appendix A
Mechanical Properties

Table A.1: Mechanical Properties

Member Designator	t (mm)	F_y (MPa)	F_u (MPa)	% Elong.
362T125-33	0.806	328	373	32.2%
362T125-44	1.078	323	403	29.3%
362T125-60	1.516	584	615	15.4%
362T125-75	1.830	374	436	34.4%
600T125-33	0.804	338	367	33.0%
600T125-44	1.091	348	376	31.9%
600T125-60	1.485	429	592	25.0%
600T125-75	1.835	389	446	33.1%
362S162-33	0.791	336	371	32.1%
362S162-44	1.078	308	388	29.5%
362S162-60	1.547	391	548	26.8%
362S162-75	1.874	454	562	21.0%
600S162-33	0.807	327	380	31.1%
600S162-44	1.081	339	376	34.0%
600S162-60	1.544	373	545	27.6%
600S162-75	1.828	368	424	33.8%

Notes: Tabulated values are the averages of three coupon tests

Appendix B

Specimen Dimensions and Test Assembly Configurations

Table B.1: Physical Dimensions of Test Materials

Member Designator	Base Steel Thickness, t (mm)	Web Depth, H (mm)	Flange Width, D (mm)	Lip Length, L (mm)	Inside Bend Radius, R (mm)
362T125-33	0.806	92	32		NR
362T125-44	1.078	92	32		NR
362T125-60	1.516	92	32		NR
362T125-75	1.830	92	32		NR
600T125-33	0.804	152	32		NR
600T125-44	1.091	152	32		NR
600T125-60	1.485	152	32		NR
600T125-75	1.835	152	32		NR
362S162-33	0.791	92	41	12.7	3.38
362S162-44	1.078	92	41	12.7	3.18
362S162-60	1.547	92	41	12.7	3.18
362S162-75	1.874	92	41	12.7	3.20
600S162-33	0.807	152	41	12.7	3.07
600S162-44	1.081	152	41	12.7	3.20
600S162-60	1.544	152	41	12.7	3.58
600S162-75	1.828	152	41	12.7	3.48

NR = not recorded

Table B.2: Configuration of Test Samples

Test Series Designation	Test Sample Configuration		Screw Location	Stud Section	Track Section
TS1-33	Interior toe-to-toe	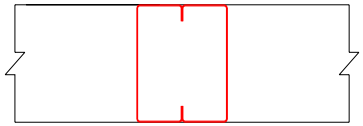	1 #10 in each flange	362S162-33	362T125-33
TS1-44	Interior toe-to-toe		1 #10 in each flange	362S162-44	362T125-44
TS1-60	Interior toe-to-toe		1 #10 in each flange	362S162-60	362T125-60
TS1-75	Interior toe-to-toe		1 #10 in each flange	362S162-75	362T125-75
TS2-33	Interior back-to-back	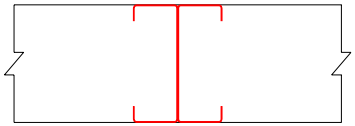	1 #10 in each flange	362S162-33	362T125-33
TS2-44	Interior back-to-back		1 #10 in each flange	362S162-44	362T125-44
TS2-60	Interior back-to-back		1 #10 in each flange	362S162-60	362T125-60
TS2-75	Interior back-to-back		1 #10 in each flange	362S162-75	362T125-75
TS3-33	Interior toe-to-toe	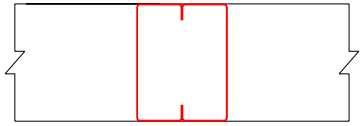	1 #10 in each flange	600S162-33	600T125-33
TS3-44	Interior toe-to-toe		1 #10 in each flange	600S162-44	600T125-44
TS3-60	Interior toe-to-toe		1 #10 in each flange	600S162-60	600T125-60
TS3-75	Interior toe-to-toe		1 #10 in each flange	600S162-75	600T125-75
TS4-33	End toe-to-toe	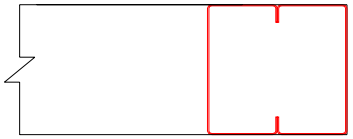	1 #10 in each flange	362S162-33	362T125-33
TS4-44	End toe-to-toe		1 #10 in each flange	362S162-44	362T125-44
TS4-60	End toe-to-toe		1 #10 in each flange	362S162-60	362T125-60
TS4-75	End toe-to-toe		1 #10 in each flange	362S162-75	362T125-75
TS5-33	End back-to-back	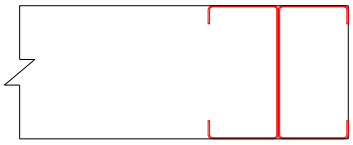	1 #10 in each flange	362S162-33	362T125-33
TS5-44	End back-to-back		1 #10 in each flange	362S162-44	362T125-44
TS5-60	End back-to-back		1 #10 in each flange	362S162-60	362T125-60
TS5-75	End back-to-back		1 #10 in each flange	362S162-75	362T125-75
TS6-33	End toe-to-toe		1 #10 in each flange	600S162-33	600T125-33
TS6-44	End toe-to-toe		1 #10 in each flange	600S162-44	600T125-44
TS6-60	End toe-to-toe		1 #10 in each flange	600S162-60	600T125-60
TS6-75	End toe-to-toe		1 #10 in each flange	600S162-75	600T125-75

Table B.2: Configuration of Test Samples (cont'd)

Test Series Designation	Test Sample Configuration		Screw Location	Stud Section	Track Section
TS7-33	End single stud, closed web		1 #10 in each flange	362S162-33	362T125-33
TS7-44	End single stud, closed web		1 #10 in each flange	362S162-44	362T125-44
TS7-60	End single stud, closed web		1 #10 in each flange	362S162-60	362T125-60
TS7-75	End single stud, closed web		1 #10 in each flange	362S162-75	362T125-75
TS8-33	End single stud, open web		1 #10 in each flange	362S162-33	362T125-33
TS8-44	End single stud, open web		1 #10 in each flange	362S162-44	362T125-44
TS8-60	End single stud, open web		1 #10 in each flange	362S162-60	362T125-60
TS8-75	End single stud, open web		1 #10 in each flange	362S162-75	362T125-75
TS9-33	Interior back-to-back	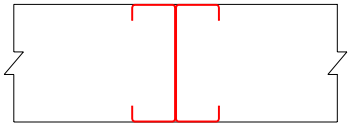	1 #8 in each flange	362S162-33	362T125-33
TS9-44	Interior back-to-back		1 #8 in each flange	362S162-44	362T125-44
TS9-60	Interior back-to-back		1 #8 in each flange	362S162-60	362T125-60
TS9-75	Interior back-to-back		1 #8 in each flange	362S162-75	362T125-75
TS10-33	**Not Tested**	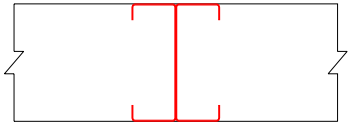			
TS10-44	Interior back-to-back		1 #12 in each flange	362S162-44	362T125-44
TS10-60	Interior back-to-back		1 #12 in each flange	362S162-60	362T125-60
TS10-75	Interior back-to-back		1 #12 in each flange	362S162-75	362T125-75
TS11-33	Interior back-to-back	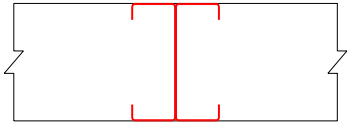	1 #12 bottom flange only	362S162-33	362T125-33
TS11-44	Interior back-to-back		1 #12 bottom flange only	362S162-44	362T125-44
TS11-60	Interior back-to-back		1 #12 bottom flange only	362S162-60	362T125-60
TS11-75	Interior back-to-back		1 #12 bottom flange only	362S162-75	362T125-75
TS12-33	Interior back-to-back	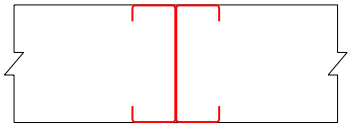	1 #12 top flange only	362S162-33	362T125-33
TS12-44	Interior back-to-back		1 #12 top flange only	362S162-44	362T125-44
TS12-60	Interior back-to-back		1 #12 top flange only	362S162-60	362T125-60
TS12-75	Interior back-to-back		1 #12 top flange only	362S162-75	362T125-75

Appendix C

Test Results

Table C.1: Summary of Test Results

Test Designation	Test Sample Configuration	At 3mm def. Load / Web (kN)	Web Crippling Load / Web (kN)	Punch Through Load / Web (kN)	Maximum Load / Web (kN)	Failure Mode(s)	Stud			Track	
							Depth (mm)	Thickness	Yield (MPa)	Thickness (mm)	Tensile (MPa)
TS1-33-1	Interior toe-to-toe	1.177	1.954		2.839	WC - Def	92	0.791	336	0.806	373
TS1-33-2	Interior toe-to-toe	1.110	1.885		2.447	WC - Def - SPU	92	0.791	336	0.806	373
TS1-44-1	Interior toe-to-toe	2.608	3.678		4.142	WC - Def - SPU	92	1.078	308	1.078	403
TS1-44-2	Interior toe-to-toe	3.223	3.590		4.657	WC - Def	92	1.078	308	1.078	403
TS1-60-1	Interior toe-to-toe	6.452	8.618		9.221	WC - SS (bot)	92	1.547	391	1.516	615
TS1-60-2	Interior toe-to-toe	7.158	8.743		9.121	WC - SS/ST (top)	92	1.547	391	1.516	615
TS1-75-1	Interior toe-to-toe	8.075	11.26		15.78	WC - SS/ST (top)	92	1.874	454	1.830	436
TS1-75-2	Interior toe-to-toe	NR	NR		16.23	WC - SS/ST (top)	92	1.874	454	1.830	436
TS2-33-1	Interior back-to-back	1.150	1.857		2.684	WC - Def	92	0.791	336	0.806	373
TS2-33-2	Interior back-to-back	1.422	2.124		2.486	WC - Def	92	0.791	336	0.806	373
TS2-44-1	Interior back-to-back	2.595	4.036		5.230	WC - Def	92	1.078	308	1.078	403
TS2-44-2	Interior back-to-back	2.622	3.570		4.723	WC - SPU	92	1.078	308	1.078	403
TS2-60-1	Interior back-to-back	6.931		9.554	9.554	PT	92	1.547	391	1.516	615
TS2-60-2	Interior back-to-back	6.459		9.721	9.976	PT -SS	92	1.547	391	1.516	615
TS2-75-1	Interior back-to-back	6.828			12.28	SS	92	1.874	454	1.830	436
TS2-75-2	Interior back-to-back	5.935			13.53	SS	92	1.874	454	1.830	436
TS3-33-1	Interior toe-to-toe	1.580	1.911		2.049	WC - Def	152	0.807	327	0.804	367
TS3-33-2	Interior toe-to-toe	1.324	1.839		1.839	WC - Def	152	0.807	327	0.804	367
TS3-44-1	Interior toe-to-toe	3.325	3.596		5.147	WC - Def	152	1.081	339	1.091	376
TS3-44-2	Interior toe-to-toe	3.134	3.633		4.362	WC - Def	152	1.081	339	1.091	376
TS3-60-1	Interior toe-to-toe	6.941	8.327		8.327	WC - Def - SPU	152	1.544	373	1.485	592
TS3-60-2	Interior toe-to-toe	7.253	8.384		8.384	WC - Def - SPU	152	1.544	373	1.485	592
TS3-75-1	Interior toe-to-toe	8.470	10.62		10.68	WC - Def - SPU	152	1.828	368	1.835	446
TS3-75-2	Interior toe-to-toe	9.317	10.44		10.44	WC - Def - SPU	152	1.828	368	1.835	446
TS4-33-1	End toe-to-toe	1.529	1.644		1.838	WC - Def	92	0.791	336	0.806	373
TS4-33-2	End toe-to-toe	1.550	1.585		1.749	WC - Def	92	0.791	336	0.806	373
TS4-44-1	End toe-to-toe	2.211	2.790		3.239	WC - Def	92	1.078	308	1.078	403
TS4-44-2	End toe-to-toe	2.701	3.229		3.386	WC - Def	92	1.078	308	1.078	403
TS4-60-1	End toe-to-toe	4.386	6.061		6.520	WC - Def	92	1.547	391	1.516	615
TS4-60-2	End toe-to-toe	5.460	6.106		7.826	WC - Def	92	1.547	391	1.516	615
TS4-75-1	End toe-to-toe	7.481	9.847		12.81	WC - SS (top)	92	1.874	454	1.830	436
TS4-75-2	End toe-to-toe	8.264	9.679		12.62	WC - SS (all)	92	1.874	454	1.830	436

Notes: WC = Web Crippling
SS = Screw shear (t = top, bot = bottom, or all)
SPU = Screw Pull-out
PT = Track Punch-through
Def = Excessive Deformation
ST = Screw Tension
TS1 to TS8 connections use one #10 SD Hex screw in both flanges
TS9 connections use one #8 SD Wafer-head screw in both flanges
TS10 connections use one #12 SD Hex screw in both flanges
TS11 connections use one #12 SD Hex screw in the bottom flange only
TS12 connections use one #12 SD Hex screw in the top flange only

Table C.1: Summary of Test Results (cont'd)

Test Designation	Test Sample Configuration	At 3mm def. Load / Web (kN)	Web Crippling Load / Web (kN)	Punch Through Load / Web (kN)	Maximum Load / Web (kN)	Failure Mode(s) 0	Stud			Track	
							Depth (mm)	Thickness	Yield (MPa)	Thickness (mm)	Tensile (MPa)
TS5-33-1	End back-to-back	1.801	2.196		2.530	WC - Def	92	0.791	336	0.806	373
TS5-33-2	End back-to-back	1.525	2.187		2.041	WC - Def	92	0.791	336	0.806	373
TS5-44-1	End back-to-back	3.606	3.739		4.248	WC - Def	92	1.078	308	1.078	403
TS5-44-2	End back-to-back	3.906		4.163	4.409	PT	92	1.078	308	1.078	403
TS5-60-1	End back-to-back	NR		8.709	8.709	PT	92	1.547	391	1.516	615
TS5-60-2	End back-to-back	5.567		8.710	8.710	PT	92	1.547	391	1.516	615
TS5-75-1	End back-to-back	7.571		11.75	12.61	PT-SS (bot)	92	1.874	454	1.830	436
TS5-75-2	End back-to-back	NR		NR	NR	PT	92	1.874	454	1.830	436
TS6-33-1	End toe-to-toe	1.481	1.722		1.722	WC - Def	152	0.807	327	0.804	367
TS6-33-2	End toe-to-toe	1.138	1.575		1.575	WC - Def	152	0.807	327	0.804	367
TS6-44-1	End toe-to-toe	2.267	2.921		2.921	WC - Def	152	1.081	339	1.091	376
TS6-44-2	End toe-to-toe	2.145	2.850		2.850	WC - Def	152	1.081	339	1.091	376
TS6-60-1	End toe-to-toe	5.155	6.573		6.573	WC - Def - SPU	152	1.544	373	1.485	592
TS6-60-2	End toe-to-toe	5.374	6.447		6.496	WC - Def - SPU	152	1.544	373	1.485	592
TS6-75-1	End toe-to-toe	6.699	7.819		8.314	WC - Def - SS (top)	152	1.828	368	1.835	446
TS6-75-3	End toe-to-toe	7.026	8.126		8.554	WC - Def- SPU	152	1.828	368	1.835	446
TS7-33-1	End single stud, closed web	0.802	1.258		1.832	WC - Def	92	0.791	336	0.806	373
TS7-33-2	End single stud, closed web	0.782	1.396		1.804	WC - Def	92	0.791	336	0.806	373
TS7-44-2	End single stud, closed web	2.308	2.687		3.287	WC - Def	92	1.078	308	1.078	403
TS7-44-3	End single stud, closed web	2.021	2.668		3.629	WC - Def	92	1.078	308	1.078	403
TS7-60-1	End single stud, closed web	3.831	5.039		5.253	WC - Def	92	1.547	391	1.516	615
TS7-60-2	End single stud, closed web	3.743	5.682		5.883	WC - Def	92	1.547	391	1.516	615
TS7-75-1	End single stud, closed web	5.990	7.310		9.938	WC - SS (all)	92	1.874	454	1.830	436
TS7-75-2	End single stud, closed web	7.252	8.225		8.357	WC - SS (all)	92	1.874	454	1.830	436
TS8-33-1	End single stud, open web	1.190	1.491		1.763	WC - Def	92	0.791	336	0.806	373
TS8-33-3	End single stud, open web	1.296	1.754		1.754	WC - Def	92	0.791	336	0.806	373
TS8-44-2a	End single stud, open web	2.091	3.350		5.331	WC - Def - SPU	92	1.078	308	1.078	403
TS8-44-3	End single stud, open web	2.585	3.680		5.878	WC - Def	92	1.078	308	1.078	403
TS8-60-1	End single stud, open web	4.671	7.092		9.113	WC - Def	92	1.547	391	1.516	615
TS8-60-2	End single stud, open web	4.789	NR		7.943	WC - Def	92	1.547	391	1.516	615
TS8-75-1	End single stud, open web	7.689	11.94		15.89	WC - SPU	92	1.874	454	1.830	436
TS8-75-2	End single stud, open web	7.667	11.23		15.44	WC - SS (top)	92	1.874	454	1.830	436

Notes: WC = Web Crippling
SS = Screw shear (t = top, bot = bottom, or all)
SPU = Screw Pull-out
PT = Track Punch-through
Def = Excessive Deformation
ST = Screw Tension
TS1 to TS8 connections use one #10 SD Hex screw in both flanges
TS9 connections use one #8 SD Wafer-head screw in both flanges
TS10 connections use one #12 SD Hex screw in both flanges
TS11 connections use one #12 SD Hex screw in the bottom flange only
TS12 connections use one #12 SD Hex screw in the top flange only

81

Table C.1: Summary of Test Results (cont'd)

Test Designation	Test Sample Configuration	At 3mm def. Load / Web (kN)	Web Crippling Load / Web (kN)	Punch Through Load / Web (kN)	Maximum Load / Web (kN)	Failure Mode(s) 0	Stud			Track	
							Depth (mm)	Thickness	Yield (MPa)	Thickness (mm)	Tensile (MPa)
TS9-33-1	Interior back-to-back	1.676	2.108		2.509	WC - Def	92	0.791	336	0.806	373
TS9-33-2	Interior back-to-back	1.532	2.162		2.831	WC - Def	92	0.791	336	0.806	373
TS9-44-1	Interior back-to-back	2.776	4.379		4.379	WC - Def - SPU	92	1.078	308	1.078	403
TS9-44-2	Interior back-to-back	2.506	3.957		4.279	WC - Def - SPU	92	1.078	308	1.078	403
TS9-60-1	Interior back-to-back	5.289			8.654	SS	92	1.547	391	1.516	615
TS9-60-2	Interior back-to-back	5.225			8.303	SS	92	1.547	391	1.516	615
TS9-75-1	Interior back-to-back	7.765			9.832	SS	92	1.874	454	1.830	436
TS9-75-2	Interior back-to-back	8.789			10.20	SS	92	1.874	454	1.830	436
TS10-33-1	Not Tested										
TS10-33-2	Not Tested										
TS10-44-1	Interior back-to-back	2.529	4.460		6.007	WC - Def	92	1.078	308	1.078	403
TS10-44-2	Interior back-to-back	2.499	4.246	4.876	4.876	WC - PT	92	1.078	308	1.078	403
TS10-60-1	Interior back-to-back	5.342		9.088	10.11	PT (Tearing)	92	1.547	391	1.516	615
TS10-60-2	Interior back-to-back	6.841		11.27	11.27	PT (Tearing)	92	1.547	391	1.516	615
TS10-75-1	Interior back-to-back	7.541		12.60	14.38	PT (Tearing)	92	1.874	454	1.830	436
TS10-75-2	Interior back-to-back	7.459		13.91	13.91	PT (Tearing)	92	1.874	454	1.830	436
TS11-33-1	Interior back-to-back	1.122	2.204		2.204	WC	92	0.791	336	0.806	373
TS11-33-2	Interior back-to-back	1.195		2.130	2.577	PT	92	0.791	336	0.806	373
TS11-44-1	Interior back-to-back	2.108		3.852	3.852	PT	92	1.078	308	1.078	403
TS11-44-2	Interior back-to-back	1.892		3.766	4.254	PT	92	1.078	308	1.078	403
TS11-60-1	Interior back-to-back	4.087		6.919	6.919	PT	92	1.547	391	1.516	615
TS11-60-2	Interior back-to-back	3.946		7.021	7.021	PT	92	1.547	391	1.516	615
TS11-75-1	Interior back-to-back	6.225		11.25	11.82	PT	92	1.874	454	1.830	436
TS11-75-2	Interior back-to-back	5.962		10.75	11.76	PT	92	1.874	454	1.830	436
TS12-33-1	Interior back-to-back	0.961			1.570	Track Def - SPU	92	0.791	336	0.806	373
TS12-33-2	Interior back-to-back	1.129			1.572	Track Def - No SPU	92	0.791	336	0.806	373
TS12-44-1	Interior back-to-back	1.927			3.138	Track Def - No SPU	92	1.078	308	1.078	403
TS12-44-2	Interior back-to-back	1.820			2.466	Track Def - No SPU	92	1.078	308	1.078	403
TS12-60-1	Interior back-to-back	3.386			4.727	Track Def - No SPU	92	1.547	391	1.516	615
TS12-60-2	Interior back-to-back	3.510			4.760	Track Def - No SPU	92	1.547	391	1.516	615
TS12-75-1	Interior back-to-back	6.061			8.654	Track Def - No SPU	92	1.874	454	1.830	436
TS12-75-2	Interior back-to-back	5.785			7.782	Track Def - No SPU	92	1.874	454	1.830	436

Notes: WC = Web Crippling
SS = Screw shear (t = top, bot = bottom, or all)
SPU = Screw Pull-out
PT = Track Punch-through
Def = Excessive Deformation
ST = Screw Tension
TS1 to TS8 connections use one #10 SD Hex screw in both flanges
TS9 connections use one #8 SD Wafer-head screw in both flanges
TS10 connections use one #12 SD Hex screw in both flanges
TS11 connections use one #12 SD Hex screw in the bottom flange only
TS12 connections use one #12 SD Hex screw in the top flange only

82

Appendix D

Test Load vs. Displacement Curves

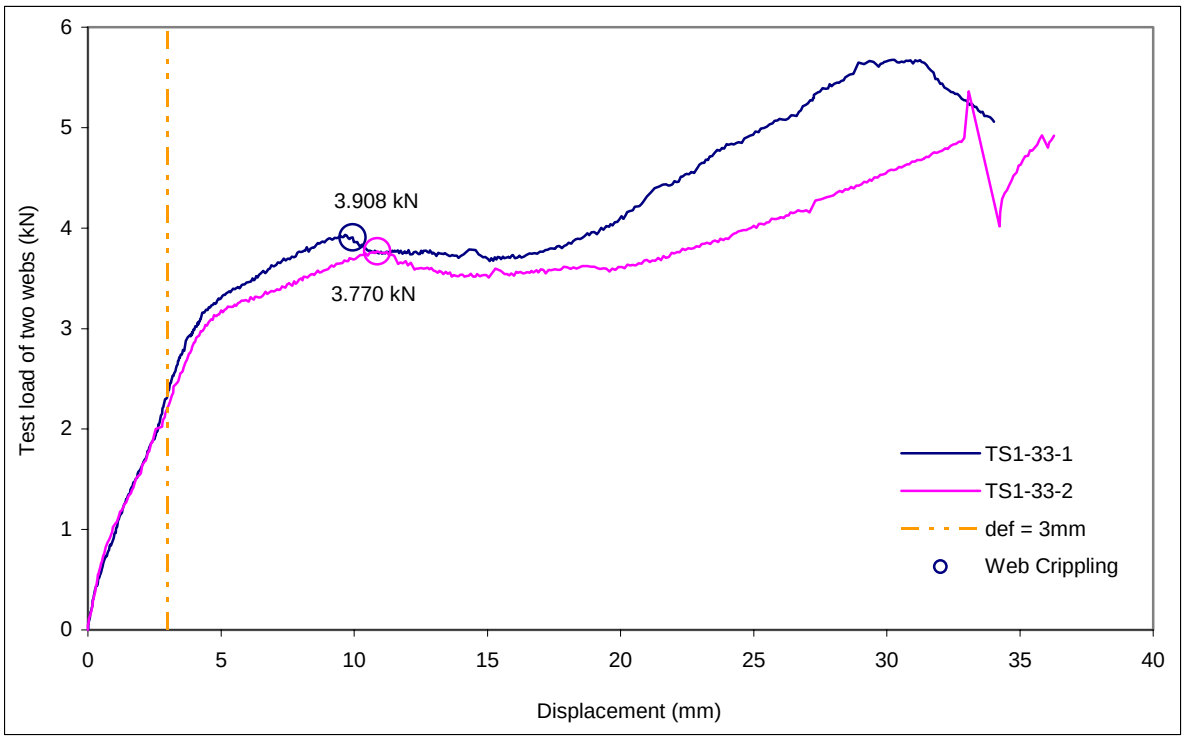

Figure D1.1: Test Load vs. Displacement, TS1-33 Series

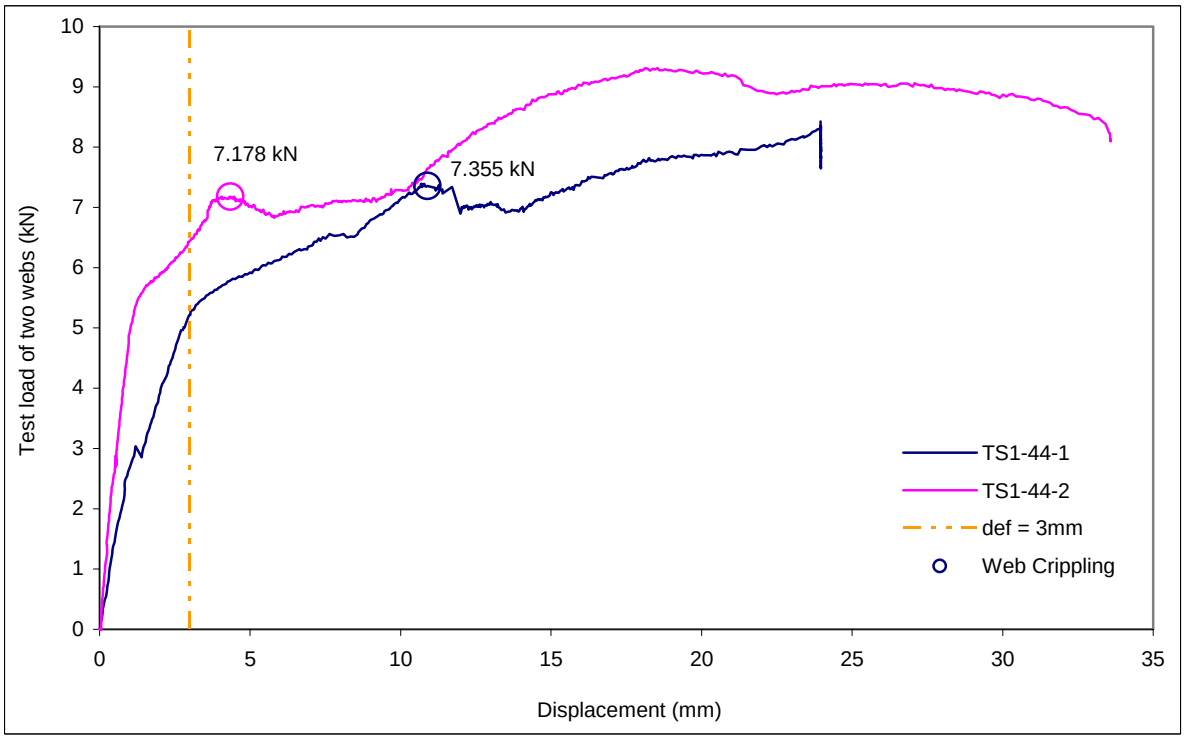

Figure D1.2: Test Load vs. Displacement, TS1-44 Series

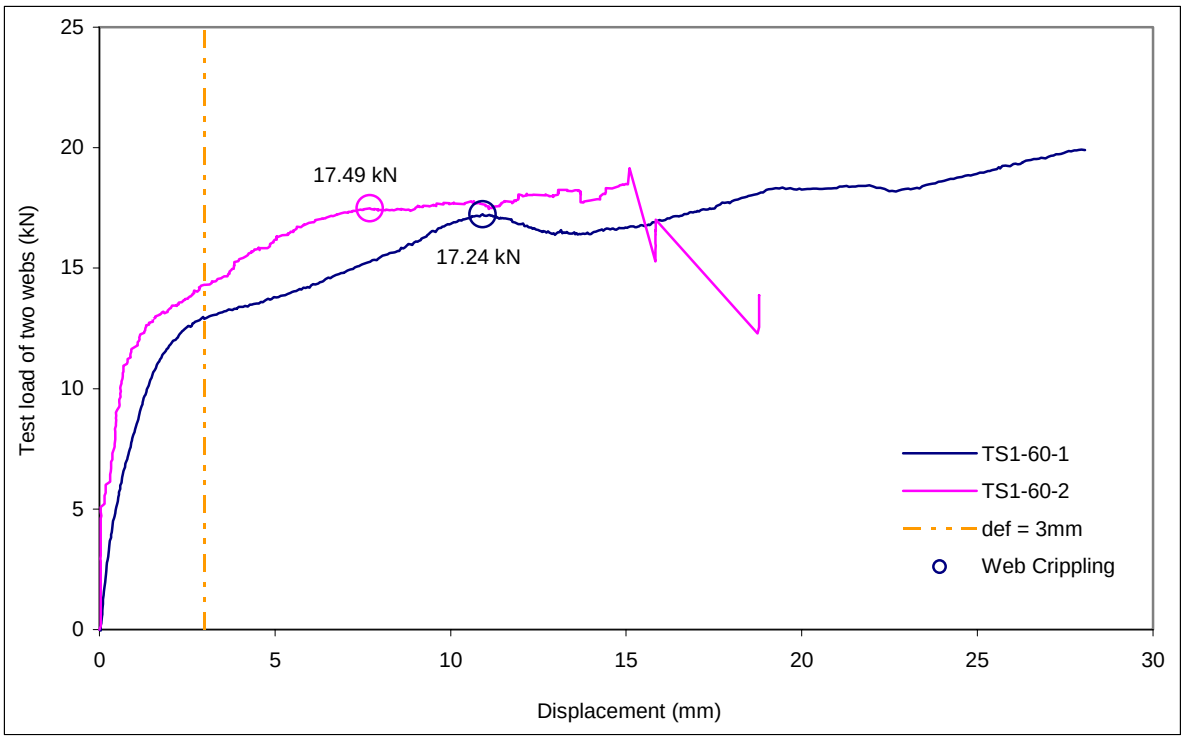

Figure D1.3: Test Load vs. Displacement, TS1-60 Series

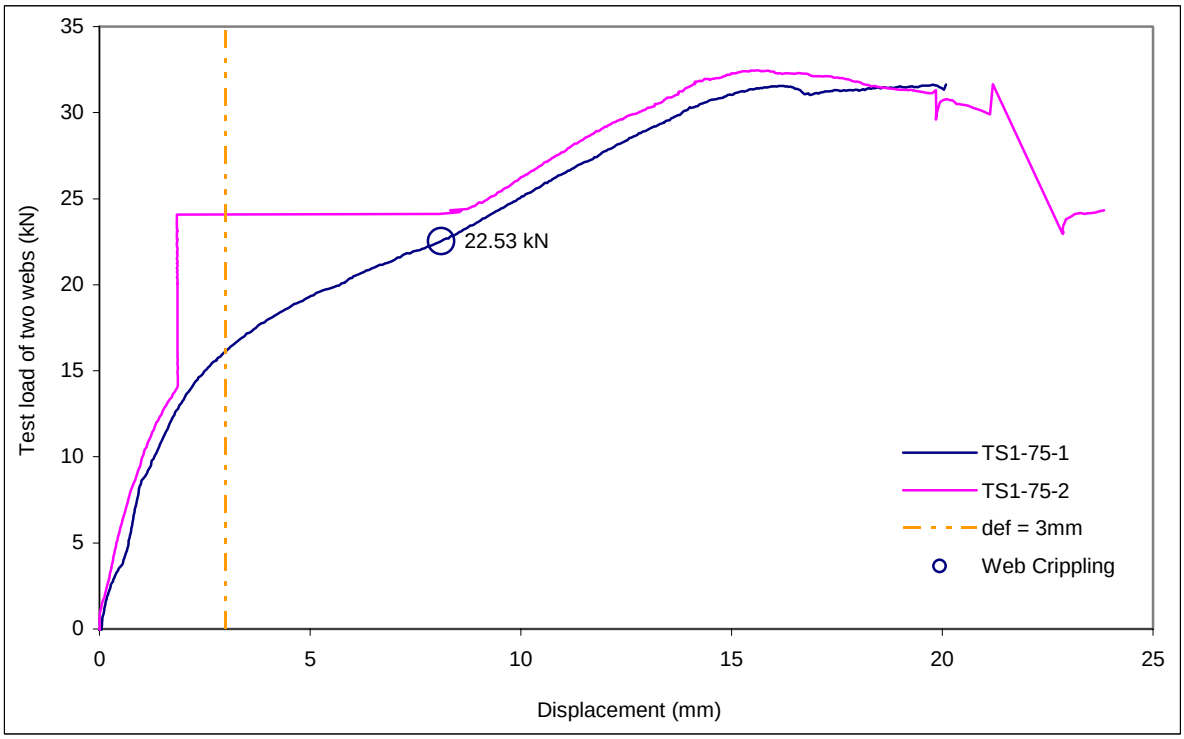

Figure D1.4: Test Load vs. Displacement, TS1-75 Series

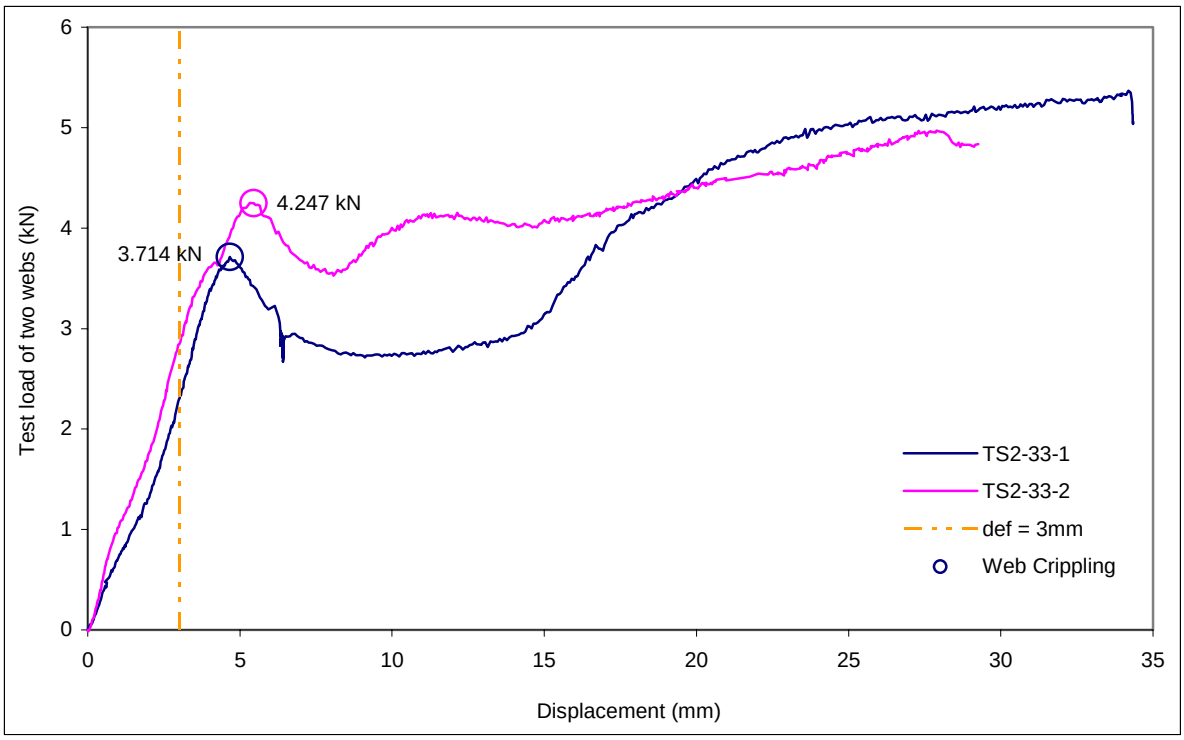

Figure D2.1: Test Load vs. Displacement, TS2-33 Series

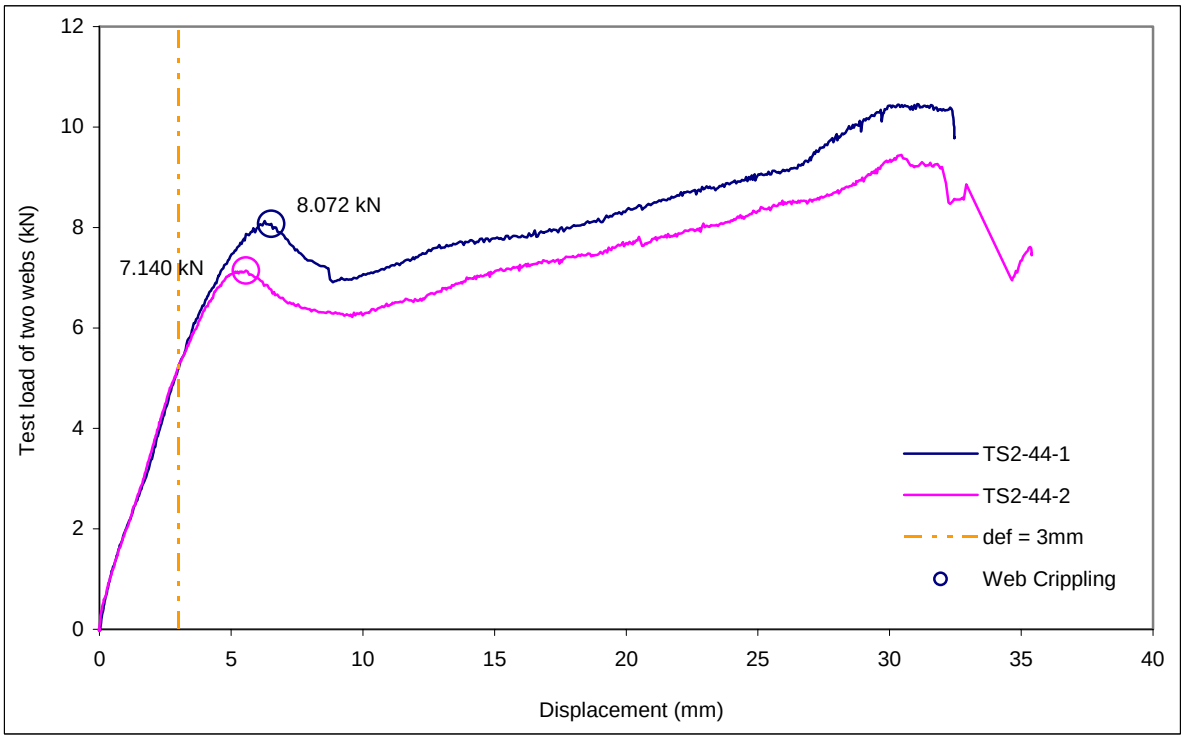

Figure D2.2: Test Load vs. Displacement, TS2-44 Series

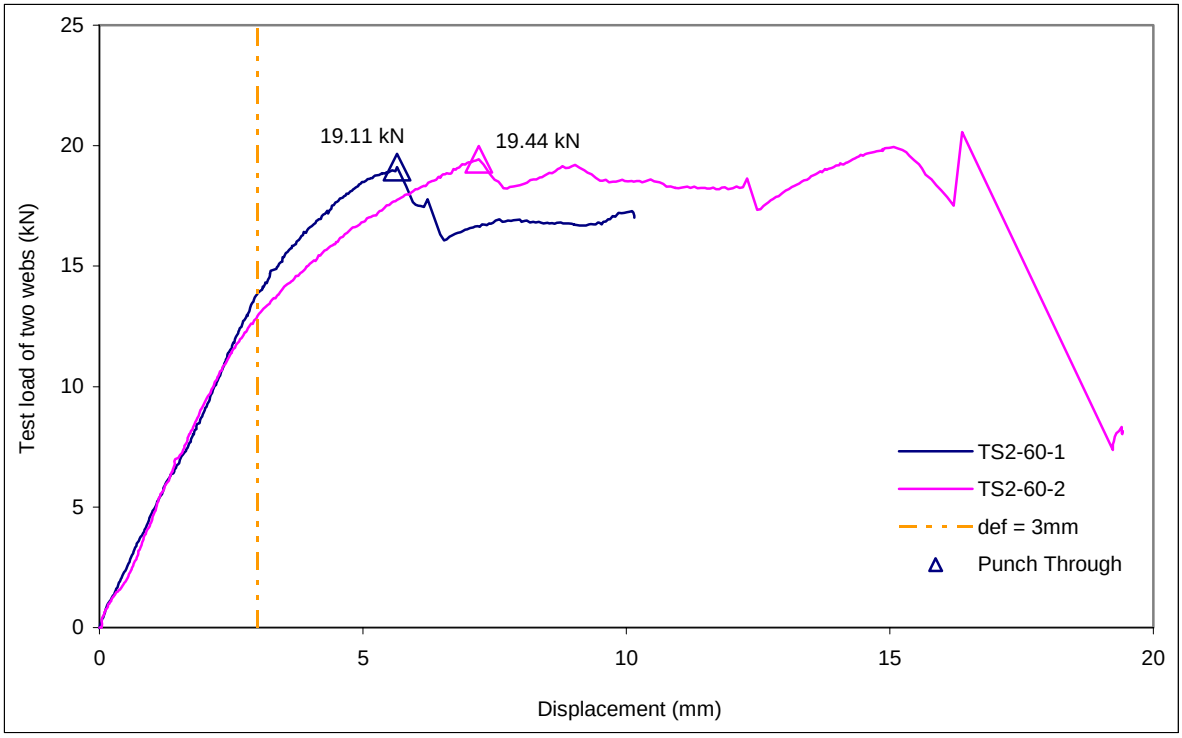

Figure D2.3: Test Load vs. Displacement, TS2-60 Series

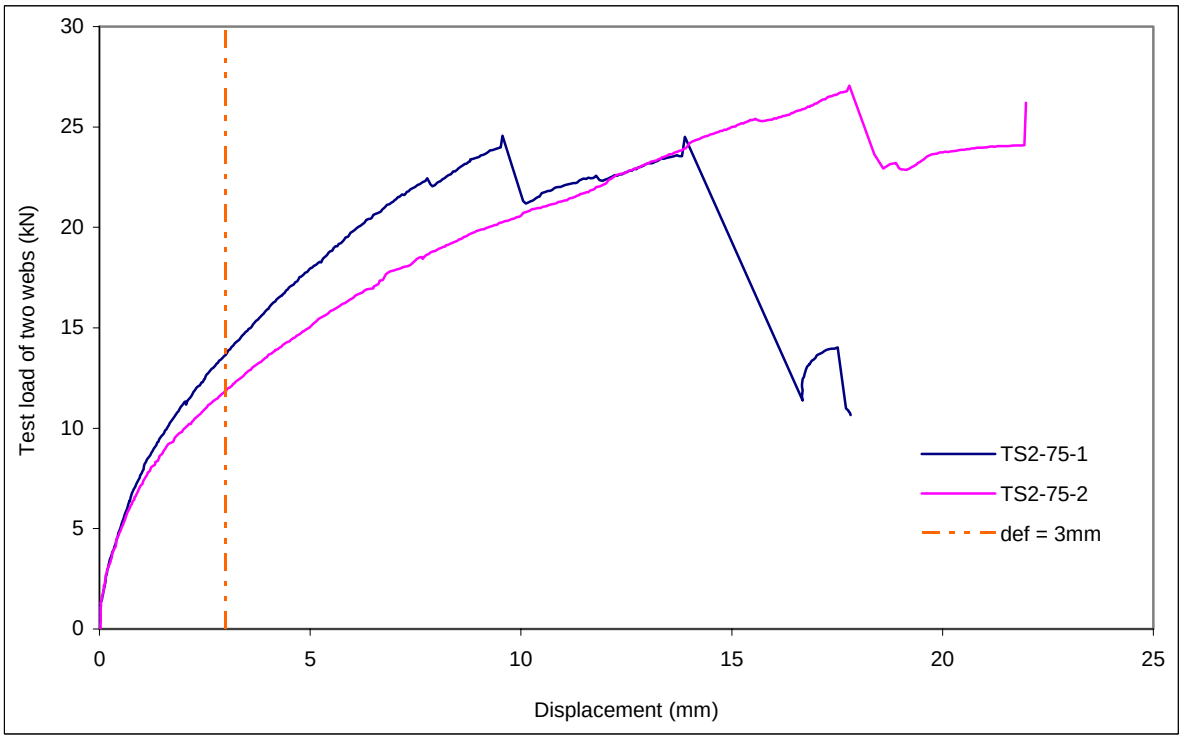

Figure D2.4: Test Load vs. Displacement, TS2-75 Series

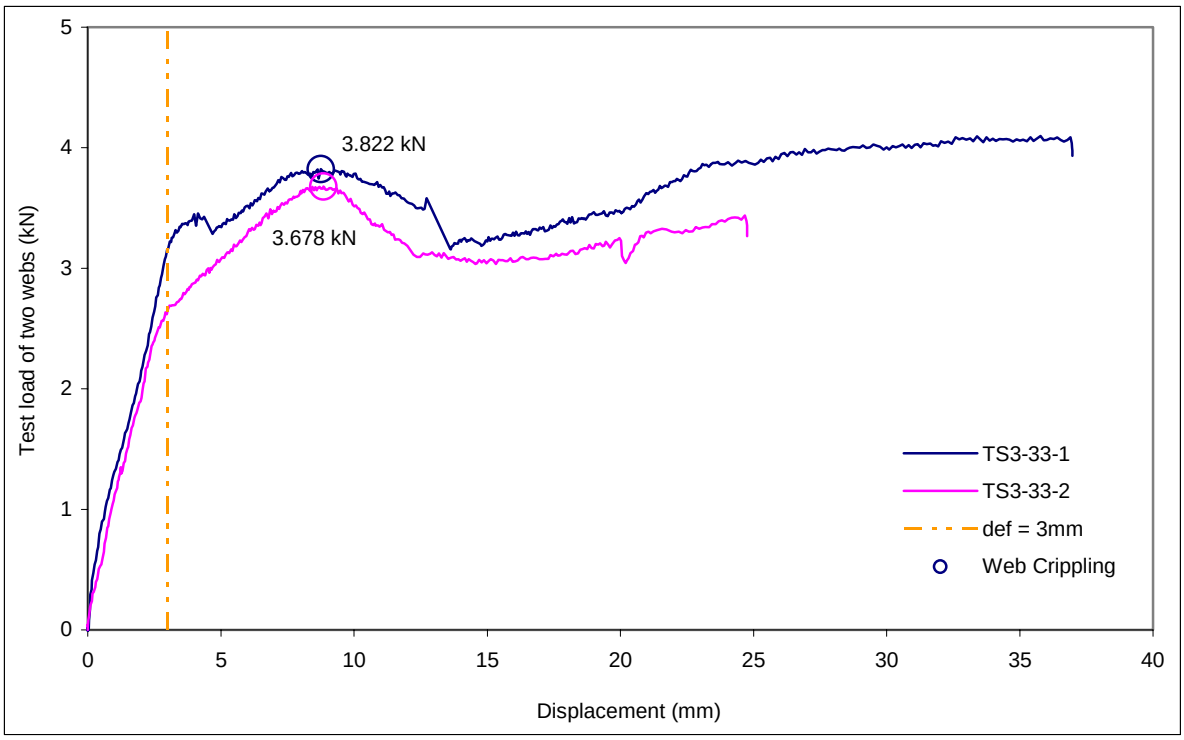

Figure D3.1: Test Load vs. Displacement, TS3-33 Series

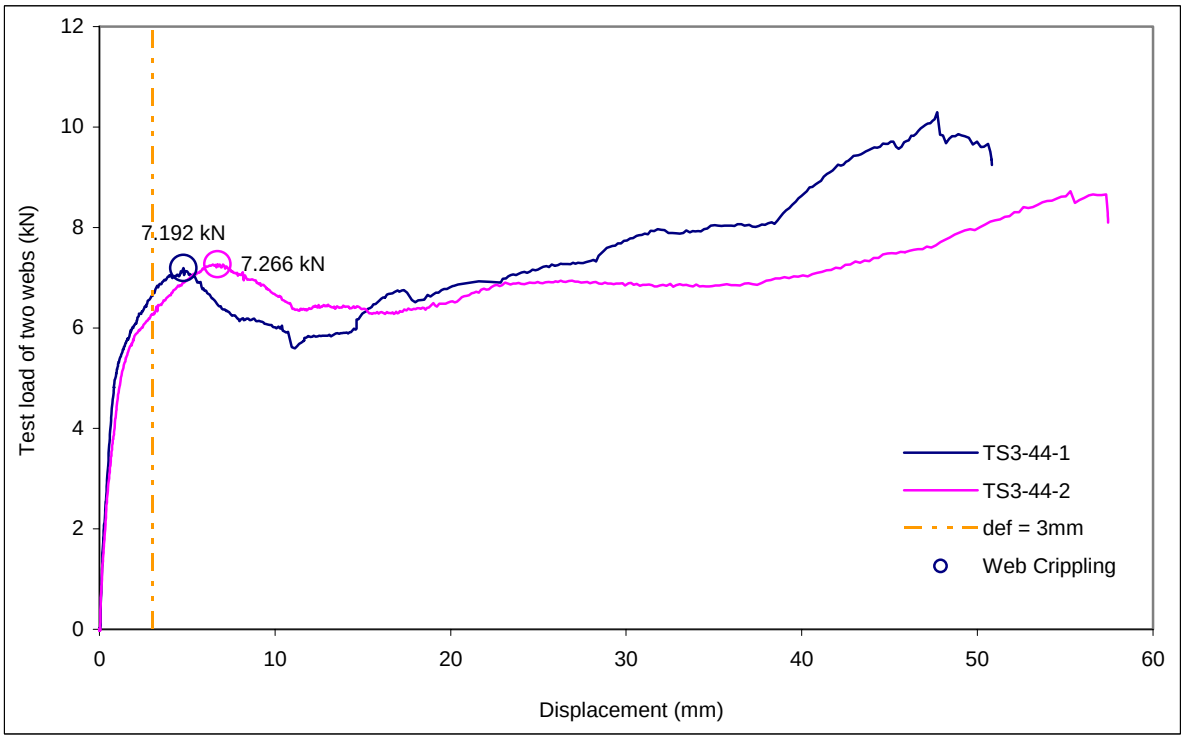

Figure D3.2: Test Load vs. Displacement, TS3-44 Series

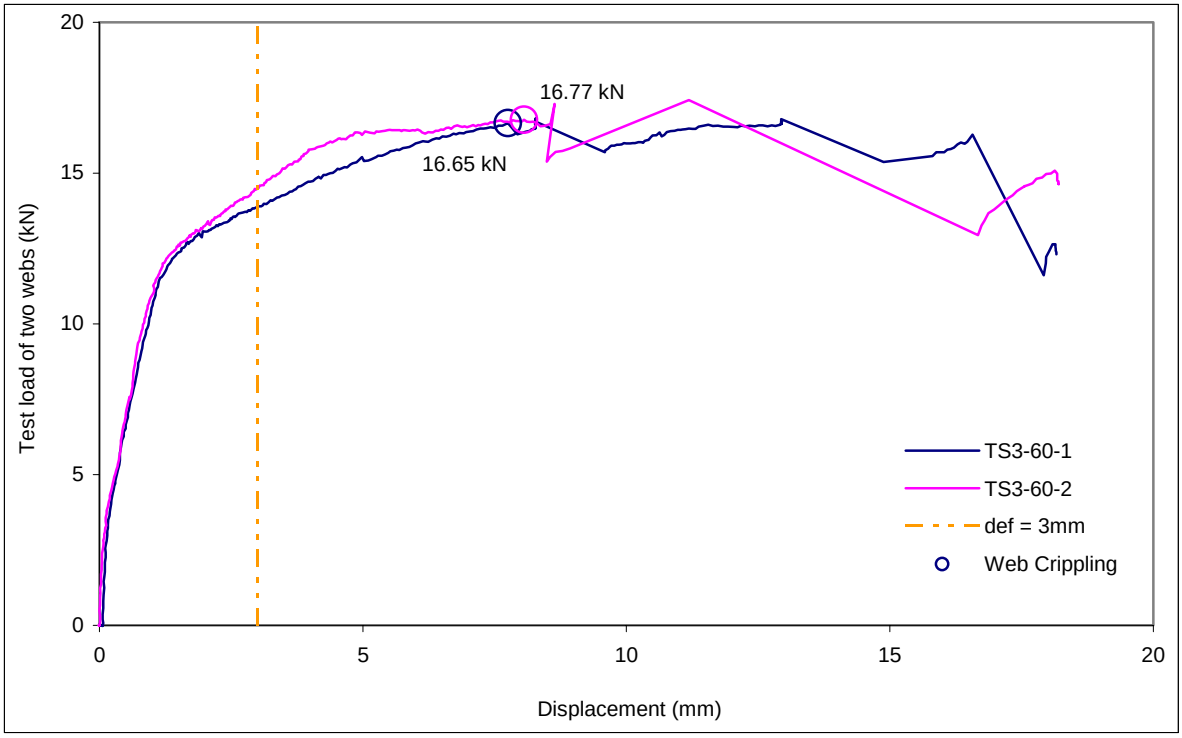

Figure D3.3: Test Load vs. Displacement, TS3-60 Series

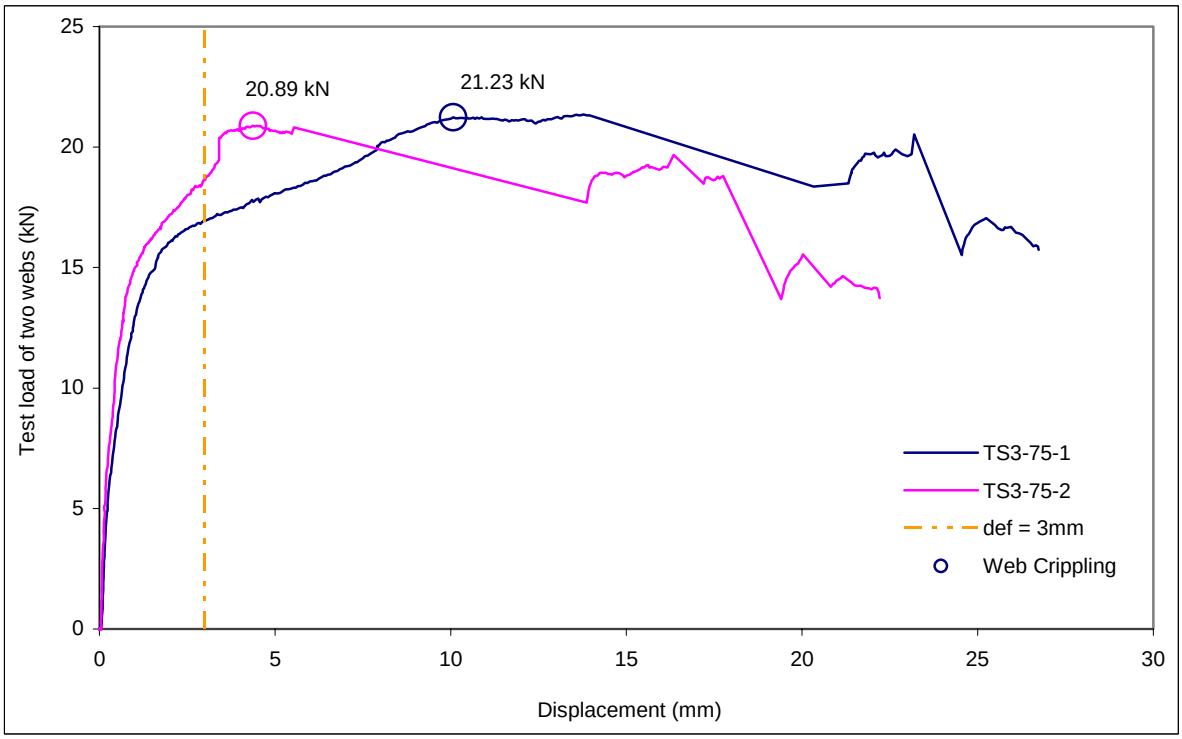

Figure D3.4: Test Load vs. Displacement, TS3-75 Series

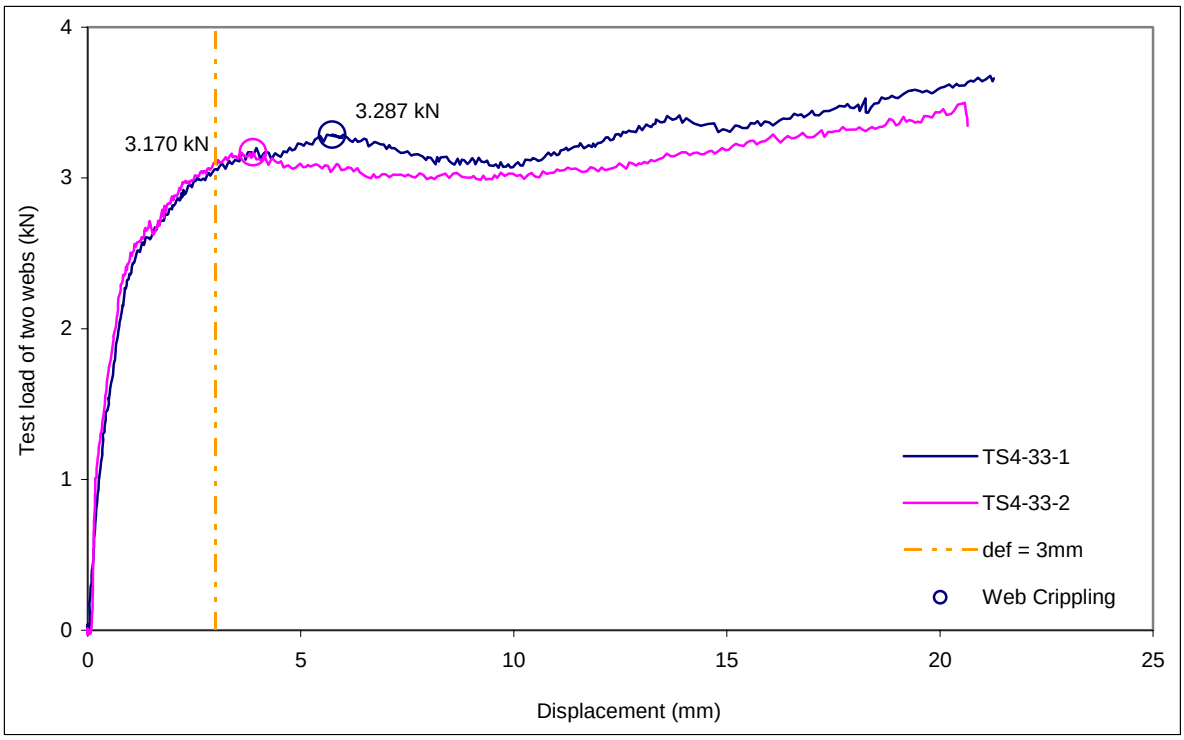

Figure D4.1: Test Load vs. Displacement, TS4-33 Series

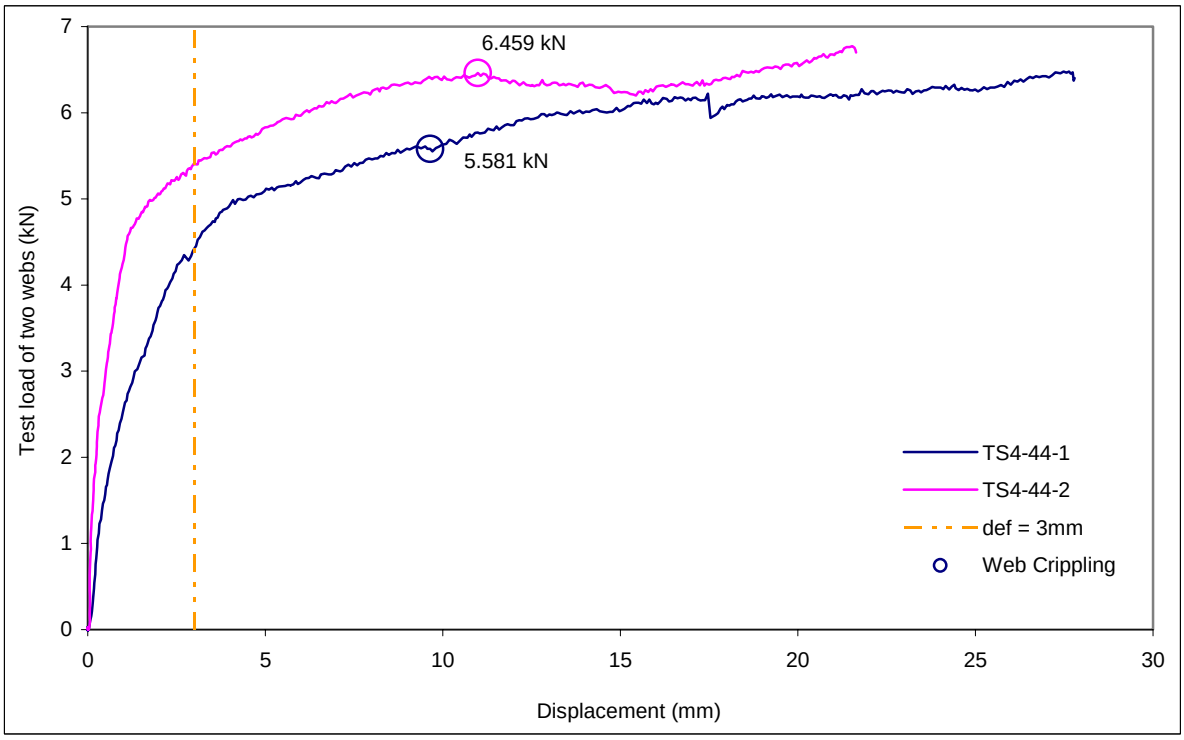

Figure D4.2: Test Load vs. Displacement, TS4-44 Series

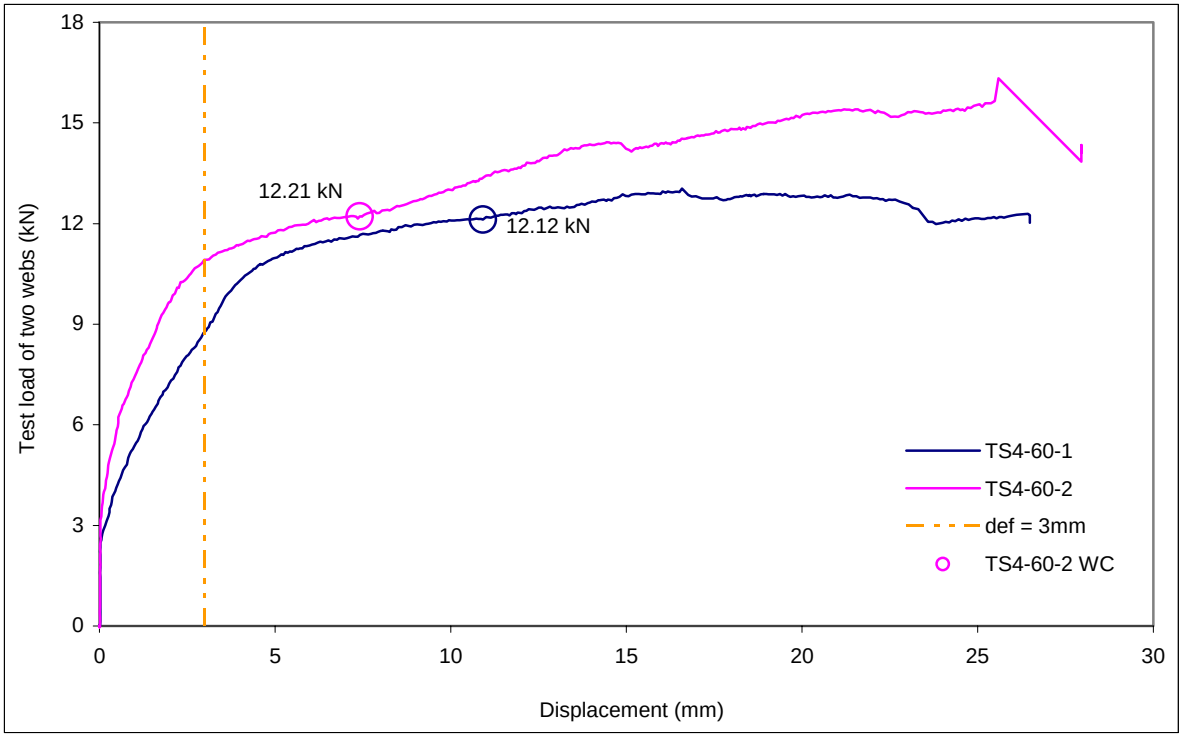

Figure D4.3: Test Load vs. Displacement, TS4-60 Series

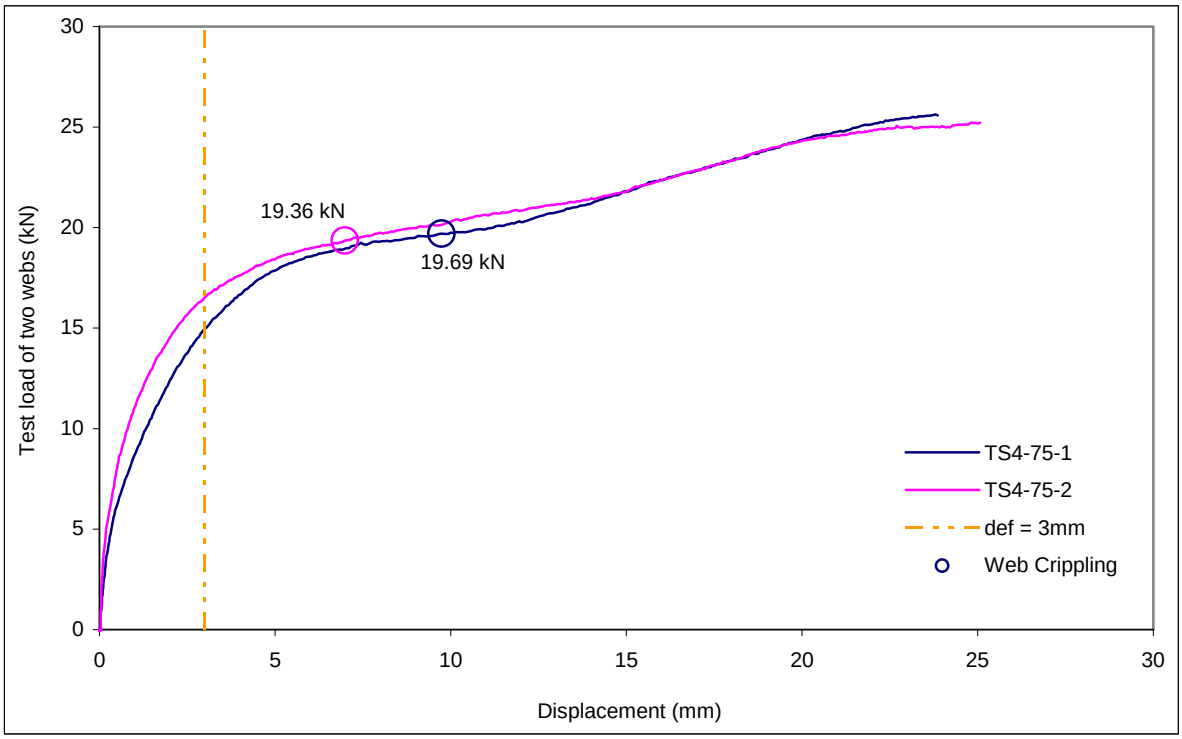

Figure D4.4: Test Load vs. Displacement, TS4-75 Series

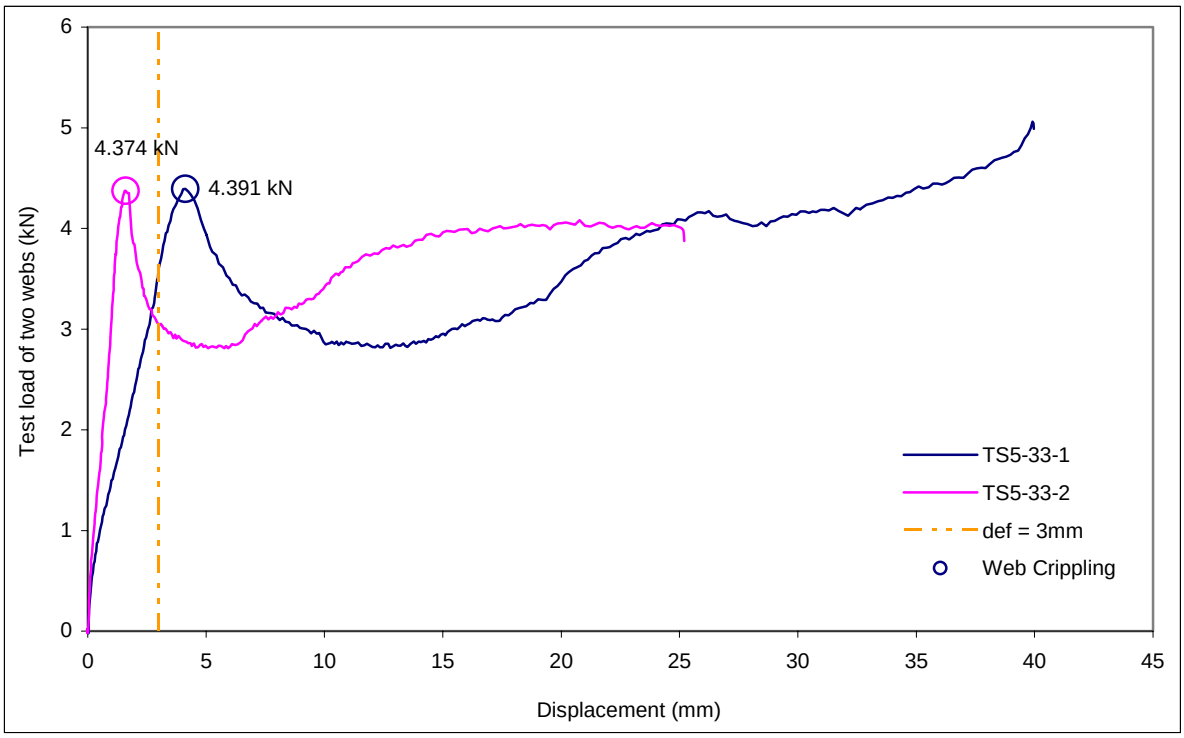

Figure D5.1: Test Load vs. Displacement, TS5-33 Series

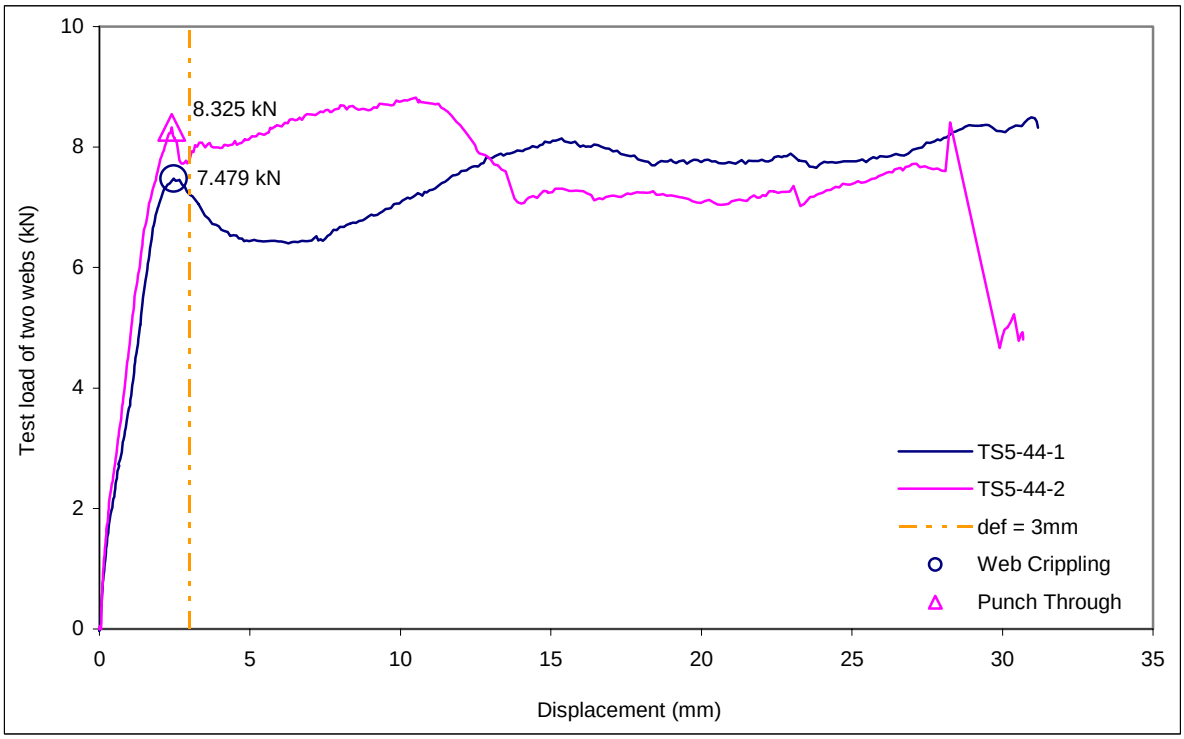

Figure D5.2: Test Load vs. Displacement, TS5-44 Series

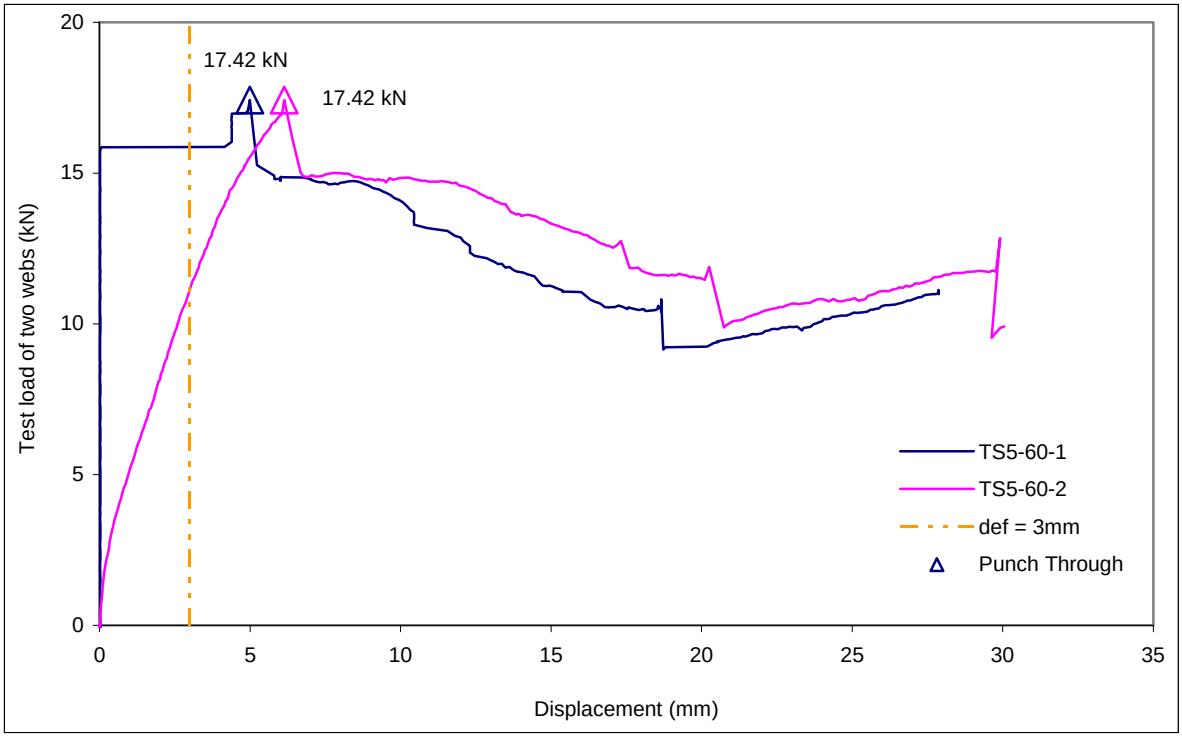

Figure D5.3: Test Load vs. Displacement, TS5-60 Series

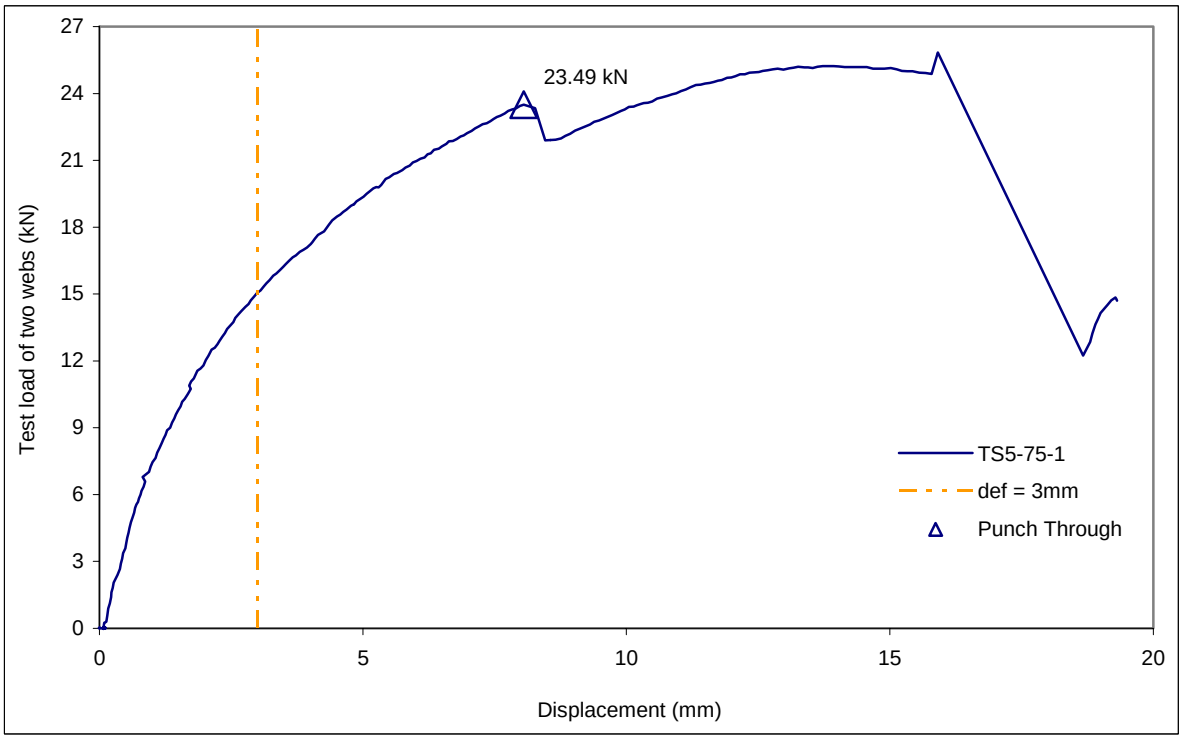

Figure D5.4: Test Load vs. Displacement, TS5-75 Series

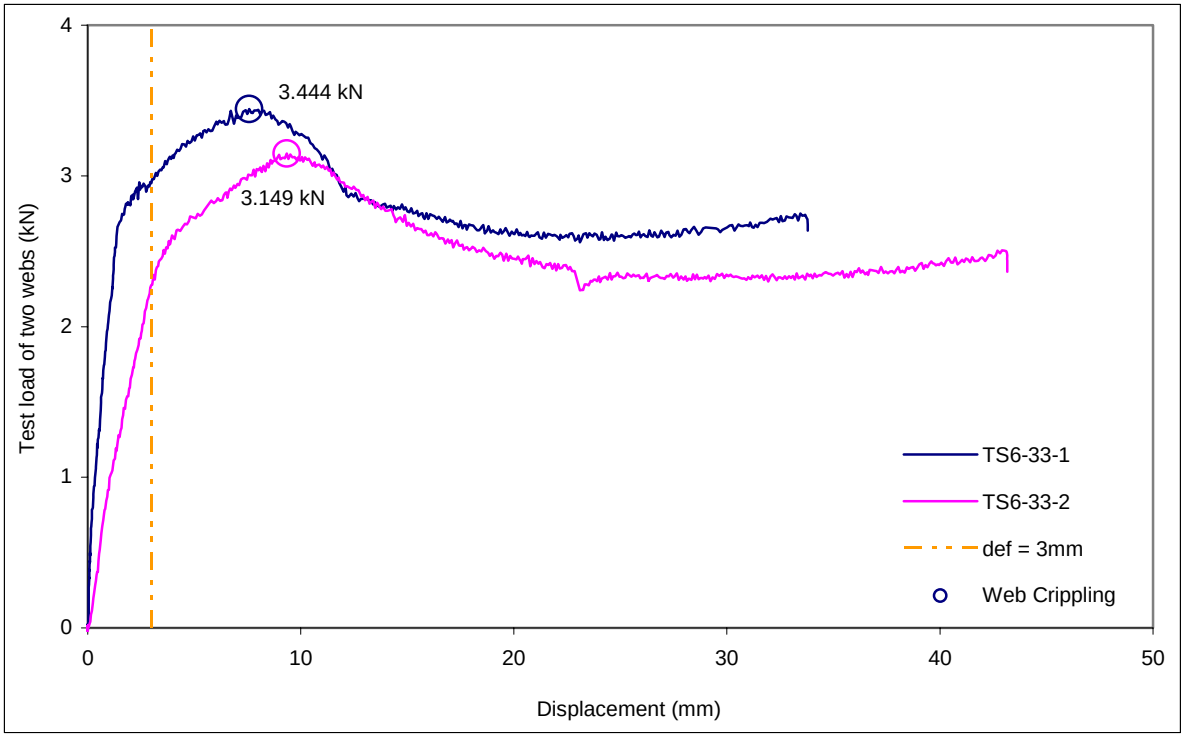

Figure D6.1: Test Load vs. Displacement, TS6-33 Series

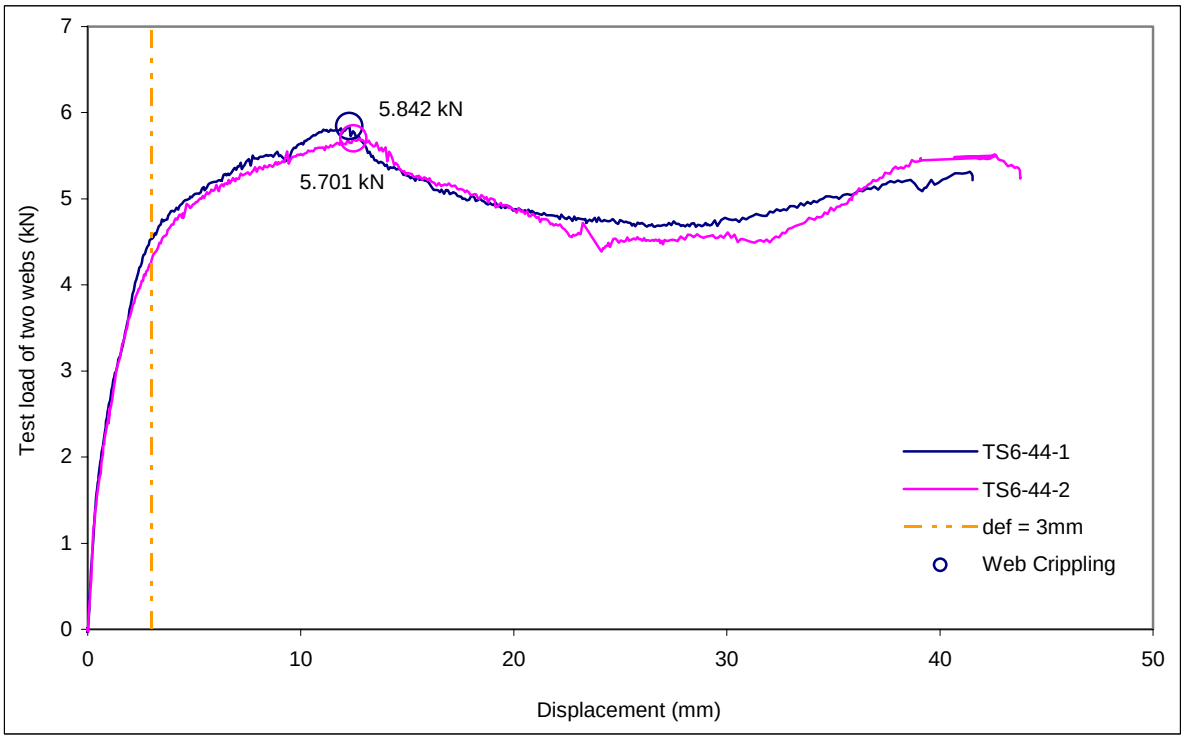

Figure D6.2: Test Load vs. Displacement, TS6-44 Series

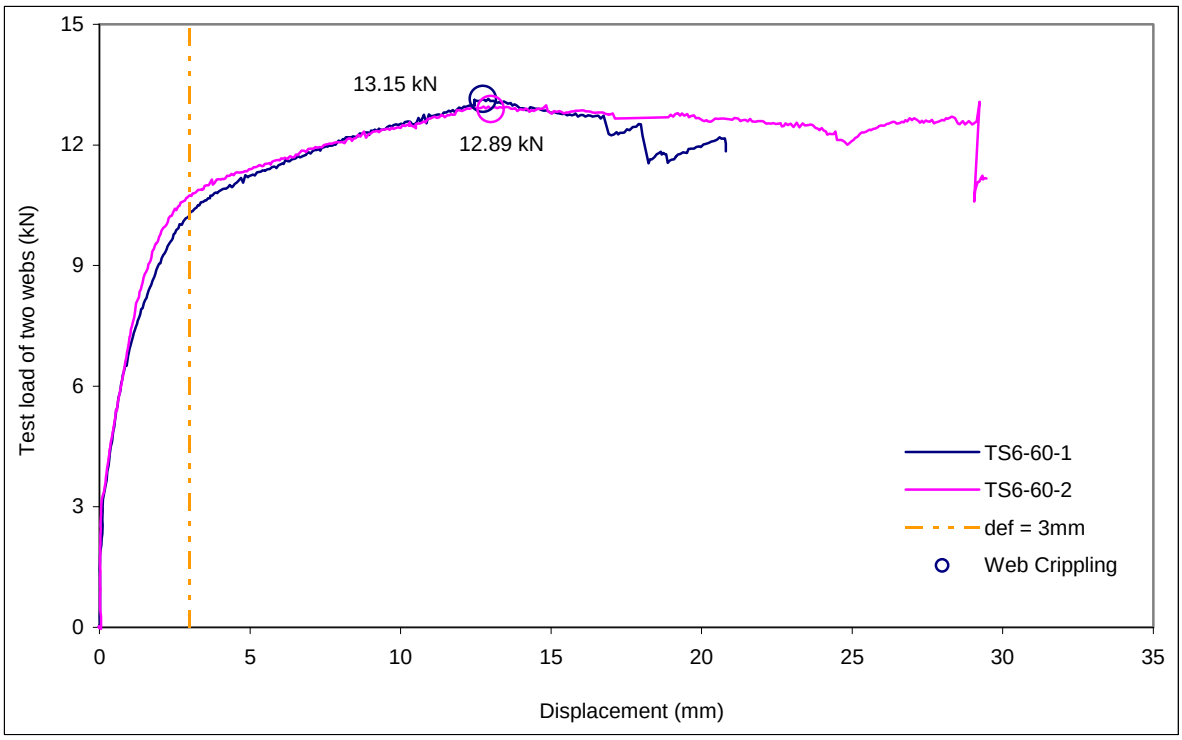

Figure D6.3: Test Load vs. Displacement, TS6-60 Series

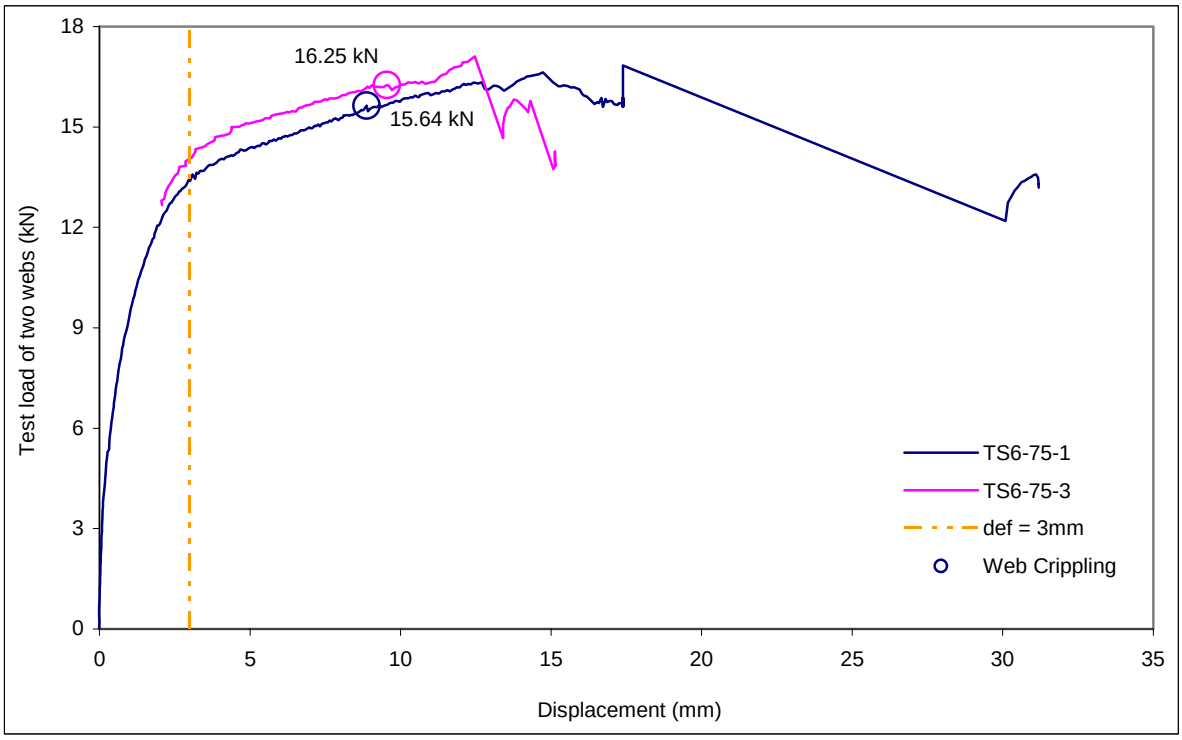

Figure D6.4: Test Load vs. Displacement, TS6-75 Series

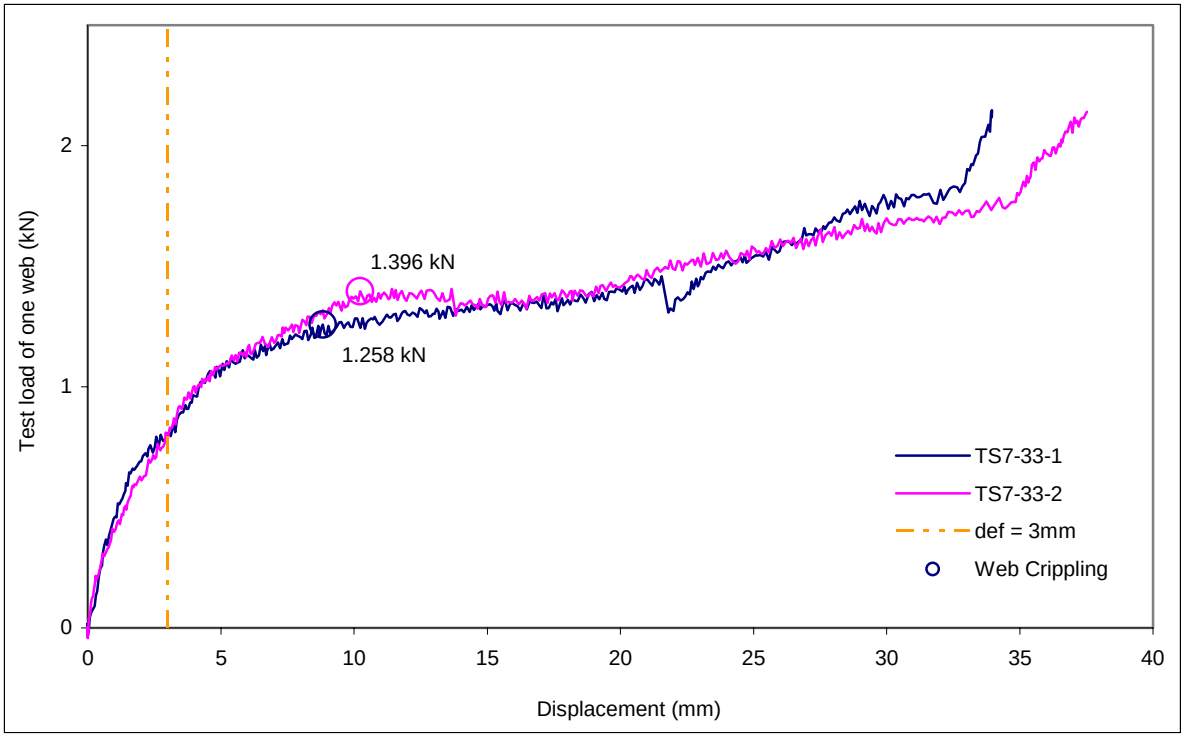

Figure D7.1: Test Load vs. Displacement, TS7-33 Series

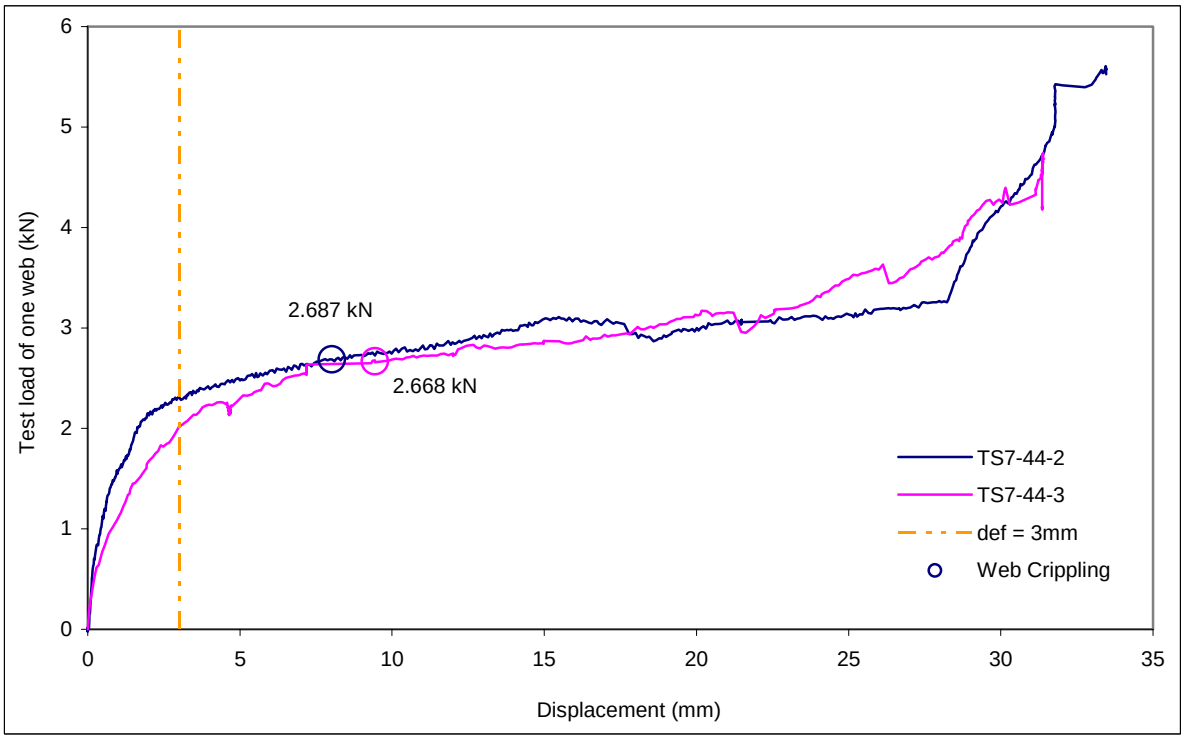

Figure D7.2: Test Load vs. Displacement, TS7-44 Series

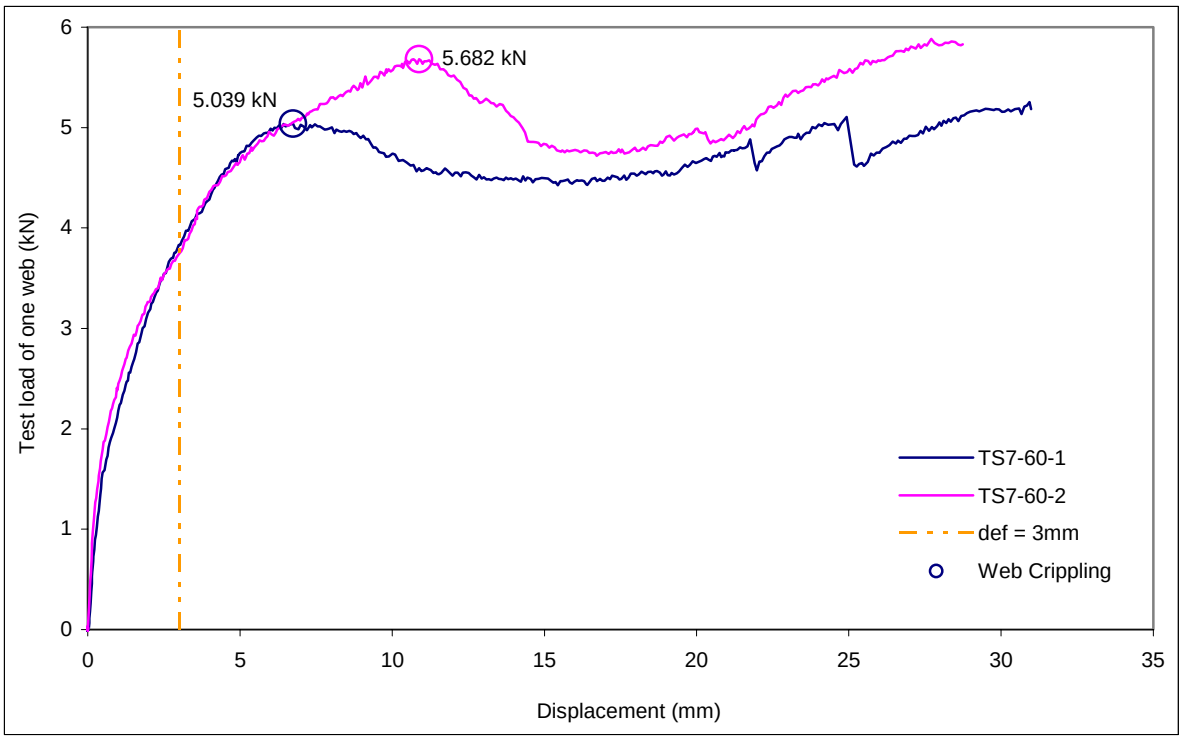

Figure D7.3: Test Load vs. Displacement, TS7-60 Series

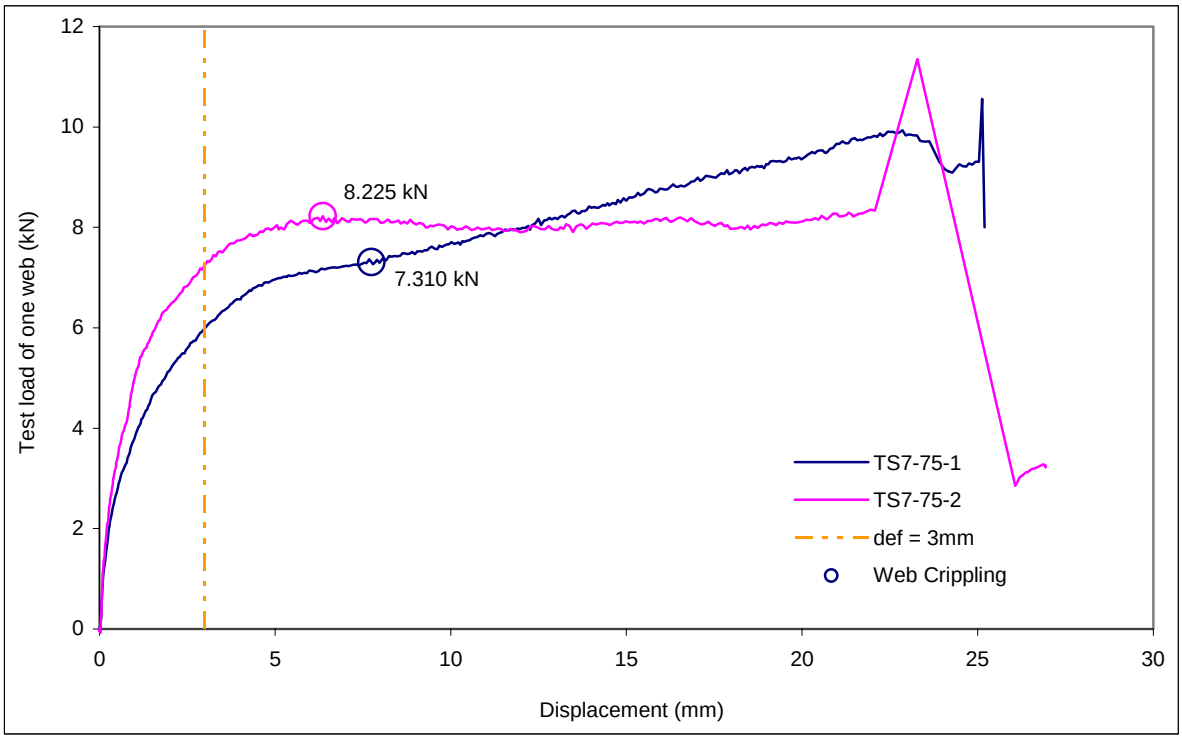

Figure D7.4: Test Load vs. Displacement, TS7-75 Series

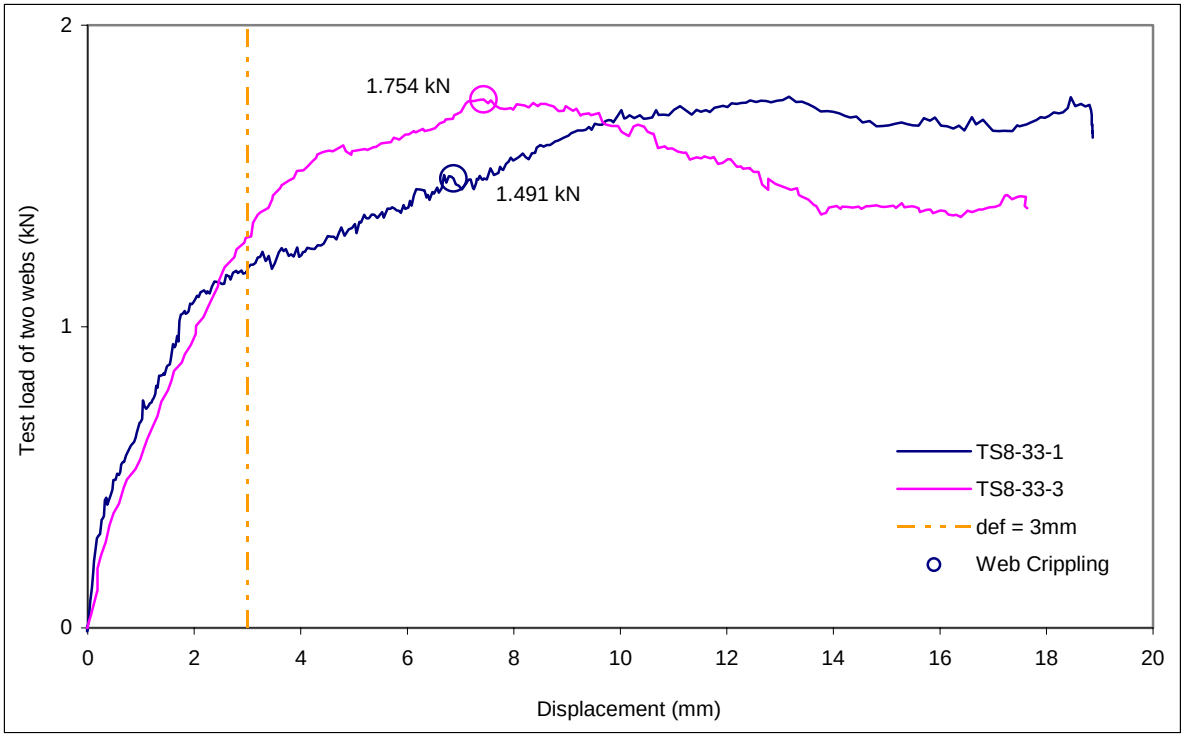

Figure D8.1: Test Load vs. Displacement, TS8-33 Series

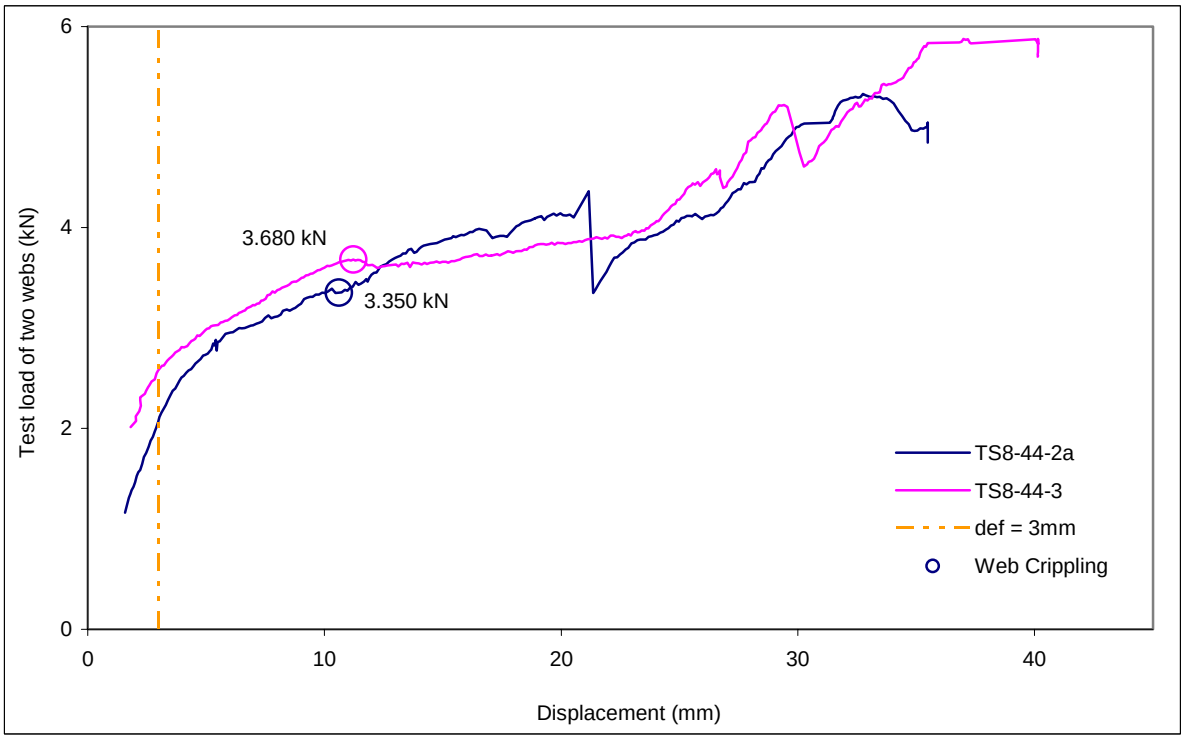

Figure D8.2: Test Load vs. Displacement, TS8-44 Series

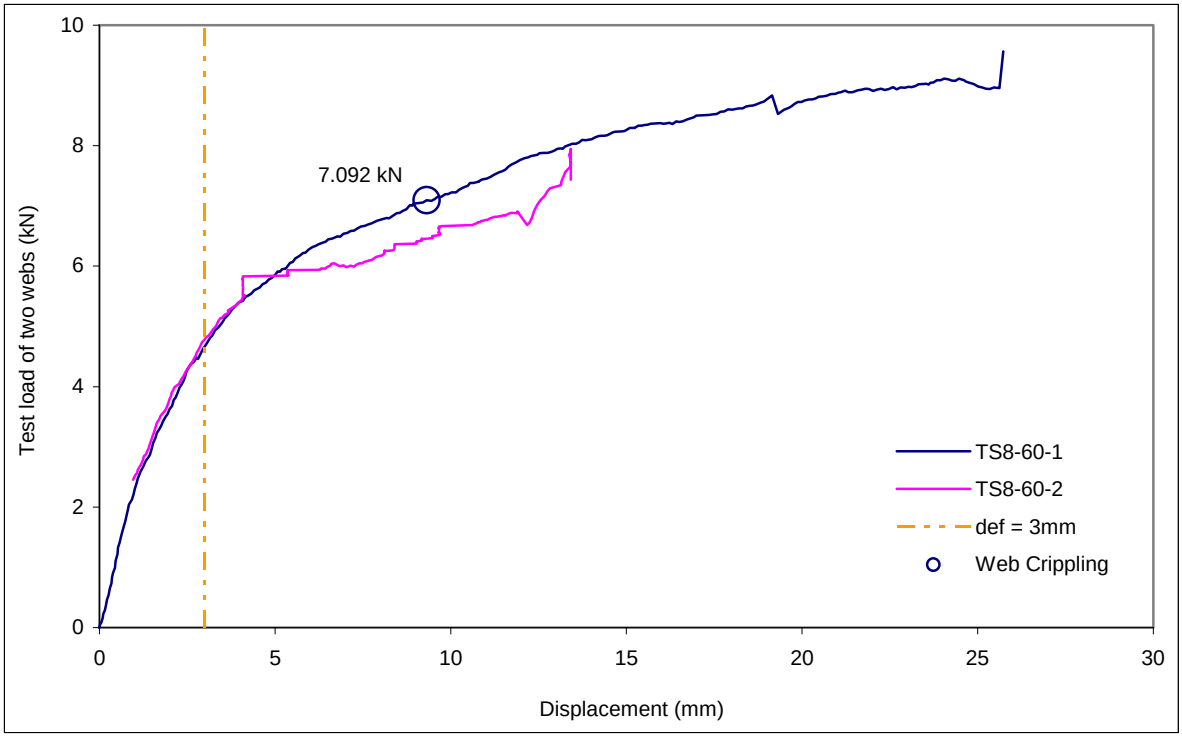

Figure D8.3: Test Load vs. Displacement, TS8-60 Series

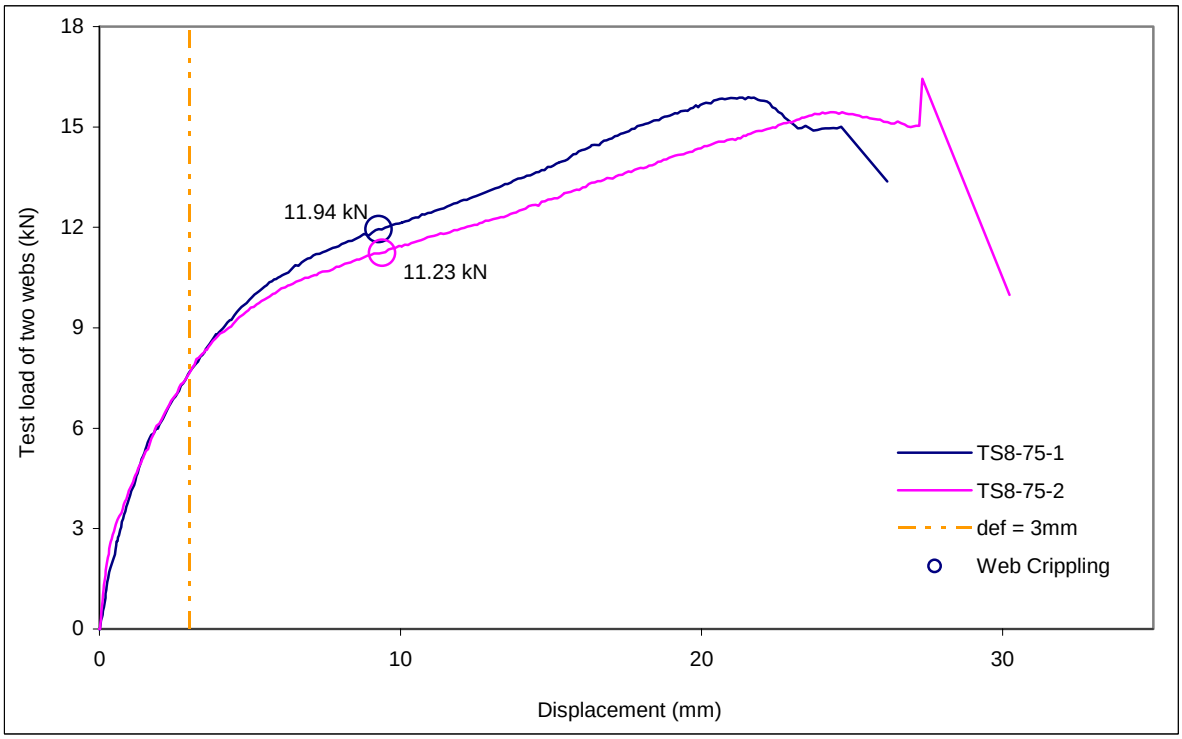

Figure D8.4: Test Load vs. Displacement, TS8-75 Series

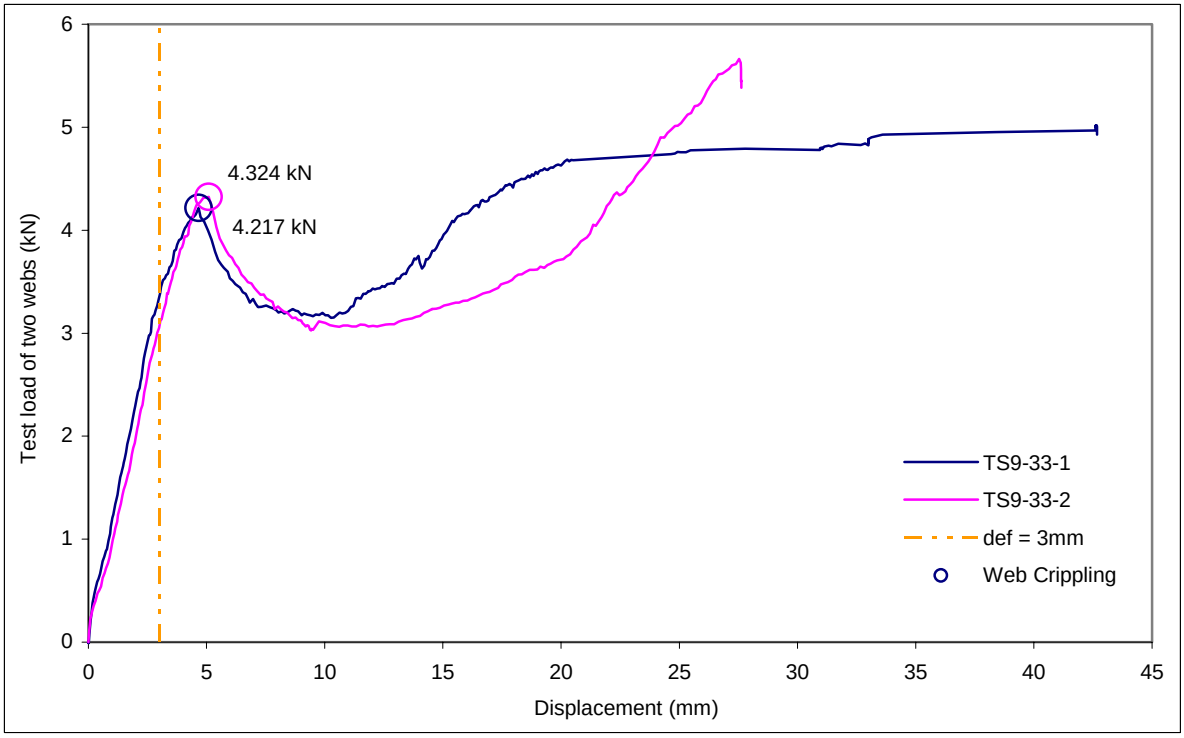

Figure D9.1: Test Load vs. Displacement, TS9-33 Series

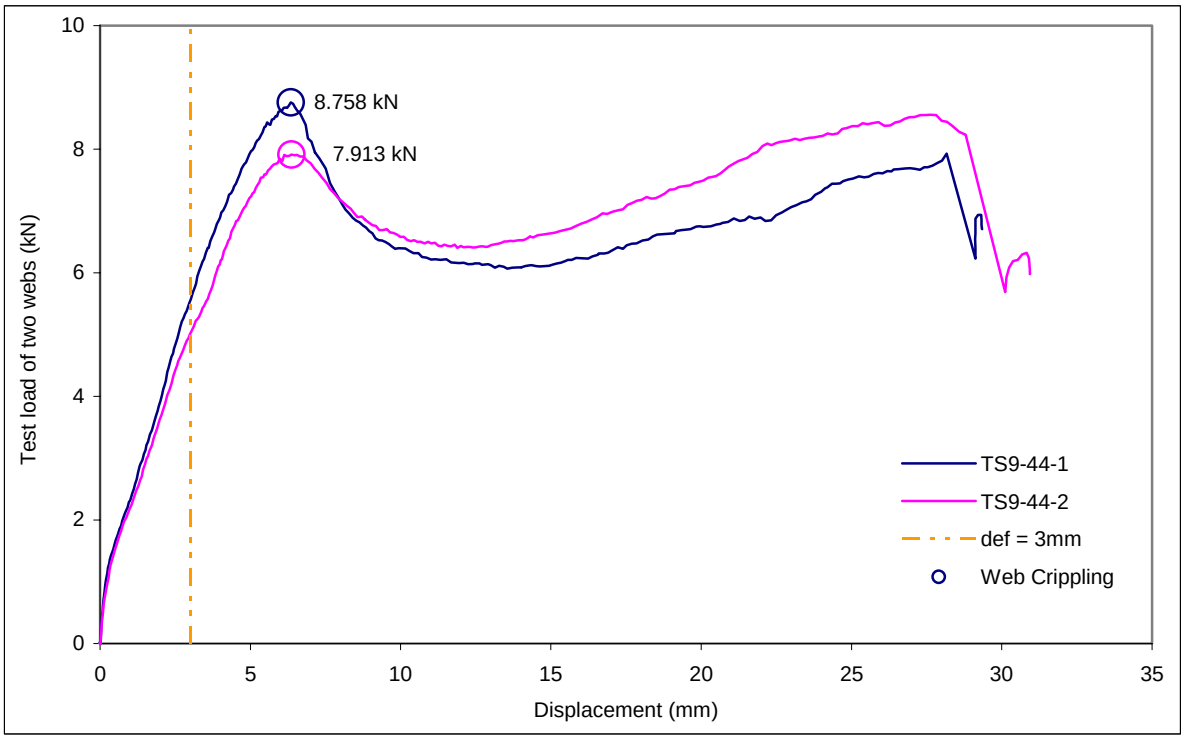

Figure D9.2: Test Load vs. Displacement, TS9-44 Series

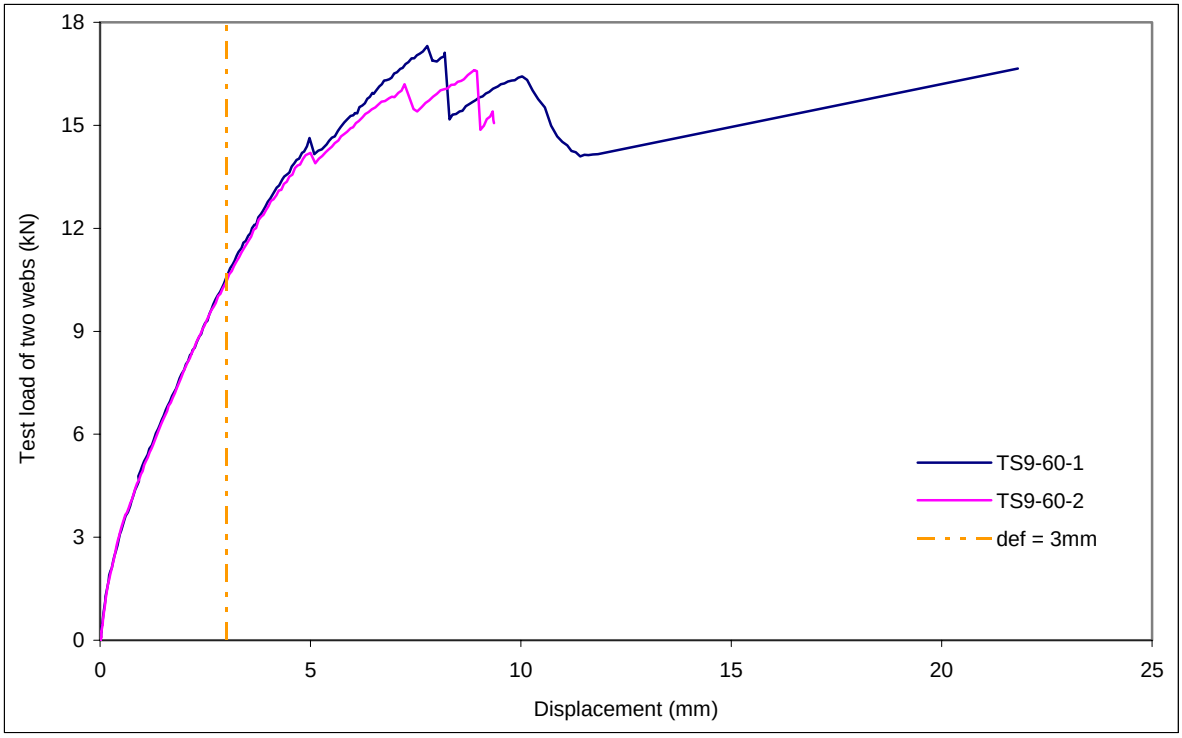

Figure D9.3: Test Load vs. Displacement, TS9-60 Series

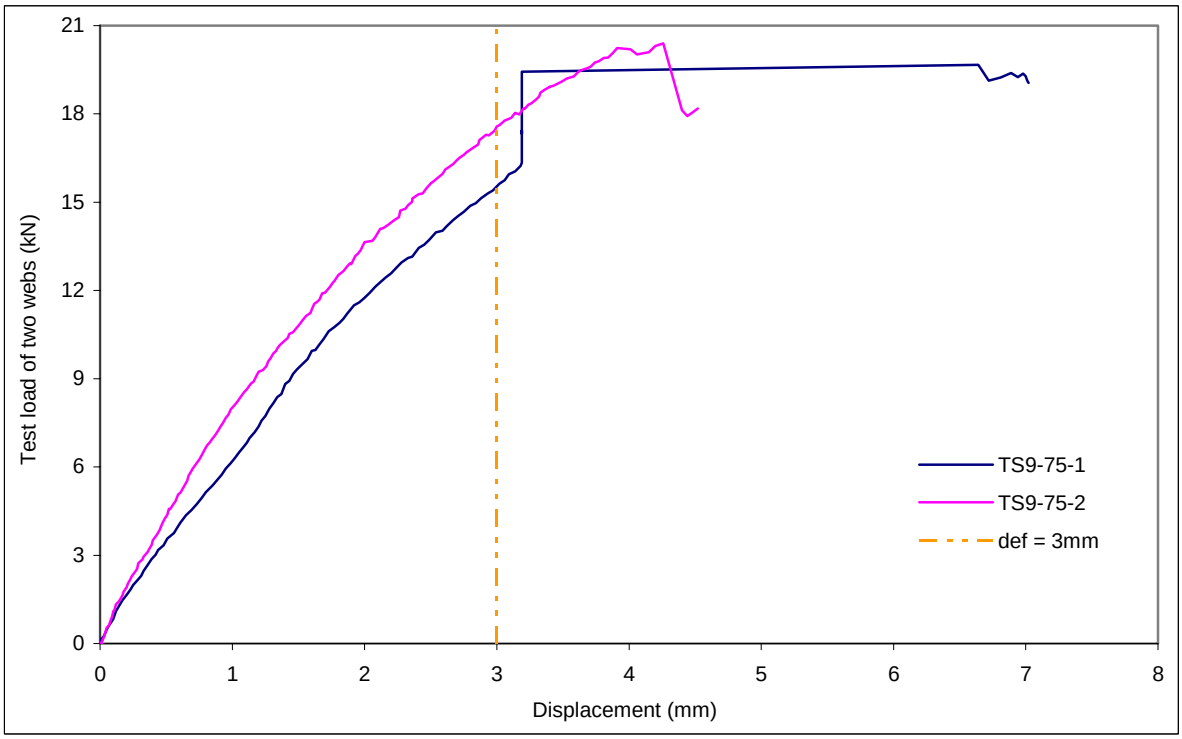

Figure D9.4: Test Load vs. Displacement, TS9-75 Series

No TS10-33-1 or TS10-33-2 Tests

Figure D10.1: Test Load vs. Displacement, TS10-33 Series

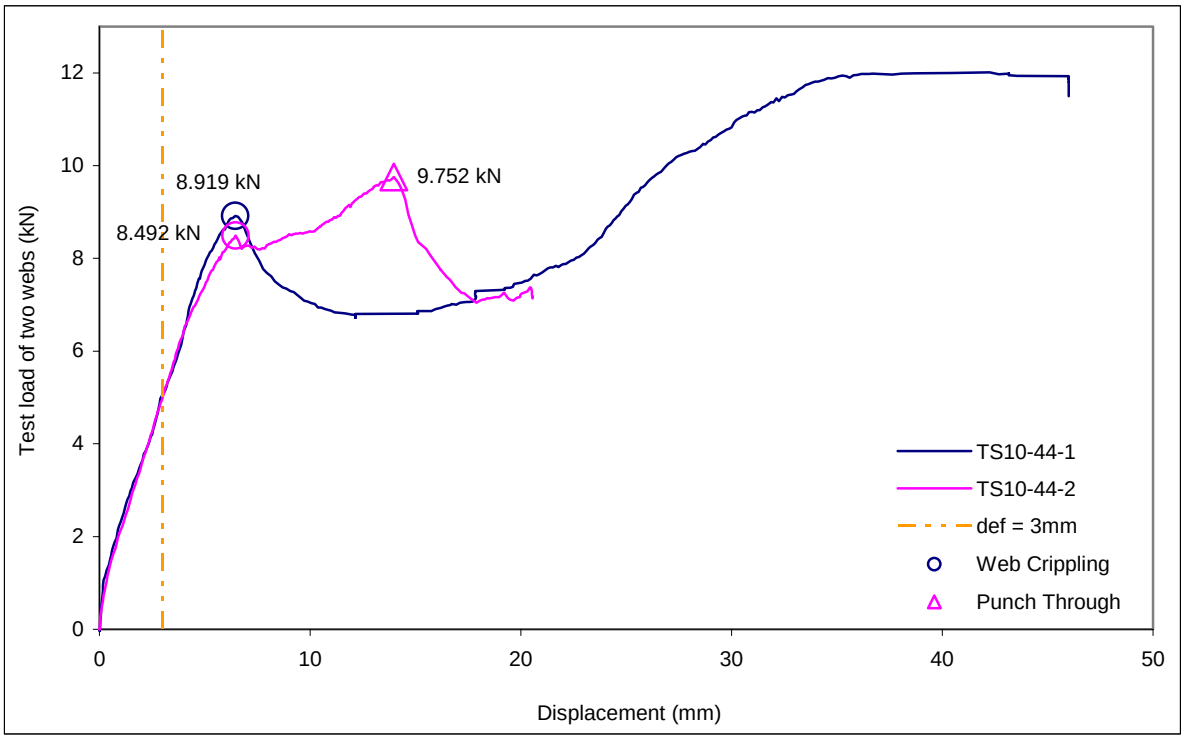

Figure D10.2: Test Load vs. Displacement, TS10-44 Series

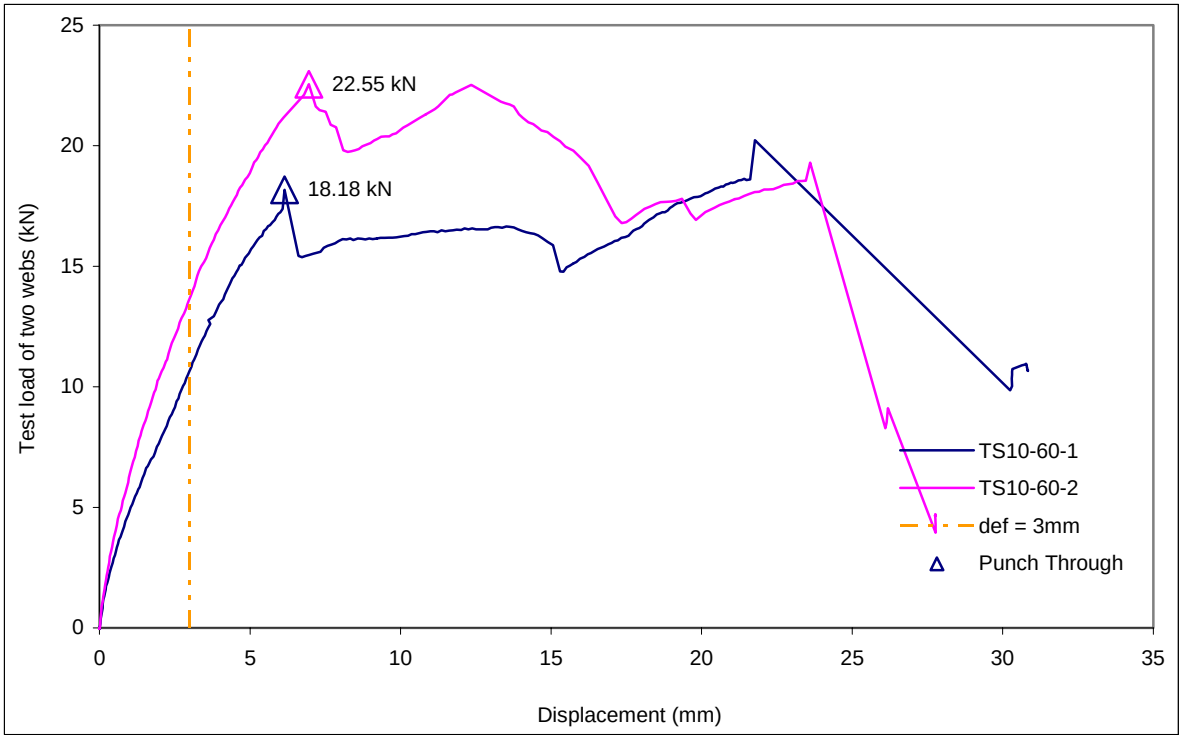

Figure D10.3: Test Load vs. Displacement, TS10-60 Series

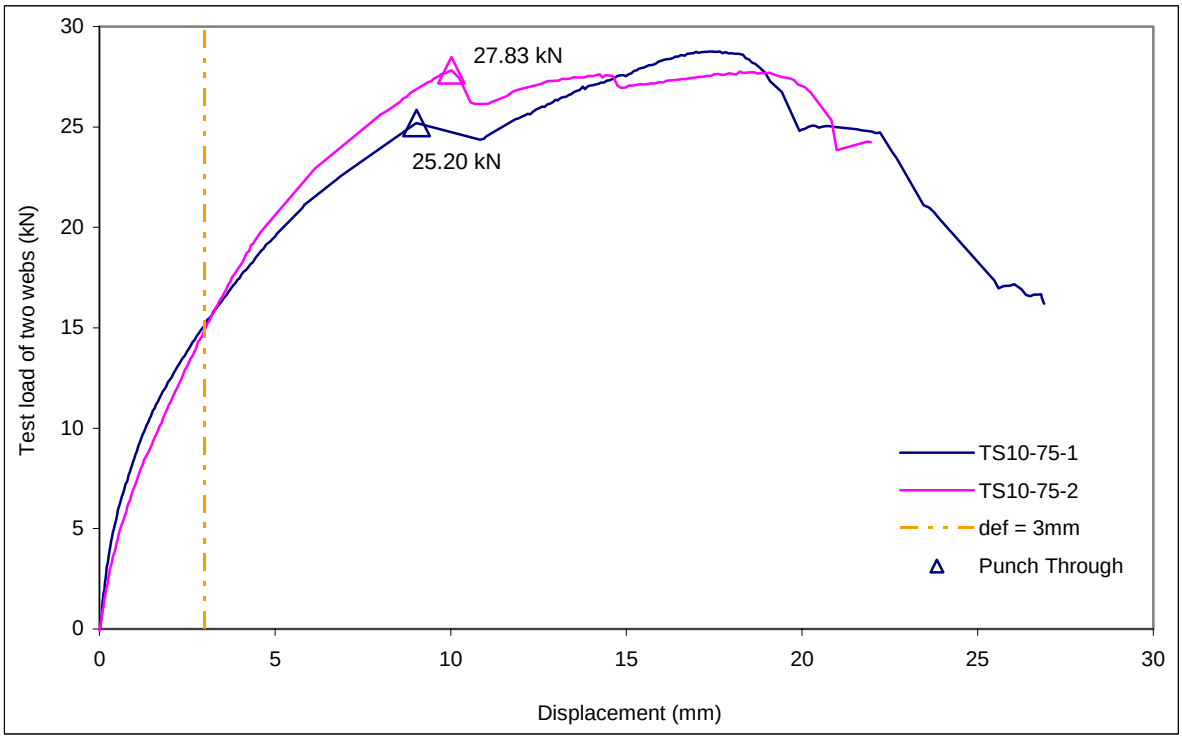

Figure D10.4: Test Load vs. Displacement, TS10-75 Series

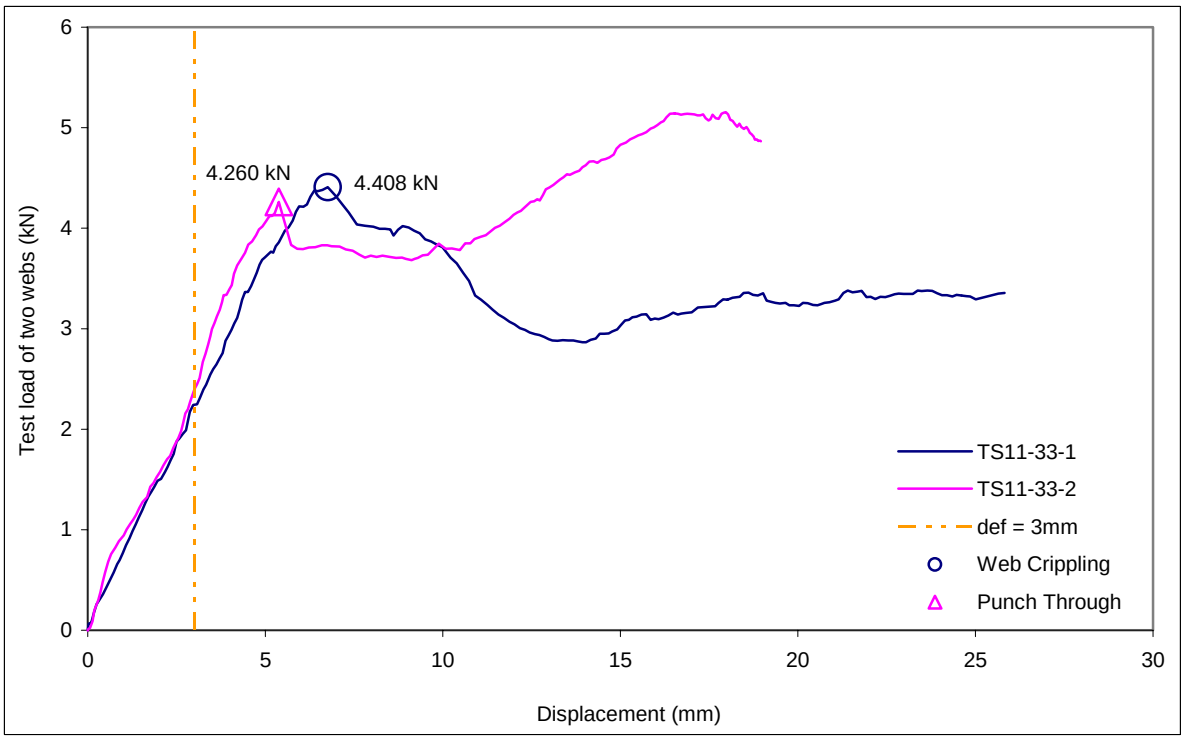

Figure D11.1: Test Load vs. Displacement, TS11-33 Series

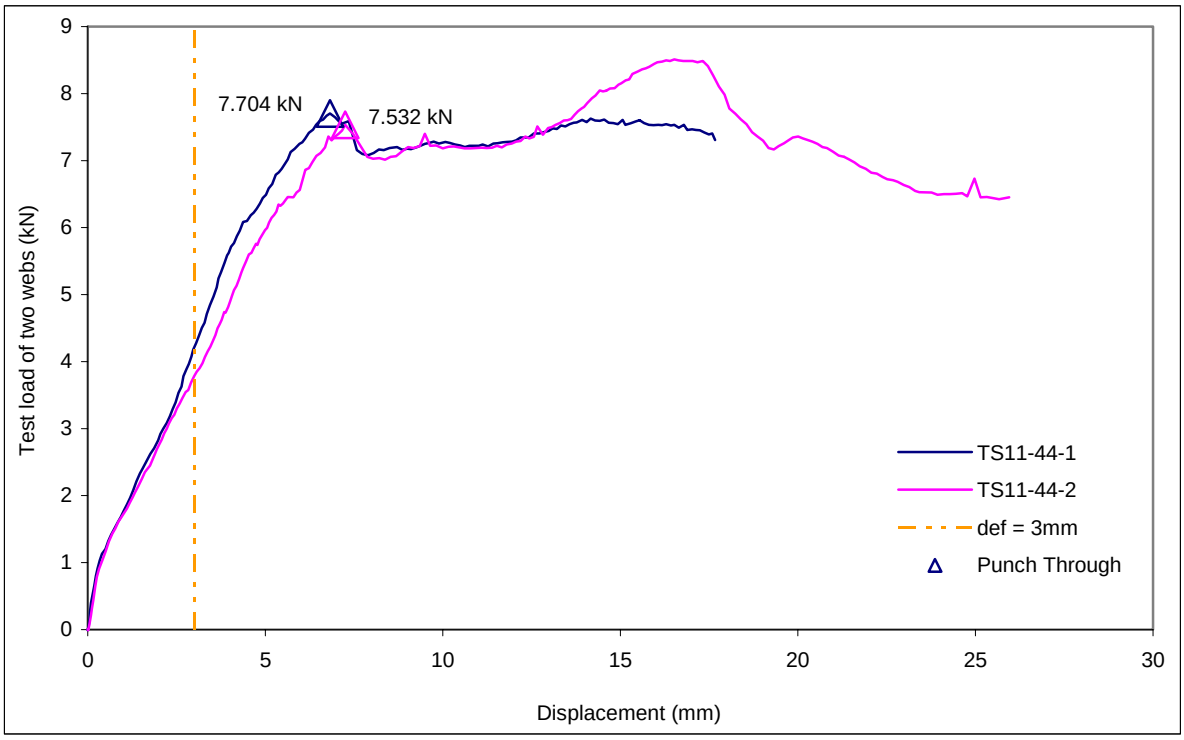

Figure D11.2: Test Load vs. Displacement, TS11-44 Series

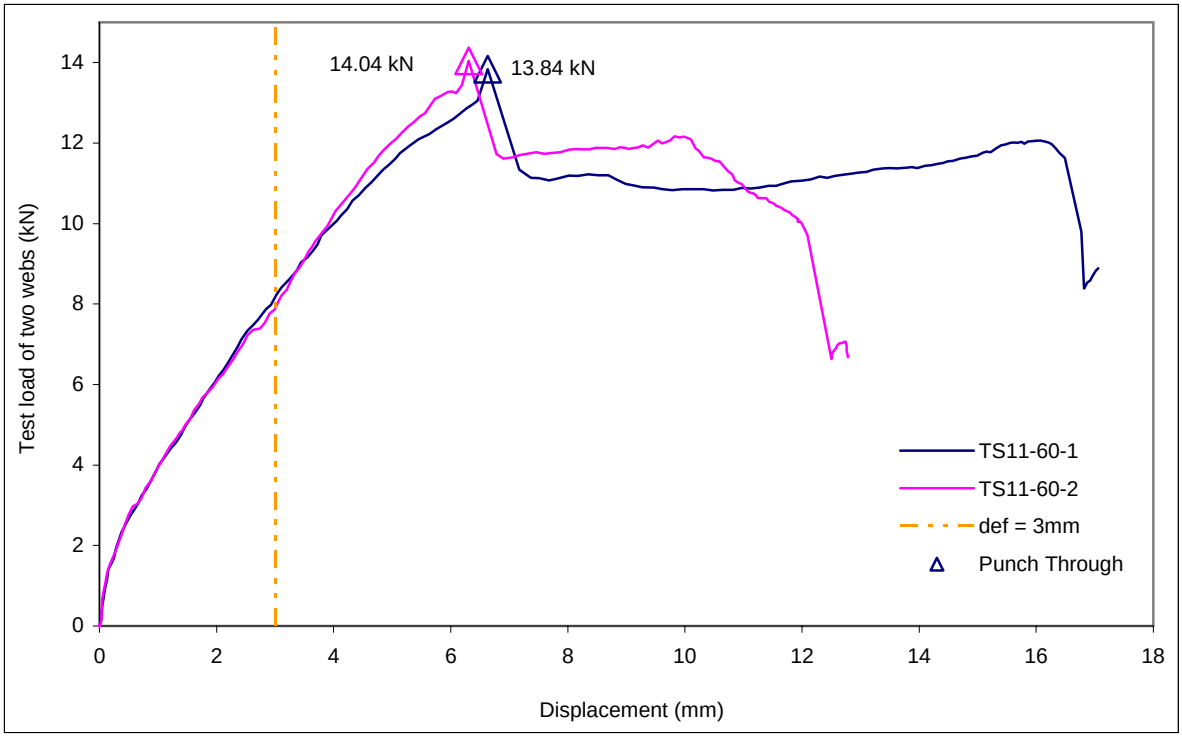

Figure D11.3: Test Load vs. Displacement, TS11-60 Series

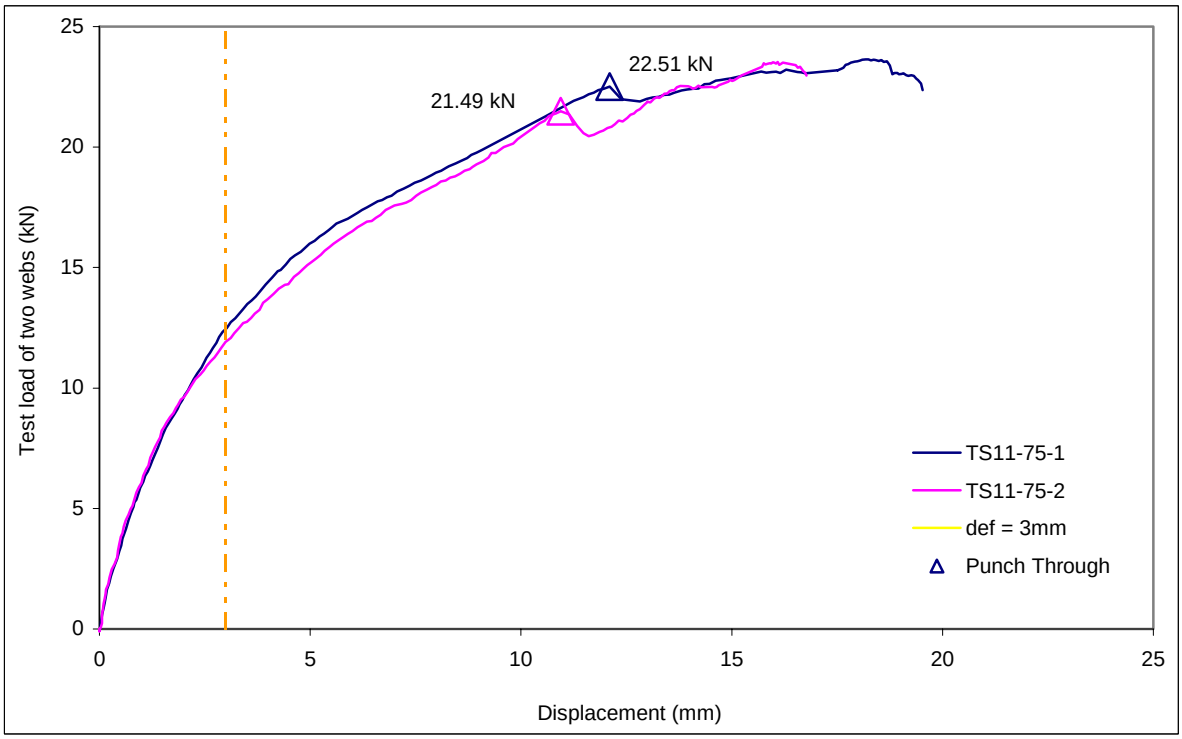

Figure D11.4: Test Load vs. Displacement, TS11-75 Series

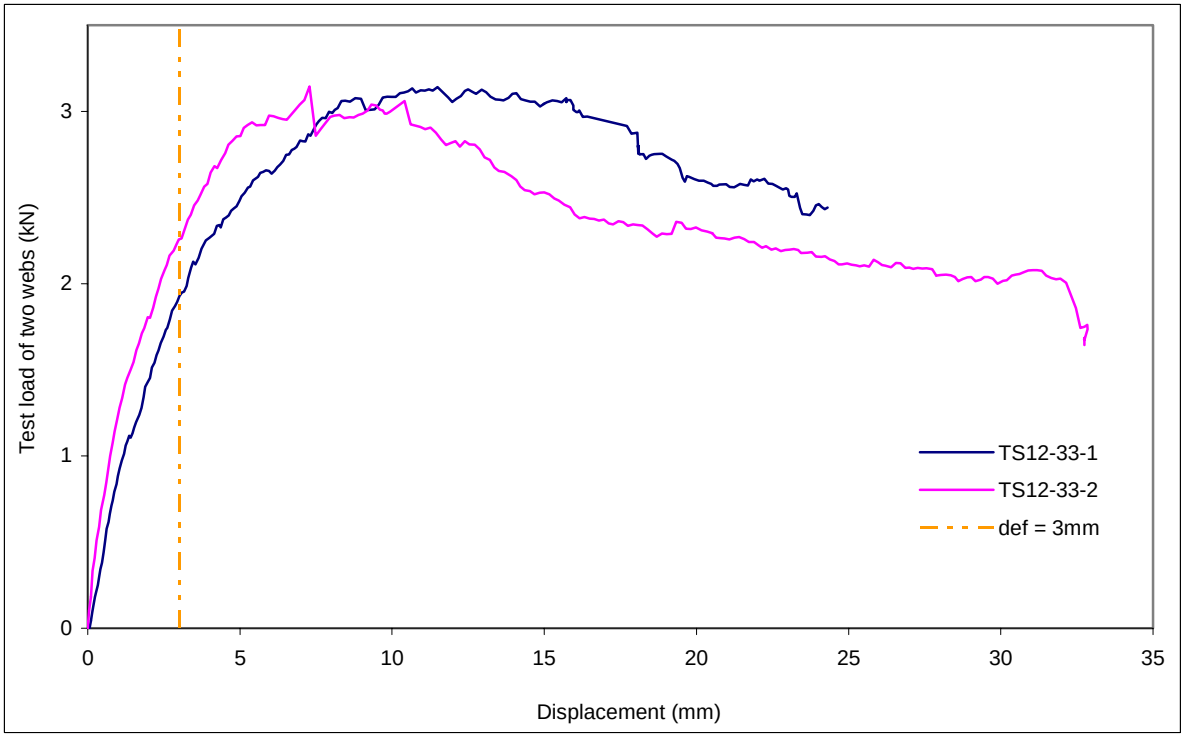

Figure D12.1: Test Load vs. Displacement, TS12-33 Series

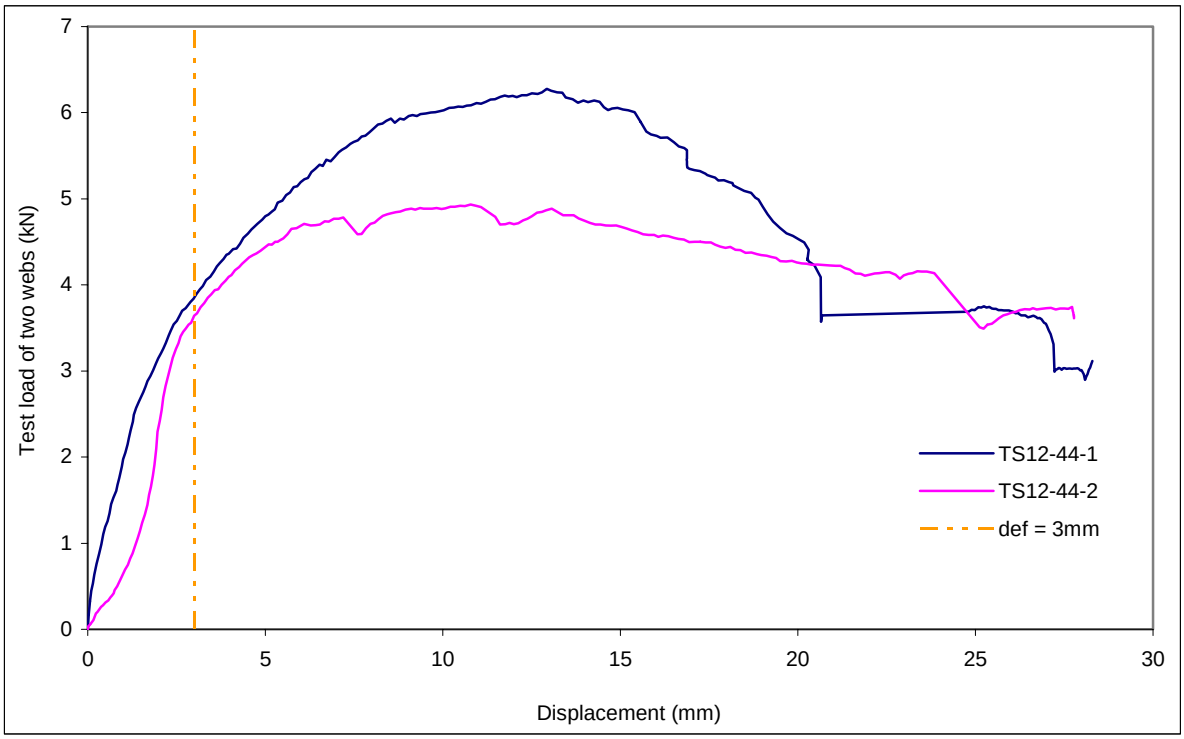

Figure D12.2: Test Load vs. Displacement, TS12-44 Series

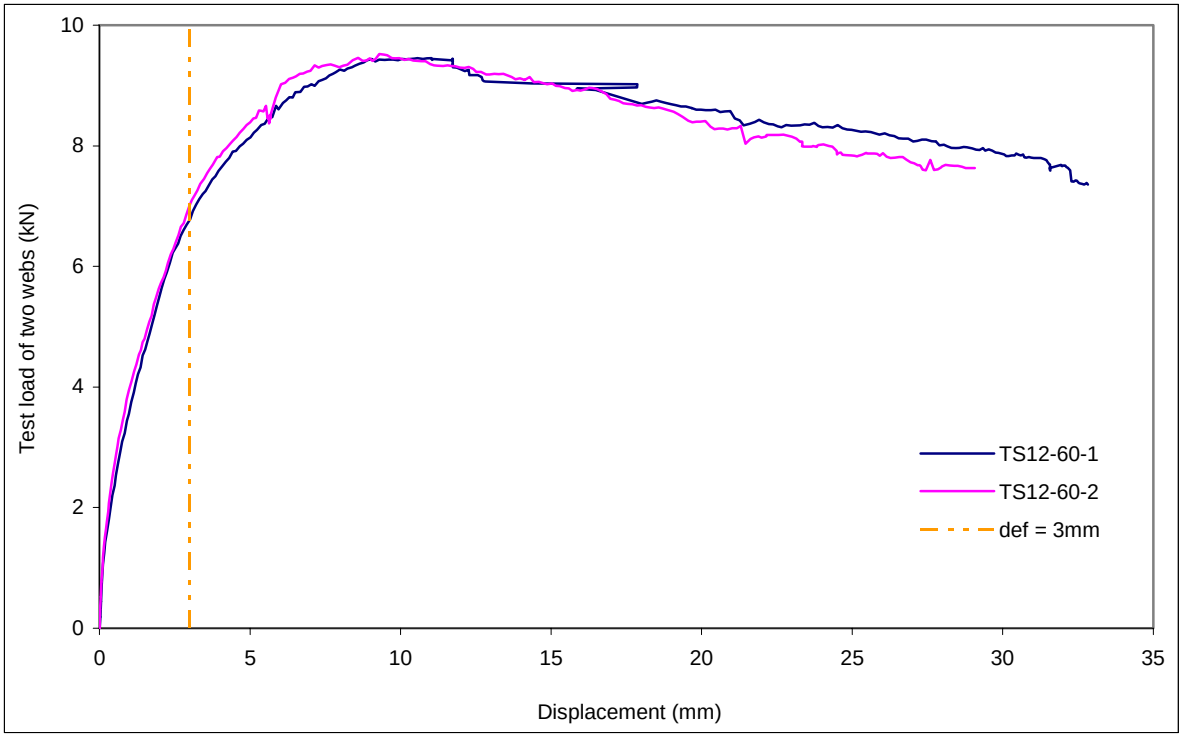

Figure D12.3: Test Load vs. Displacement, TS12-60 Series

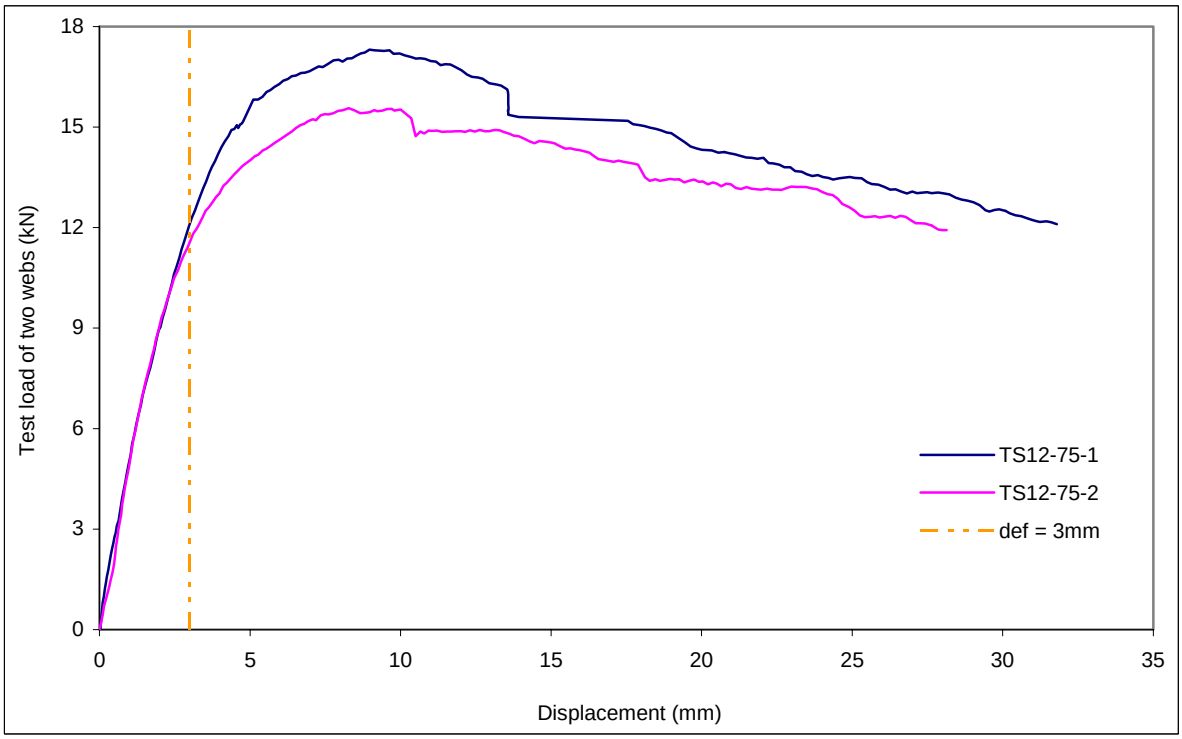

Figure D12.4: Test Load vs. Displacement, TS12-75 Series

References

AISI (2007a). *North American Specification for the Design of Cold-Formed Steel Structural Members*, AISI S100-07, American Iron and Steel Institute, Washington, DC.

AISI (2007b). *North American Standard for Cold-Formed Steel Framing – Wall Stud Design*, AISI 211-07, American Iron and Steel Institute, Washington, DC.

ASTM (2005). *Standard Test Methods and Definitions for Mechanical Testing of Steel Products,* ASTM A370-05. American Society for Testing and Materials, West Conshohocken, PA.

CSA (2007). *North American Specification for the Design of Cold-Formed Steel Structural Members*, CAN/CSA-S136-077, Canadian Standards Association, Mississauga, ON.

CSSBI (2006). *Lightweight Steel Framing Design Manual.* Canadian Sheet Steel Building Institute. Cambridge, ON.

Beshara, B., and Schuster, R. M. (2002). Web Crippling of Cold Formed Steel Members, *Proceedings of the 16th International Specialty Conference on Cold-Formed Steel Structures*, University of Missouri-Rolla, Rolla, MO.

Bolte, W.G. (2003). Behaviour of Cold-Formed Steel Stud-to-Track Connections, *Thesis presented to the faculty of the University of Missouri-Rolla in partial fulfillment for the degree Master of Science*, , University of Missouri-Rolla, Rolla, MO.

Daudet, L.R. (2001). "Recent Research on Stud/Track Connections", October 2001 Newsletter, Light Gauge Steel Engineers Association, Washington, DC.

Drysdale, R.G., and Breton, N. (1991). *Strength and Stiffness Characteristics of Steel Stud Backup Walls Designed to Support Brick Veneer*, Part 1 of the McMaster University Laboratory Test Program on Brick Veneer/Steel Stud Wall Systems, McMaster University, ON.

Fox, S.R., and Schuster, R.M. (2000). "Lateral Strength of Wind Loadbearing Wall Stud-to-Track Connections", *Proceedings of the Fifteenth International Specialty Conference on Cold-Formed Steel Structures*, University of Missouri-Rolla, Rolla, MO.

Fox, S.R. (2001). "Lateral Strength of Welded Stud-to-Track Connections", Canadian Cold Formed Steel Research Group report, University of Waterloo, Waterloo, ON.

Gerges, R.R., and Schuster, R.M. (1998) "Web Crippling of Single Web Cold Formed Steel Members Subjected to End-One-Flange Loading," *Proceedings of the 14th International Specialty Conference on Cold-Formed Steel Structures*, University of Missouri-Rolla, Rolla, MO.

Lewis, V., Fox, S.R., and Schuster, R.M. (1999). *A Further Study into the Web Crippling Behaviour at the Stud to Track Connection*, Canadian Cold Formed Steel Research Group report, University of Waterloo, Waterloo, ON.

Marinovic, I. (1994). Thin-walled Metal Structural Members, M.S. Thesis, Cornell University, Ithaca, NY.

Prabakaran, K., and Schuster, R. M. (1998). "Web Crippling Behavior of Cold Formed Steel Members," *Proceedings of the 14th International Specialty Conference on Cold-Formed Steel Structures,* University of Missouri-Rolla, Rolla, MO.

Schumacher, C., Fox, S.R., and Schuster, R.M. (1998). *Web Crippling Behaviour of Laterally Loaded Cold Formed Steel Studs at the Stud/Track Connection*, Canadian Cold Formed Steel Research Group report, University of Waterloo, Waterloo, ON.

Wallace, J.A., and Schuster, R.M. (2004). *Web Crippling of Cold Formed Steel Multi-Web Deck Sections Subjected to End One-Flange Loading*, Proceedings of the 17th International Specialty Conference on Cold-Formed Steel Structures, University of Missouri-Rolla, Rolla, MO.

Yu, W.W. (1985). "Cold Formed Steel Design", John Wiley and Sons Inc., New York, NY.